Vera Viana
Helena Mena Matos
João Pedro Xavier
Editors

Polyhedra and Beyond

Contributions from Geometrias'19,
Porto, Portugal, September 05-07

Birkhäuser

Trends in Mathematics

Trends in Mathematics is a series devoted to the publication of volumes arising from conferences and lecture series focusing on a particular topic from any area of mathematics. Its aim is to make current developments available to the community as rapidly as possible without compromise to quality and to archive these for reference.

Proposals for volumes can be submitted using the Online Book Project Submission Form at our website www.birkhauser-science.com.

Material submitted for publication must be screened and prepared as follows:

All contributions should undergo a reviewing process similar to that carried out by journals and be checked for correct use of language which, as a rule, is English. Articles without proofs, or which do not contain any significantly new results, should be rejected. High quality survey papers, however, are welcome.

We expect the organizers to deliver manuscripts in a form that is essentially ready for direct reproduction. Any version of TEX is acceptable, but the entire collection of files must be in one particular dialect of TEX and unified according to simple instructions available from Birkhäuser.

Furthermore, in order to guarantee the timely appearance of the proceedings it is essential that the final version of the entire material be submitted no later than one year after the conference.

More information about this series at http://www.springer.com/series/4961

Vera Viana • Helena Mena Matos
João Pedro Xavier

Editors

Polyhedra and Beyond

Contributions from Geometrias'19,
Porto, Portugal, September 05-07

Birkhäuser

Editors
Vera Viana (iD)
Faculty of Architecture
University of Porto
Porto, Portugal

Helena Mena Matos
Faculty of Sciences
University of Porto
Porto, Portugal

João Pedro Xavier
Faculty of Architecture
University of Porto
Porto, Portugal

Foreword

Leonardo da Vinci's approximately 60 illustrations for the book *The Divine Proportion* presented polyhedra for the very first time in history so spectacularly that they seemed to jump out of the paper as three-dimensional representations. 1800 years after Plato and Archimedes, they caused a true "polyhedra mania": Nuremberg artists Albrecht Durer, Wenzel Jamnitzer, and Lorenz Stoer drew polyhedra extensively; Dutchmen Simon Stevin and Claes Pietersz van Deventer published about them; Johannes Kepler rediscovered the complete list of regular polyhedra from the time of the Greeks and added two new ones in 1619 by including pentagrams. In the seventeenth century, the interest in the artistic presentation of polyhedra declined although their mathematical study continued. In 1809, Frenchman Louis Poinsot discovered two new solids by allowing intersecting faces. Englishman John Flinders Petrie added three infinite regular polyhedra in 1926, in collaboration with Canadian Donald Coxeter. American architect Buckminster Fuller caused an artistic revival, and his designs were so influential that the 1996 Nobel Prize winners in chemistry who discovered the C60 molecule gave it the name *Buckminsterfullerene*, although the shape of that molecule corresponds to the truncated icosahedron, already known to Archimedes. 2011 Chemistry Nobel Prize winner Daniel Shechtman likes to emphasize the divine proportion in his quasicrystals. In Europe, the work of Dutch artist Maurits Cornelis Escher led to a revival of the artistic study of polyhedra, and later Belgian Luc Tuymans and Danish Icelander Olafur Eliasson also represented them. Eventually, polyhedra conquered the whole world as they even inspired versatile Chinese artist Ai Weiwei, for instance. Thus, artistically and scientifically the polyhedral topic surely still is of interest. And perhaps even more than before, as modern 3D-software brings it within reach of any motivated computer enthusiast.

This was amply illustrated at the Geometrias'19 Conference in Porto, of which this book collects some highlights (not necessarily in order of their presentation at the conference). Some contributions were developed further into full papers, for the purpose of their inclusion in this book. The participants still hold vivid memories of the presentation on synthetic methods for constructing polyhedra, where one could actually see a snub cube being created on the screen, as the result of a kind of

equilibrium process. Anyone who ever tried to draw a snub cube using even the most sophisticated 3D-software, quickly experiences this is impossible, thus confirming the fact that it can't be constructed in a finite number of steps with lines and circular arcs. Historical aspects are emphasized by a contribution on small stellated dodecahedrons in Genoa, Italy, and that is quite unusual, as Kepler-Poinsot solids do not seem so popular. A paper on confocal quadratic surfaces gives a more theoretical *intermezzo*, while regular participants of geometry-related conferences are probably happy to see a continuation of the work on concave deltahedral rings. This contrasts with the considerations on the gyroid, which is probably new to most readers. Admittedly, double-layered polyhedra are beautiful—even if one doesn't grasp what they are about! Geodesic structures can't be omitted in any self-respecting conference on polyhedra, while Vittorio Giorgini's organic structures are, regrettably, less well-known. Even Gaudí can be a topic, when combined with John Pickering's form-finding method. Several talks and workshops about pedagogical aspects were on the conference program too, during the conference, and the introduction to solid tessellations, included in this book, is but one of them. This variety of subjects of the Porto Geometrias'19 Conference, presented in an open exchange, created a pleasant ambience that will hopefully filter through these selected papers.

Dirk Huylebrouck holds a PhD in mathematics from the University of Ghent, Belgium. He lectured in Congo and Burundi for 12 years, interrupted by assignments in Portugal and at Maryland University Europe. Next, he taught at the Faculty of Architecture of the KU Leuven (Belgium) and edited the column *The Mathematical Tourist* in the journal *The Mathematical Intelligencer*. Author of seven books in popular mathematics in Dutch, his first, *Africa + Mathematics*, has already been translated in English (2019, Springer).

Ostend, Belgium   Dirk Huylebrouck
08 December 2021

Preface

Aproged, the Portuguese Geometry and Drawing Teachers Association, invited us to organize its 5th international conference and thus, *Geometrias'19: Polyhedra and Beyond* was held in the Department of Mathematics of the Faculty of Sciences, University of Porto, in September 5–7, 2019. The aim of this conference was to bring together international experts, scholars, researchers, and students from diverse backgrounds to engage in interdisciplinary discussions on theoretical research and practical studies on polyhedra and geometrical structures under development in different fields of knowledge and institutions. The *Geometrias'19: Book of Abstracts*[1], published in its outcome, summarized the essence of this Conference, offering a clear testimony of how the atmosphere of dialog and shared knowledge created renewed mutual interests between the participants, encouraging new synergies.

This book reflects a selection of the investigations presented during *Geometrias'19* that were developed into full papers, so some contributions contain materials somehow beyond the results presented in the talks, addressing different subjects and explorations of polyhedral theory within architecture, computer science, mathematics, and structural design, broadly construed.

For their contribution to the accomplishment of this book, we are especially grateful to the Scientific Committee members and additional reviewers for their commitment in revisiting these studies, and to all the authors for the development of their research and their openness during the reviewing procedures. An additional appreciation to our Foreword's Author, for such an inspirational input.

We thank you all for your contributions and for understanding the time it took us to achieve this publication, of which we are very proud of.

Porto, Portugal

Vera Viana
Helena Mena Matos
João Pedro Xavier

---

[1]Viana, V. (Ed.). (2019). *Geometrias'19: Book of Abstracts*. Porto: Aproged. https://doi.org/10.24840/978-989-98926-8-2

Acknowledgments

Contents

List of Figures

List of Tables

Contributors

Leonardo Baglioni Sapienza University of Rome, Rome, Italy

Marco Giorgio Bevilacqua University of Pisa, Pisa, Italy

Cristina Càndito University of Genoa, Genoa, Italy

Alexandra Castro Faculty of Architecture, University of Porto, Porto, Portugal

Ilenio Celoria University of Genoa, Genoa, Italy

Federico Fallavollita University of Bologna, Bologna, Italy

Riccardo Foschi University of Bologna, Bologna, Italy

Filippo Iardella BIM and Digital Engineer, Milano, Italy

Henriette-Sophie Lipschütz Freie Universität, Berlin, Germany

Andrés Martín-Pastor Department of Graphic Engineering, ETSIE, IUACC, Universidad de Sevilla, Sevilla, Spain

Slobodan Mišić University of Arts in Belgrade, Belgrade, Serbia

Marija Obradović University of Belgrade, Belgrade, Serbia

Konrad Polthier Freie Universität, Berlin, Germany

Ulrich Reitebuch Freie Universität, Berlin, Germany

Rinus Roelofs Independent Sculptor, Hengelo, The Netherlands

José Pedro Sousa Faculty of Architecture, University of Porto, Porto, Portugal

Gianluca Stasi Ctrl+Z Arquitectura, Seville, Spain

Denise Ulivieri University of Pisa, Pisa, Italy

Emmanouil Vermisso Florida Atlantic University, Boca Raton, FL, USA

Vera Viana Faculty of Architecture, CEAU, University of Porto, Porto, Portugal

João Pedro Xavier Faculty of Architecture, University of Porto, Porto, Portugal

About the Editors

Vera Viana is a Researcher in CEAU, Faculty of Architecture, University of Porto, and Director of the Portuguese Geometry and Drawing Teachers' Association.

With research interests on polyhedral geometry, the history of polyhedra, the relationships between architecture and mathematics and the transformative potential of digital culture in mathematics education, Viana authored a PhD thesis, papers, lectures, workshops, and a website on these subjects.

Viana has organized the Geometrias conferences and contributed to other international conferences and congresses as co-chair, scientific reviewer, and sessions moderator. Editorial Board member of the Nexus Network Journal.

Helena Mena Matos is Assistant Professor at the Department of Mathematics of the Faculty of Sciences of the University of Porto and member of the Mathematics Research Centre of the University of Porto. In addition to teaching and research in fundamental mathematics, she has a strong interest in the connections between mathematics and the visual arts and dedicates part of her time to the dissemination of mathematics. Faculty of Sciences, University of Porto, Porto, Portugal

João Pedro Xavier is an architect and full professor at the Faculty of Architecture, University of Porto, where he received his degree in 1985 and his PhD in Architecture in 2005.

He worked in Álvaro Siza's office from 1986 to 1999. At the same time, he established his own practice as an architect.

Xavier is a member of the research teams *Architecture: Theory, Project, History* and *Digital Fabrication Laboratory*. The relationship between architecture and mathematics, especially perspective, is his main research interest.

He is correspondent editor of the *Nexus Network Journal*, **and Council member of the** *European Association for Architectural Education*. Faculty of Architecture, University of Porto, Porto, Portugal

Chapter 1
Synthetic Methods for Constructing Polyhedra

Leonardo Baglioni, Federico Fallavollita, and Riccardo Foschi

Abstract In this paper, we propose an explanation and application of the synthetic method to the representation of the Platonic and Archimedean Solids (PS and AS). The intention is to illustrate the potential of this method in a historical and theoretical context. The study of regular and semiregular polyhedra in this sense is an ideal theme to illustrate the heuristic potential of drawing. Therefore, some synthetic constructions of PS and AS are proposed, defining the constructive algorithms of these figures. The working environment used is the mathematical representation method; for some constructions, parametric and physical simulating tools were used. Particular attention is dedicated to two different synthetic methods: the first, is the construction of the snub cube through paper folding and the second, is a more general method that exploits a physical simulator engine.

Introduction

The synthetic method, as Gino Loria explains in the booklet *I metodi matematici* [1, pp. 77–83], is part of mathematical methods. In particular, we refer to what Loria defines as method of existential construction. He inserts this method among those special to geometry and explains that Euclid never reasoned on a figure whose construction he had not previously taught. In continuation, stating that this serves as a demonstration of the existence of the figures of which the definition was given [1, p. 77]. As an example, he proposes the proof of the existence of the PS through the known Euler formula:

$$F + V - E = 2$$

L. Baglioni
Sapienza University of Rome, Rome, Italy
e-mail: leonardo.baglioni@uniroma1.it

F. Fallavollita (✉) · R. Foschi
University of Bologna, Bologna, Italy
e-mail: federico.fallavollita@unibo.it; riccardo.foschi2@unibo.it

Then he says *n* is the number of sides of each face and *m*, the edges. He declares this:

$$nF = 2E, mV = 2E$$

He deduces and concludes that the only possible regular solids are the tetrahedron, the hexahedron, the octahedron, the icosahedron, and the dodecahedron and that, to prove their arithmetic and geometric existence, it is useful to start from their actual construction.

In these constructions, Loria explains how to build the five PS in space by giving instructions that are nothing more than algorithms that, step by step, allow us to build the solids. This *existential method* for Loria has a mathematical dignity equal to all the other methods illustrated in the essay. In particular, at the beginning of the essay, Loria distinguishes the analytical method from the synthetic one and tries to give a definition to both. According to his own words, if we follow the first (Analysis), the theorem is reduced to be demonstrated or the problem to be solved to another one, that is then judged to be simpler. To the new one, the same procedure is applied and continued until we get to a known or already treated proposition. Following the second one (Synthesis), a series of considerations is established which gradually leads to the desired purpose [1, p. 03].

The synthetic method, therefore, is typical of descriptive geometry, that uses drawing as a research tool for the study of properties and relationships of figures in space. In a more general statement, we can say that a synthetic method uses the construction, representation, and visualization as main instruments to explore geometry.

Today, the synthetic method, thanks to the advent of the digital revolution, has acquired particular importance in the world of geometry. The digital drawing has a higher accuracy than the analogical one and, above all, allows us to draw directly in space. Nevertheless, there is a character of representation that, more than any other, has been enhanced by digital, and that is its constructive aspect. Geometry deals in abstract terms with procedures and methods that can be replicated in reality by means of physical instruments. Construction as a mental process at the base of geometric operations in the plane and in space finds a fertile field of application in the virtual world, greatly enhancing the heuristic power of representation. This makes it possible to review old and new geometry problems that previously were impossible to solve synthetically, according to Migliari [2, p. 28].

Taking inspiration from Loria's considerations, we propose the construction of some PS and AS through the synthetic method and attempt, in this way, to show the experimental potential of drawing. In particular, we focus on the construction of the snub cube and the snub dodecahedron and propose procedures that can be implemented in a parametric modeller and a physical engine.[1] For example, it is possible to construct, through the synthetic method, the snub cube applying the origami properties in Hartl and Kwickert [3].

Another interesting construction, and more general, is the one used to build a snub cube, or a dodecahedron, starting from its net and exploiting the attractive

---

[1] In these experimentations, we used Grasshopper (Version 6 SR19) and Kangaroo 2.

forces of some vertices. In the algorithm proposed through a physical engine in a mathematical environment, it is possible to see, in real time, the envelope of the solid.

The Synthetic Approach for the Constrction of PS and AS

The history of polyhedra shows how, for the study of their properties, their physical construction through models, generally wooden models, allowed their exploration and investigation. If we look at the images attributed to Leonardo Da Vinci which accompany the pages of the treatise by Luca Pacioli, *De Divina Proportione* (1496), we can see how they are a kind of perspective representations. To verify this, it is sufficient to compare two upper and lower faces of one figure, for example, the *Duodecedron Planus Vacuus*, which in reality are parallel to realize how they undergo a perspective foreshortening.

This leads to thinking about the use of a model wooden as a reference and then transported on paper, perhaps by means of one of the many perspective machines that were developing in those years. The physical realization of a regular polyhedron in its full form is as simple as instructive. Take the case of the dodecahedron: from the net of the 12 pentagonal faces, we proceed to their juxtaposition in such a way that the various edges coincide with each other, so that three faces identify a single vertex; the final model is the regular dodecahedron (Fig. 1.1). In this construction, the *existential demonstration method* referred to by Gino Loria, fully manifests itself, namely the verification that the only spatial configuration that can be derived from 12 equal pentagonal faces arranged to define a closed volume, corresponds exclusively to that of the dodecahedron.

In digital representation,[2] particularly in the mathematical one, it is possible to generate the representation of regular polyhedra with the same constructive approach that we have just described. In graphical methods, on the other hand, the remarkable properties of polyhedra, such as the golden ratios established between the lengths of the edges between the various polyhedra, are instrumental to their representation. In a digital environment, starting from the net of three pentagonal faces adjacent to each other, we rotate them in space, so that the vertices are positioned at the point of intersection between the circumferences that describe the movement of the vertices. Once the first solid angle is constructed, we can proceed by radial symmetry to identify the other faces. With this approach, it is possible to construct all the regular

---

[2] By digital representation methods, we mean the set of principles and theories underlying three-dimensional representation software. Among these, we distinguish two different digital representation methods: the mathematical representation method and the polygonal (or numerical) representation method. The first one represents entities in a continuous way by means of parametric mathematical equations (such as, for example, NURBS). The second one approximates shapes by means of polyhedral entities (mesh).
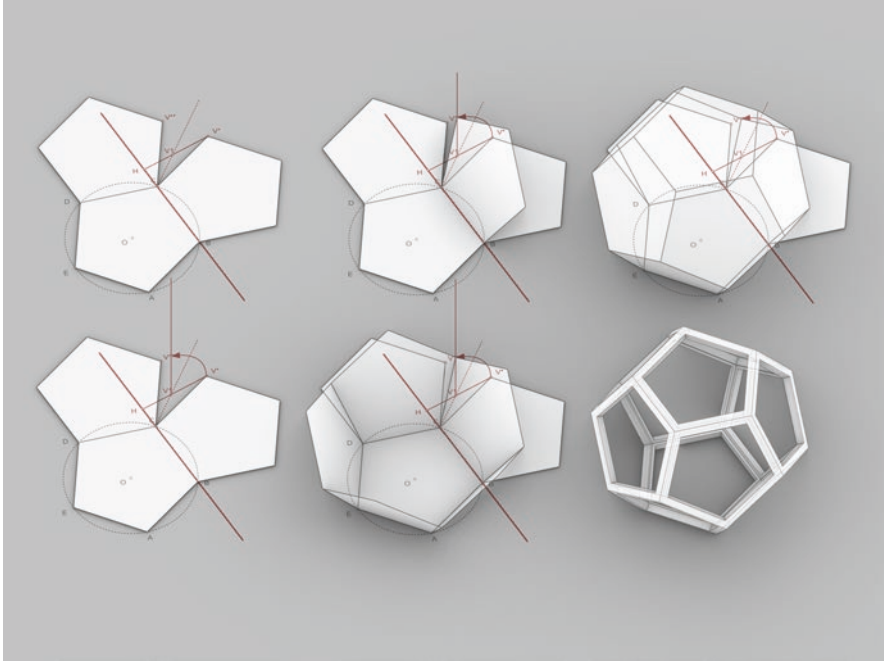
Fig. 1.1 Construction of a dodecahedron in digital representation

polyhedra, verify their remarkable properties,[3] and generate a new net; this can allow us to construct its physical model. Finally, the possibility of implementing the described steps through VPL (visual programming language) software, integrated in a mathematical environment, becomes an excellent tool for communication purposes. Thanks to these applications, it is possible to interact in real time with the described entities, to vary their parameters and dimensions, to describe the vacuous form of the polyhedron, or to explicit the entire construction process for a complete learning of the represented subject (Fig. 1.2).

The semiregular [4] polyhedra[4] are all deducible from operations carried out on the PS. These operations are flat sections that can be traced to three main types:

– planar section of the PS symmetric with respect to the vertices;
– planar section of the PS symmetric with respect to the edges followed by symmetrical sections at their vertices;
– inscribing within the faces of the PS, a polygon having the same number of sides but rotated in the same direction through a certain angle.

---

[3] For example, the characteristic of being circumscribable in a sphere and, at the same time, of circumscribing a sphere, or the property of having equal solid angles.

[4] Semiregular polyhedra are convex polyhedra defined by regular polygons of different types.
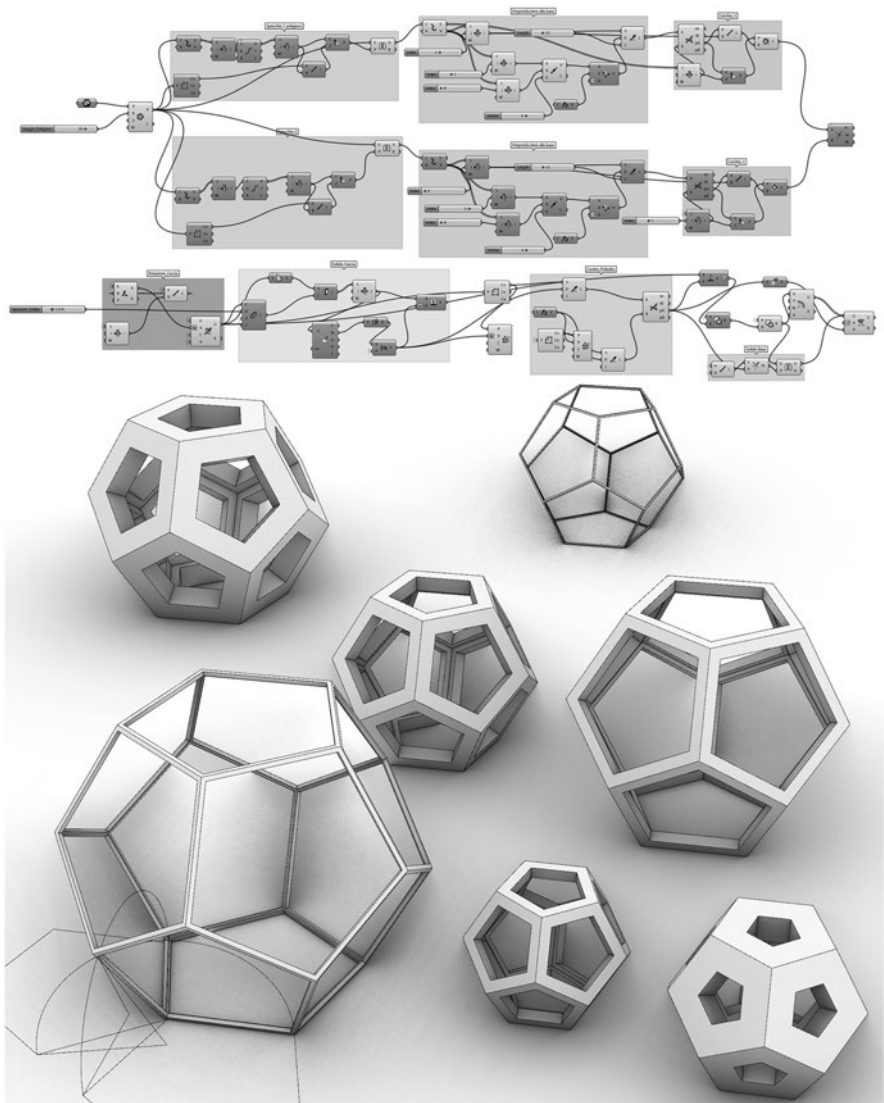
Fig. 1.2 Construction process of the dodecahedron through the synthetic method

Each of these main operations is followed by different variations, as shown in Table 1.1, to define all the 13 semiregular convex polyhedra, and it is interesting to remember that the same operation, carried out on PS dual, leads to the same AS.

The flat sections carried out on the PS are regulated by different types of ratios that define the subdivisions of the edges and can be obtained by graphic

Table 1.1 Geometrical operations to construct Archimedean Solids from Platonic Solids

Operation	Variation	Derivation
1. Planar section of the PS symmetric with respect to the vertices and...	1.1 Passing through the edges centres	Cuboctahedron From Cube and Octahedron
		Icosidodecahedron From Dodecahedron and Icosahedron
	1.2 Passing through the third point of the edges	Truncated Tetrahedron From Tetrahedron
		Truncated Octahedron From Octahedron and Cube
		Truncated Icosahedron From Icosahedron and Dodecahedron
	1.3 So that the central segment of the edge connects twice the number of face sides	Truncated Cube From Cube and Octahedron
		Truncated Dodecahedron From Dodecahedron and Icosahedron
	1.4 Beyond the midpoints of the edges and leading to reversely homothetical or inverted polygons inscribed within the faces	Truncated Tetrahedron From Tetrahedron
		Truncated Octahedron From Octahedron and Cube
		Truncated Cube From Cube and Octahedron
		Truncated Icosahedron From Icosahedron and Dodecahedron
		Truncated Dodecahedron From Dodecahedron and Icosahedron
2. Planar section of the PS symmetric with respect to the edges followed by symmetrical sections at their vertices	2.1 To obtain polygons homothetical with respect to the faces centres inscribed within the faces	Rhombicuboctahedron From Cube and Octahedron
		Rhombicosidodecahedron From Dodecahedron and Icosahedron
	2.2 To obtain polygons having twice the number of sides inscribed within the faces	Truncated Cuboctahedron From Cube and Octahedron
		Truncated Icosidodecahedron From Dodecahedron and Icosahedron
3. Inscribed within the faces of the PS, a polygon having the same number of sides, but rotated in the same direction through a certain angle		Snub Cube From Cube and Octahedron
		Snub Dodecahedron From Dodecahedron and Icosahedron

constructions by means of straightedge and compass[5] (SE&C). For this reason, all the proportions that link the PS and the AS by means of graphic constructions allow us to represent them graphically with an adequate level of accuracy (Fig. 1.3).

Actually, the semiregular snub cube and snub dodecahedron[6] have a geometric genesis that makes their representation impossible without admitting the introduction of obvious approximations. The snub cube is constructed by placing smaller squares on the faces of the cube which are slightly rotated. Then the vertices of these squares are connected such that, in each vertex, there are one square and four triangles. To draw the snub cube, it is possible to adopt the graphic method proposed by Dragomir and Gheroghiu [5, pp. 214–215]. The method consists in dividing the edge of the PS starting from a ratio defined by the equation

$$2\alpha^3 - 4\alpha^2 + 4\alpha - 1 = 0$$

from which the α value is equal to 0.352 ... In digital language, we encounter a problem in the construction of the mathematical model, because of the approximation that the procedure involves. In fact, the value of α cannot be expressed through a graphic construction with SE&C. This leads to an error in the construction of the solid because the tolerance of the program does not recognize the vertices of the solid belonging to the circumscribed sphere. The same problem arises for the construction of the last chiral solid, the snub dodecahedron. In 2002, Weissbach and Martini [6, pp. 121–133] demonstrated analytically that it is not possible to construct the last two chiral solids via SE&C, but it is possible to construct the two polyhedra using the properties of *origami*. The art of paper folding can be used to solve classical construction problems of geometry [7], such as the trisection of an arbitrary angle or doubling the cube, using a few paper folds. We propose a reinterpretation of the demonstration made by Hartl and Kwickert, conducted with analytical language, through a synthetic construction that exploits the properties of paper folding.

Paper folding can be simulated in parametric drawing, by using geometric constraints which control the relationships of objects with respect to each other [8]. In this way, digital synthetic language expresses all its constructional power and introduces a new character of geometry, that is the system of logical relations between entities. The object of the representation is therefore the whole relational-generative process, and no longer the single entity, according to a language that still finds in geometry the main interpretative support. In the case of the snub cube, the aim of the paper folding construction is to find a vertex *A* of the semiregular polyhedron related to the vertex *C* of the cube that envelops it.

---

[5] For example, the rhombicuboctahedron can be generated by dividing the edge of a circumscribed hexahedron into three parts according to the ratio 1: $\sqrt{2}$: 1. The length defined by the irrational value $\sqrt{2}$ is easily identifiable from a graphic construction that makes use of the diagonal of a square of side equal to 1 unit.

[6] These two polyhedra enjoy the chiral property for which the symmetry generates differences.

Truncated Tetrahedron from Tetrahedron   Truncated Tetrahedron from Tetrahedron   Cuboctahedron from Cube

Icosidodecahedron from Dodecahedron   Truncated Octahedron from Octahedron   Rombicosidodecahedron from Dodecahedron

Truncated Icosahedron from Icosahedron   Truncated Cube from Cube   Truncated Cube from Octahedron

Truncated Dodecahedron from Dodecahedron   Rhombicuboctahedron from Cube   Truncated Cuboctahedron from Cube

Truncated Icosidodecahedron from Dodecahedron   Snub Cube from Octahedron   Snub Dodecahedron from Icosahedron

Fig. 1.3 Graphical constructions of Archimedean Solids starting from Platonic Solids

Starting from one square face of the cube, we call the top edge, *g*, and the bottom left, corner *P* (Fig. 1.4 – *origami*).

We divide the edge of the base into four equal parts and call the second point from the left, *Q*. We trace the two vertical lines from the other two points and name the second, *h*. The problem is to find the folding line (i.e. the symmetry axis) so that *P* goes to *P'* in *g* and *Q* goes to *Q'* in *h*. This fold is exactly the sixth axiom of Humiaki Huzita. Those axioms describe what can be constructed using a sequence
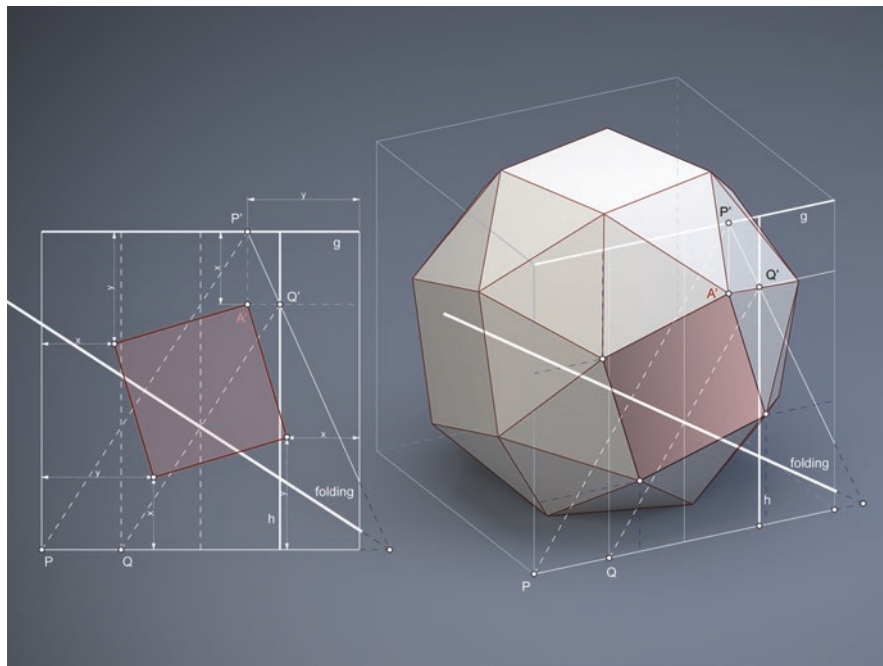
Fig. 1.4 Snub cube construction through paper folding

of creases with at most two point or line alignments at once. This fold allows us to find the points P' and Q', which give the coordinates of the vertex $A1$ of the snub cube.

It is possible to simulate the first fold correctly by inserting constructive constraints in the mathematical modeller. Once point $A1$ has been found, through symmetry, it is possible to find all the missing vertices and edges of the snub cube. This synthetic method allows us to obtain the accurate construction of the chiral AS.

Hartl and Kwickert [3, 9] did not find a similar elegant folding construction for the snub dodecahedron. In the authors' opinion, this issue is traceable to the infinite number of folding constructions, and they found the nicest among them. For this reason, we decided to apply a different approach, proposing a parametrical one based on *Live Physics* engine.

The General Synthetic Method to Construct a Polyhedron

The last synthetic method presented here allows us to construct any regular and semiregular polyhedra from its net. This method, therefore, is the most flexible, and allows us to accurately construct even the snub cube and the snub dodecahedron. The construction principle is very simple and is based on the physical simulation of
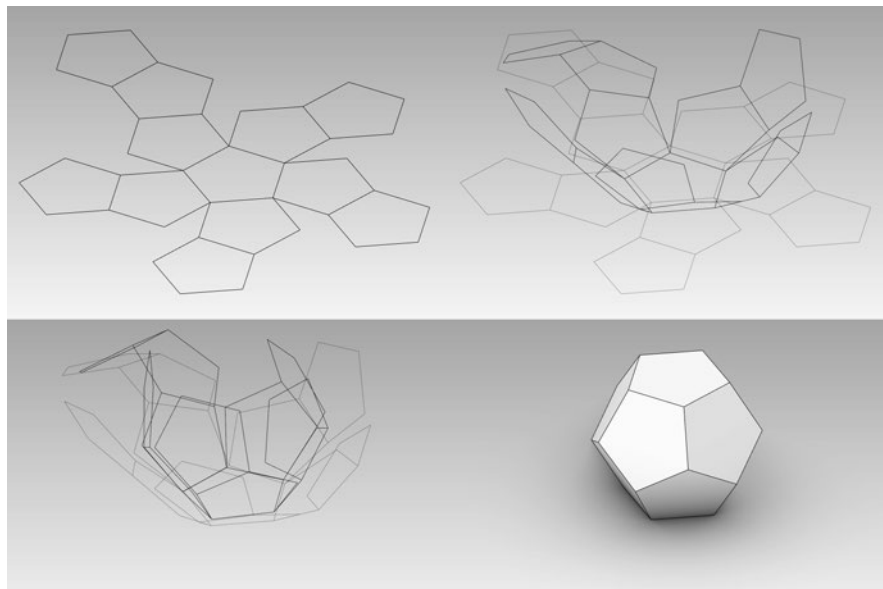
Fig. 1.5 The construction of the snub cube, first algorithm

its solid construction. As Loria explains, if you actually try to build a regular polyhedron in the real world, the easiest thing to do is to draw a possible net and rotate the faces until the free edges touch. In this way, the possible convex final solution is the one sought. It is evident that another final combination of faces is not possible unless the faces are rotated in the opposite direction: some clockwise and the others counterclockwise. In addition, in the latter case, the final result would not be a closed polyhedron. We have developed two procedures. The second one is the more effective and therefore is the final synthetic method that we here propose. The first one worked automatically with polyhedra as the dodecahedron (Fig. 1.5).

For other polyhedra, as the octahedron, you have to manually guide the algorithm to find the right spatial configuration. In fact, the first algorithm can lead to an imploded flat configuration. The reason for this is due to the possible mount/valley movement of the faces. In order to apply this simple method, we have employed a physics engine within a mathematical modelling environment.[7]

The first procedure (Fig. 1.6) consists of these steps:

1. plan a possible net of the regular and semiregular polyhedron to be built (in the figure, it is a dodecahedron);
2. set some constraints. Some vertices must remain fixed in the transformation (in the case studied, we chose the five vertices of the central face); and all the edges must remain the same length;

[7] See note 1.
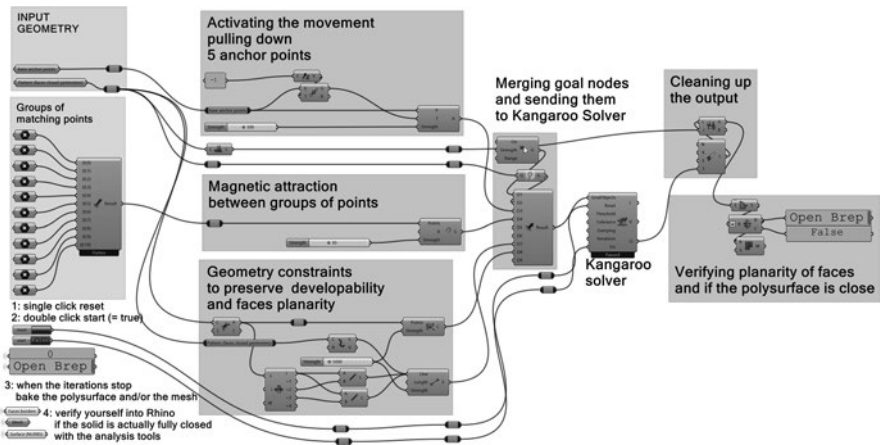
Fig. 1.6 The visualization of the first algorithm for the construction of a polyhedron starting from its net

3. select the pairs of vertices that have to merge in the final configuration; the vertices must be chosen with consistency and, of course, it is not necessary to apply these forces to all the vertices of the figure;
4. start the simulation. If the parameters are correct and well balanced, you will obtain the desired polyhedron.

To start the simulation, it is necessary to apply an initial thrust, otherwise, the vertices will all remain in the same plane. We applied an initial downthrust to the vertices of the central face. In the mathematical virtual space, self-intersections are possible, so there is no danger that inconsistent rotations of the faces will be generated; if this happens, the algorithm just takes more time to reach the result. The delicate issue of this physical algorithm is the balancing of forces and the mount/valley problem. We have noticed that when the individual weights of the forces are not well balanced, the algorithm generates imploded solids and fails to close the figure in an adequate time. In order to overcome this problem, it is necessary to experimentally find the right balance by calibrating the forces involved. Once the right balance is found, the figure begins to form and, in a short time, the solid is obtained (it is also possible to calibrate the time and speed of construction of the figure).

In the case of the dodecahedron, this algorithm gives no problem, because the only final spatial configuration is the platonic solid of 12 faces. In other cases, as the octahedron, sometimes you have to manually guide the algorithm to avoid the mount/valley problem (Fig. 1.7).

The parameters that we can control in the first algorithm are the pairs of vertexes (points) that must meet and the amount of attractive power applied to them.

The first procedure has been improved, in order to solve the mount/valley problem and to transform the algorithm into a complete automatic process. In order to accomplish this task, we added a new force in the process. Therefore, the final
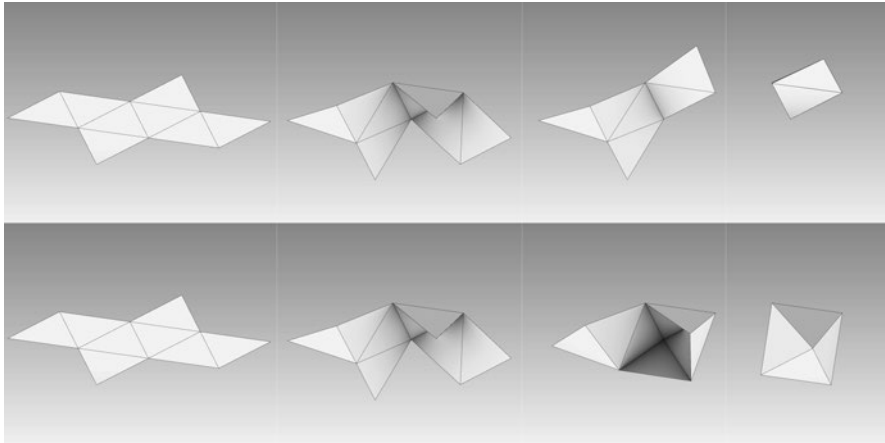
Fig. 1.7 The construction of the octahedron, first algorithm: the problem of the mount/valley
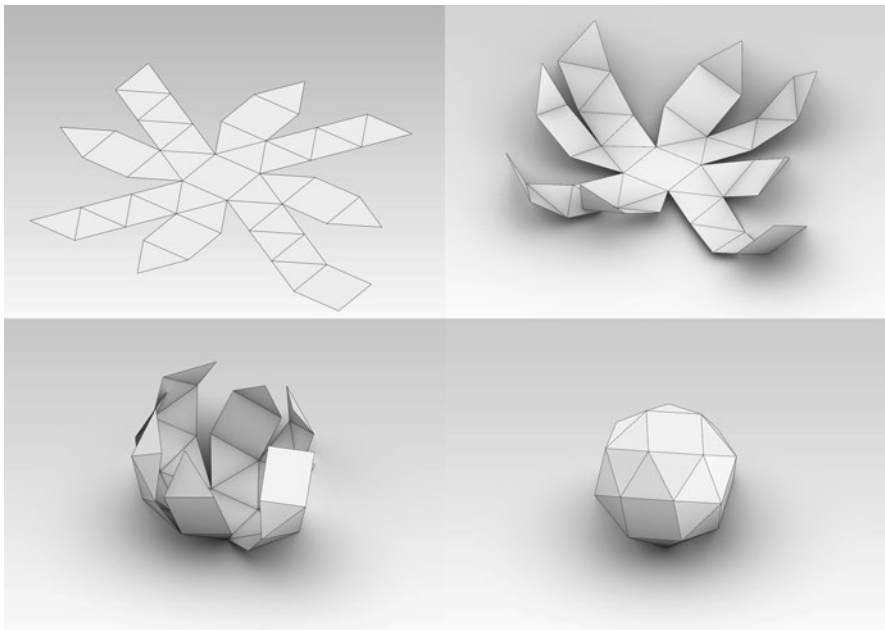
Fig. 1.8 The construction of the snub cube, second algorithm

procedure consists of four principal steps. The new step consists of applying a folding power to all the faces of the flat net. This folding power starts to fold the faces in the same direction in respect to the normal plane (of the net) and their edges. In this way, we can assure the convexity of the final solid and we do not have the mount/valley problem (Fig. 1.8). Once the edges and vertices of the solids are close,

we stop the first power, and we leave only the second power activated: the attraction power of the vertices. Automatically, the faces join and form the final polyhedron. The parameters that we can control on the second algorithm are the folding power and the folding angles between the faces. In the folding power, we can adjust the amount of power and the folding angle to assign. These consent to easily control the movement of the folding in an interactive and experimental way; when you assign a certain angle, all the faces will fold until they reach that angle. Therefore, after some attempts, you can visualize and understand which angle comes closer to the final configuration.

Furthermore, this final procedure is simpler than the first one, because we do not need to assign the attractive power to the pairs of points. This power is assigned to all the vertices within a certain distance range of space. Therefore, only when two points reach this distance range, the power can start its influence in the algorithm. In conclusion, we can summarize the steps of the final procedure

(Fig. 1.9):

1. Plan a possible net of the regular and semiregular polyhedron to be built (in the figures, it is a snub dodecahedron and a snub dodecahedron).
2. Select the edges in respect of the desired folding angle you want to assign.
3. The algorithm consents to select two different folding angles to assign to some edges. Select the amount of power you want to apply to the folding power.
4. You can control the distance range and the amount of power of the attractive power between the vertices.
5. Start the engine. If the algorithm fails to construct the final polyhedron, you just need to change the angles of the folding power or the amount of power.
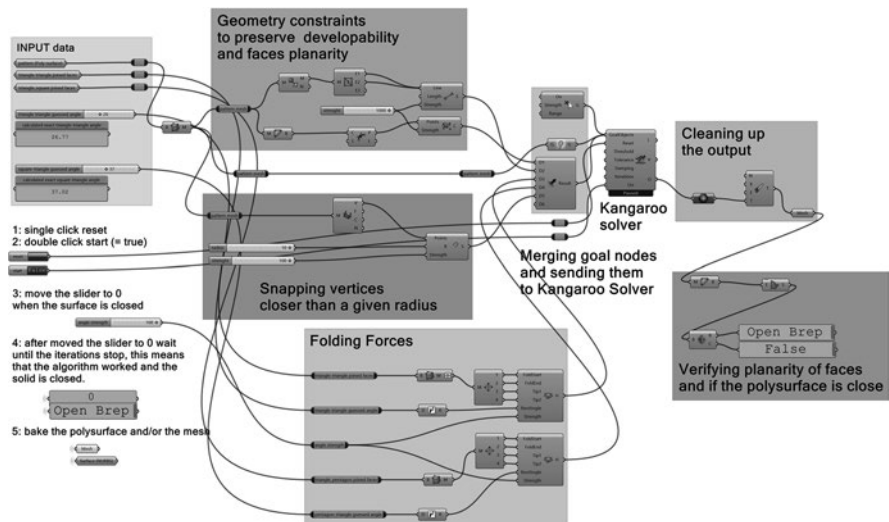
Fig. 1.9 The visualization of the second algorithm for the construction of a polyhedron starting from its net
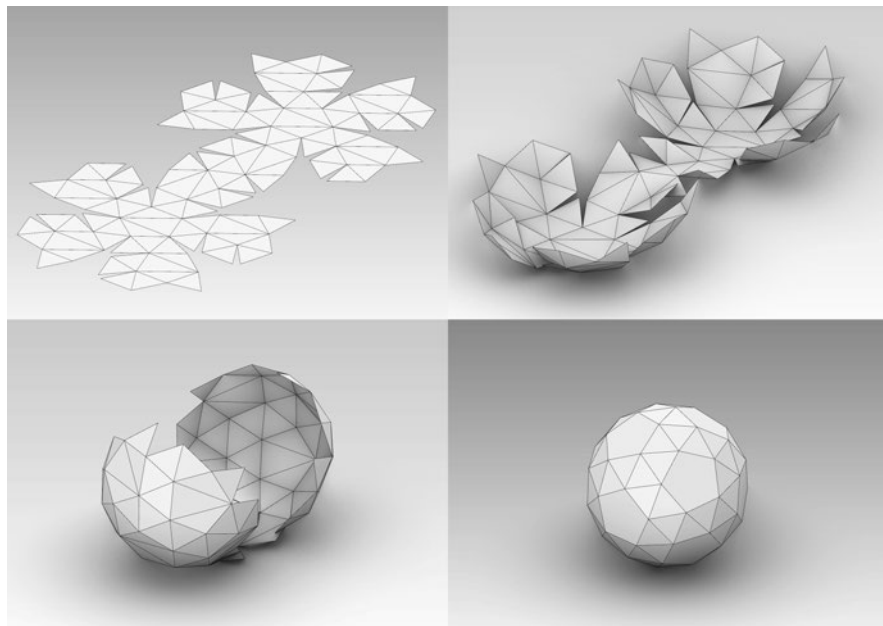
Fig. 1.10 The construction of the snub dodecahedron, second algorithm

it is easy to experimentally reach the right angles to obtain the desired polyhedron. The slider of the folding power can control the speed of the construction process. The bigger this value, the faster the movement will be and vice versa.

In the algorithm, we have included a check that automatically allows us to understand when the figure is correct, i.e. when the solid is perfectly closed. The software is based on the reiteration of the algorithm up to the optimization of the procedure after a certain number of attempts; the limit we have established is the tolerance of the modeller in recognizing a closed solid; therefore, when the program recognizes the presence of a closed polysurface, it stops the process. The method was tested with regular and semiregular polyhedra (Fig. 1.10), but we believe that by well balancing the forces and the attractive weights of the selected vertices, it will be possible to solve the construction of more complex polyhedra as the Catalan polyhedra. In addition, it is possible to verify the correctness of the solid by verifying some properties. For example, all the vertices must lie on the sphere that envelopes the solids, and the edges must be the same length. These properties are always verified at the end of the constructions process. A curious and fascinating thing about this method is that we can visualize the process of the construction in real time. Therefore, this method consents likewise to visualize the movement of the faces from the net to the final polyhedron. We can also calibrate the speed of the movement by adjusting the amount of power of the two forces. Unfortunately, the figures of this paper cannot show these interesting visual properties of the proposed procedure, but they can give you a clue.

Conclusions

In this paper, we are confronted with the representation of regular and semiregular polyhedra. We have seen how the traditional graphic methods allow an accurate representation of the two families of polyhedra, but they must introduce analytical formulas to solve the construction of the snub cube and the snub dodecahedron [9]. In the same way, the classical approach with the mathematical representation does not allow us to construct and synthetically solve the configuration of the two chiral AS.

We have seen how the new forms of parametric digital representation allow us to find alternative solutions to known geometric problems, as the particular case of the construction of the two solid Archimedean chirals: the snub cube and the snub dodecahedron. The representation of these two solids is linked to the impossibility of constructing them by means of a ruler and compass. This particular property can be solved through the use of analytical formulas that allow us to construct a graphical representation, as proposed by Gheorghiu and Dragomir. However, this digital representation presents two different and important problems. The first must be found in the accuracy of the construction that, in today's digital representation, introduces a constructive error; the final configuration, in fact, does not verify the remarkable properties of these polyhedra, such as the possibility to circumscribe the polyhedron with a sphere. The second problem is that the synthetic method, in this way, is not autonomous, because it makes use of a mathematical equation and no longer makes use of an exclusively synthetic language such as drawing.[8]

It is possible to elegantly solve the construction of the snub cube through paper folding, of which we have given a representation through the synthetic method.

This approach, applied to the case of the snub dodecahedron, has limitations, due to the excessive complexity of the method.

Finally, we have presented a synthetic general approach to the construction of all regular and semiregular polyhedra, simulating the constructive genesis using particle systems. In this way, we can solve the two problems mentioned above, by verifying the topological and metric properties of the solids represented, through a completely synthetic and autonomous method.

All the synthetic approaches described are based on a same visual language. These approaches, apparently very different, maintain the same constructive character typical of descriptive geometry: that is, they simulate the operations that could be carried out in reality. For example, the physical simulator allows us to translate

---

[8] Even if the mathematical digital methods are based on analytical equations (see the NURBS), they can still be counted among the synthetic methods, since the control of the forms and their relationships take place through a language of visual nature. The classical studies of Descriptive Geometry were conducted with the help of a ruler and compass, which made it possible to materialize straight lines and circles on paper without necessarily resorting to their equations. In the same way, nowadays, the available tools to scholars have increased, offering much higher accuracy and allowing the representation of relationships between entities and the control of time dimension and movement.

into the digital world the operations that would have been carried out by folding a sheet of paper and gluing the vertices together.

The analogy with the role that physical models had and have in the study and research of form is evident. This role has ancient roots and it is sufficient to recall the case cited of the polyhedra models in the images of Leonardo da Vinci. In this sense, the use of plastic models for investigation and the discovery of shapes in space has a history that unites the world of architecture with that of mathematics. For this, we recall the use of models in the Italian mathematical school12 and the use of architectural models from the Renaissance to the present day [10].

Today, the new forms of the synthetic method make it possible to explain the constructive logic of the entire generative process of the shape (see the visualization of the algorithms presented in this paper). This property has a dual value; on the one hand, it favours learning and, on the other, amplifies the experimental power of representation. Scientific and technological progresses have widened the frontiers of the synthetic method and have found in computer graphics a means of interchange between different scientific disciplines [11]. The digital image has taken on a fundamental role in research. Drawing becomes a tool for research and discovery of the properties and relationships of forms in space, increasing the heuristic capacity of the synthetic method.

References

1. Loria, G. (1935). Metodi Matematici. *Hoepli*.
2. Migliari, R. (2008). Rappresentazione come sperimentazione. *Ikhnos, 1*, 7–28.
3. Hartl, U., & Kwickert, K. (2013). Constructing the Cubus simus and the Dodecaedron simum via paper folding. *Geometriae Dedicata, 166*, 1–14. https://doi.org/10.1007/s10711-012-9781-6
4. Coxeter, H. S. M., Selwyn Longuet-Higgins, M. & Miller, J. C. P. (1954). Uniform Polyhedra. In *Philosophical Transactions of the Royal Society* 246 (pp. 401–450).
5. Gheorghiu, A., & Dragomir, V. (1978). *Geometry of structural forms*. Applied Science Publisher LTD..
6. Weissbach, B., & Martini, H. (2002). On the chiral Archimedean solids. *Contributions to Algebra and Geometry, 43*, 121–133.
7. Hull, T. (2006). *Project origami: Activities for exploring mathematics*. A. K. Peters/ CRC Press.
8. Casale, A., & Valenti, G. M. (2012). *Architettura delle superfici piegate. Le geometrie che muovono gli origami*. Edizioni Kappa.
9. Baglioni, L. (2009). I Poliedri Regolari e Semiregolari con un Approfondimento sulle Cupole Geodetiche. In R. Migliari (Ed.), *Geometria Descrittiva* (Vol. II, pp. 299–422). De Agostini Scuola.
10. Retrieved in December 2019 from http://www.dma.unina.it/~nicla.palladino/catalogo/
11. Emmer, M. (2006). *Visibili armonie. Arte Cinema Teatro e Matematica*. Bollati Boringhieri.

Leonardo Baglioni,   Architect and PhD, is an associate professor for the scientific discipline ICAR/17 at the Sapienza University of Rome, where he teaches in the courses of Drawing and Fundamentals and Applications of Descriptive Geometry in the Faculty of Architecture. His research is mainly focused on descriptive geometry, its history, and its applications, with particular interest in its renewal by means of digital representation methods. In 2006 he was part of the inter-disciplinary research group for the publication of the National Critical Edition of the treatise De prospectiva pingendi by Piero della Francesca promoted by the Piero della Francesca Foundation.

Federico Fallavollita,   Architect, is an associate professor at the Department of Architecture of the Alma Mater University of Bologna. In 2008, he earned a PhD in Sciences of Representation and Survey at the Department of History, Representation and Restoration of Architecture at Sapienza University of Rome with the thesis: The Ruled Surfaces and Developable Surfaces, a Reading through the Virtual Lab. He deals with the issues of representation and survey of architecture. He is a principal coordinator of the ERASMUS + Program – Higher Education Sector – Call 2021 – (KA220_HED) – Project title: Computer-based Visualization of Architectural Cultural Heritage (CoVHer).

Riccardo Foschi is an adjunct professor and research fellow in the field of digital representation at the Department of Architecture of the University of Bologna.
   In 2019, he earned a PhD in the field of Architectural representation with the thesis "Algorithmic Modelling of Folded Surfaces. Analysis and Design of Folded Surfaces in Architecture and Manufacturing." His research interests lie in the fields of applied digital origami, real-time rendering, computational 3D modelling, BBCC survey, and descriptive geometry.

Chapter 2
Scientific Sources and Representations of the Small Stellated Dodecahedra Painted in Genoa

Cristina Càndito and Ilenio Celoria

Abstract The present study investigates the history, significance, and depiction of a polyhedron painted in the *Room of Leda*, as part of the decorative plan of *Palazzo Balbi Senarega* in Genoa, Italy, 1655.

The illusory golden oval vault is the main element in the *Room of Leda*, painted by Valerio Castello, with *quadratura* by Andrea Seghizzi. It integrates various art forms in its painted architectural structure and figurative mythological insertions. In this same room, one can observe six small stellated dodecahedra. Although an earlier representation of this polyhedron may be found in a Venetian mosaic, Johannes Kepler was the first to describe it comprehensively, in 1619.

This study formulates some hypotheses for the meaning of these representations, drawing on scientific and symbolic sources, as well as the objective evidence that the authors observed on site, revealing that the representation of these polyhedra was altered in order to achieve an ideal shape.

The Frescoes of *Palazzo Balbi Senarega*

Palazzo Balbi Senarega is part of the Strada Nuova, a street built by the Genoese aristocracy at the time when the Republic of Genoa was at the peak of its financial and maritime commerce. Grandiose in their decoration and audacious in their illusionism, the cycle of frescoes in *Palazzo Balbi Senarega* is one of the most distinctive examples of Genoese Baroque. *Palazzo Balbi Senarega* has been part of the University of Genoa since 1972 (Fig. 2.1) together with other buildings in Via *Balbi*, listed as a *UNESCO World Heritage Site* in 2006. The building was constructed by Bartolomeo Bianco (1590–1657) from around 1616 for the brothers Giacomo and Pantaleo Balbi. In 1645, it was passed on to Francesco Maria Balbi (1619–1704). Francesco hired Pietro Antonio Corradi (1613 ca. – 1683), who trained at Bianco's workshop, to design new sections of the building, restore the front, and build the

C. Càndito (✉) · I. Celoria
University of Genoa, Genoa, Italy
e-mail: cristina.candito@unige.it; ilenio.celoria@unige.it

Fig. 2.1 *Palazzo Balbi Senarega* (Genoa, Italy): The *Room of Leda* in the second noble floor

garden with its nymphaeum.[1] From 1655, after the renovation, the second noble floor underwent the realisation of its decorative plan.

The subject of this study is the rectangular *Room of Leda* (mt. 5 × 6 × 7 maximum height), which belongs to the original nucleus of the building, and is covered by a cloister vault consisting of four partial cylindrical surfaces, with rounded intersections. The decoration by Valerio Castello (1624–1659), with *quadratura* by Andrea Seghizzi (1613–1684) displays a grandiose painted structure in the vault (Fig. 2.2): a golden oval cupola resting on four sections, each with four ionic columns, standing upon marble pedestals alternated with polylobate cornices.

Above the illusory impost, there are six painted circular windows alternated to six stellated polyhedra. The myth of Leda and Zeus, depicted in the form of a swan, is represented in a portion of sky inscribed in the central oval oculus, so to fully integrate various forms of art in accordance with the Baroque style. The reason behind the representation of a sensual but composed Leda, together with the

---

[1] For the building's history, with reference to the other sources [1].

Fig. 2.2 *Room of Leda*: orthophoto of the vault. The six polyhedra (1–6) and details of the shadows (A-B; Fig. 2.8)

presence of the four deities Venus – Amor, Minerva – Prudence and Wisdom, Diana – Chastity, Mercury – Peace and Fortune [2, p. 277] could be that Barbara Airolo (born in 1624), wife of Francesco Maria Balbi, probably used this room. It is, in fact, connected on the north side with the *Room of Hercules*, which was Francesco's room [2, p. 13].

The Small Stellated Dodecahedron: Scientific and Iconographic History

As we will try to demonstrate in this paper, the polyhedron represented six times in the vault of the *Room of Leda* is a small stellated dodecahedron, which is a geometric figure obtained by extending the faces of a regular dodecahedron until 12 pentagonal pyramids are formed (Fig. 2.3). It is a regular polyhedron with regular identical faces and edges of the same length although not convex. It can be described as a polyhedron composed of 12 stellated pentagonal faces and 12 vertices, which are the vertices of an icosahedron.

As it is known, the first systematic reference to the five regular polyhedra (tetrahedron, hexahedron, octahedron, icosahedron, and dodecahedron) is in the *Timaeus* by Plato (fifth to fourth centuries BC). Many scholars have studied this topic, but only a few showed an interest in the stellated variants of these polyhedra. The present paper does not wish to present a dissertation on the history of stellated polyhedra [3], and only cites those sources with reference to elevated or stellated dodecahedra. Texts on geometry and perspective were analysed in order to find iconographic and scientific traces of this extremely peculiar solid. Among these texts, it is worth remembering the work by Luca Pacioli (1445–1517): *De Divina Proportione* (Venice, 1509), dated 1498 in the inscription of his manuscript. In the section *Libellus in tres partiales tractatus divisus quinque corporum regularium dependentium* (cc. 1–27), Pacioli inserts 60 woodcut illustrations taken from watercolour drawings by Leonardo da Vinci, representing regular solids and their elevated (*puntuto*) and sectioned (*abscissa*) variants, in the solid and frame (*vacuo*) versions [4, 5].

We know of Pacioli's derivation of the elements on regular solids, thanks to the book *Libellus de quinque corporibus regularibus*[2] written by Piero della Francesca (1415/1416–1492), who described the relationships between platonic solids, the sphere, and some architectural elements. Piero used plan and elevation view
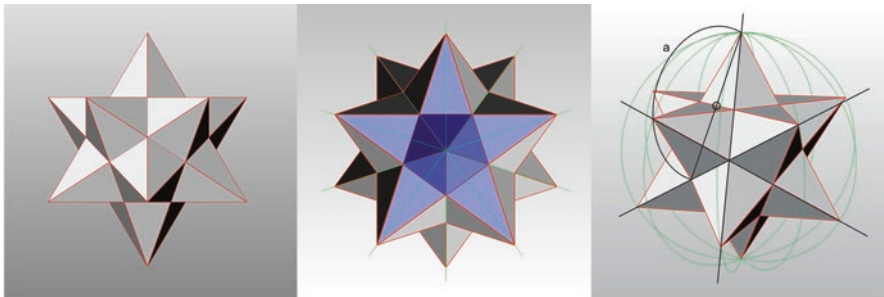
Fig. 2.3 The small stellated dodecahedron: two orthogonal (**a**, **b**) and one perspective view of the virtual model (**c**). Construction via extension of the faces of the regular dodecahedron (arch *a* for the rebatement of the pentagon's height on the apothem of the pyramid). The five-pointed star is highlighted in blue

---

[2] (1478–1482; Biblioteca Apostolica Vaticana, Ms. Cod. Vat. Urb. Lat. 632)

representations and what is today known as Cavalieri's axonometry [[6], p. 342]. Pacioli described an elevated dodecahedron which, unlike the regular solid previously described, is a generic elevated construction where the pyramids show a reduced protrusion (charts XXXI and XXXII) (Fig. 2.4a). Piero and Pacioli influenced artists who came to accomplish remarkable perspectives of regular solids [7], but we did not find, however, trace of something similar to the small stellated dodecahedron.

The interest in regular solids was shared by Albrecht Dürer (1471–1528) who, in the second book of his *Unterweisung der Messung…* (Nurnberg 1525), described regular solids and probably influenced by Pacioli, illustrated elevated polyhedra [3, p. 203]. One of his successors, Wenzel Jamnitzer (1507–1585), expressed an even deeper interest in polyhedra in his work P*erspectiva Corporum Regularium* (Nurnberg 1568), in which many complex solids can be found, but no elevated dodecahedra.

The texts on perspective by Lorenzo Sirigatti, Guidobaldo del Monte, and Piero Accolti discussed platonic polyhedra, but the only author who actually showed an elevated dodecahedron seems to be Daniele Barbaro (1514–1570) in *La pratica della perspettiva* [8, p. 111], even if the pyramids he depicted are much higher than those of the small stellated polyhedron (Fig. 2.4b). Moreover, Barbaro described a method for the perspective drawing of regular solids, and in doing so, it became a source of guidance for those who sought to take on this challenge, which was much more complex than representing parallel projections.

Drawing on previous analyses, it can be confirmed that a comprehensive description of the small stellated dodecahedron was formulated by Johannes Kepler (1571–1630) in his *Harmonices Mundi* [9, 10]. With his work, he wanted to provide a systematic treatise on plane and space tessellations, but developing this study led him also to the description of the small stellated dodecahedron (book II, pl. III) (Fig. 2.4c),[3] although it seems Kepler did not realise that this is, in fact, a regular
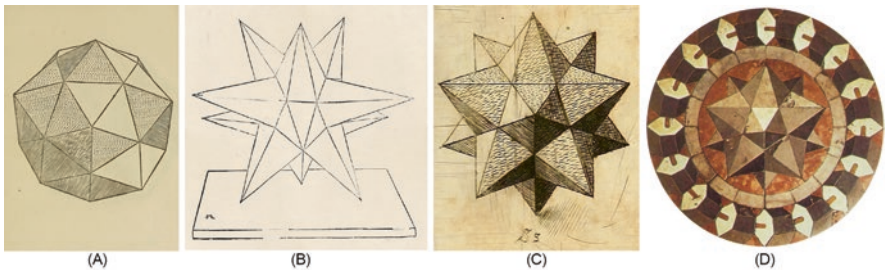
Fig. 2.4 Representations of stellated dodecahedra. (**a**) Luca Pacioli, 1509. (**b**) Daniel. Barbaro, 1569. (**c**) Johannes Kepler, 1619. (**d**) Venetian representation, 1425–1431 (?)

---

[3] Kepler also described the Great Stellated Dodecahedron (12 stellated pentagons, 20 vertices, and 30 edges), while in 1809, Louis Poinsot demonstrated the duality of two other non-convex regular polyhedra: the Great Dodecahedron and the Great Icosahedron.

polyhedron, even if not convex [11, p. 111]. Paolo Uccello (1397–1475), known for his interest in geometry and perspective, might have preceded Kepler on this (Fig. 2.4d), as can be seen in a marble inlay (Venice, Basilica di San Marco, 1425–1431 ?), where the solid is represented in a perfect axonometry, with the exception of the central pyramid, which is slightly shifted to one side.[4]

The Small Stellated Dodecahedron in the *Room of Leda*: Geometric Characteristics and Symbolic Meaning

There was a clear collaboration between Castello e Seghizzi [13, p. 73] in the representations found in the *Room of Leda*, that could explain the numerous revisions made to figures and objects during the project's execution to refine this complex composition.[5] The representation of the geometric elements in the *Room of Leda* can reasonably be attributed to Andrea Seghizzi. However, even though it is not possible to state with certainty that the *quadratura* artist did also conceive and design the decorative scheme, it is still interesting for the purpose of this study to research his training, and the possible sources he might have used. Andrea Seghizzi learned the art of *quadratura* while working in Bologna (Italy) with Girolamo Curti, known as Dentone (1575–1632), Agostino Mitelli (1609–1660), and Angelo Michele Colonna (1604–1687) [14, 15]. Further clues might come from the Jesuit College adjacent to *Palazzo Balbi Senarega*, that was partly paid for by the Balbi family itself. This connection led us to investigate the scientific literature available at the time through maths teachers or texts available in the library of the Jesuit College.

Regarding the people gravitating around the teaching of mathematics in the Genoese Jesuit College, it is useful to note that the Advanced Mathematics Course, started in 1604, was moved, alongside all other courses, to the building expressly built for that purpose in via *Balbi,* between 1636 and 1642. The first mathematics professors were Bernardo Salino (who wrote texts on geometry and was in touch with the friar Christoph Clavio), Francesco Arluno, Nicolò Cabeo (1650), and Giacomo Bonvicino (1651–56) [16, 17].

The manuscript by Bonvicino *Brevis introductio in totam mathematicam* (1654),[6] containing notes on his geometry lessons, is dated as the year before the start of the cycle of frescoes in *Palazzo Balbi Senarega*. In its 160 pages, the text deals with geometric and trigonometric constructions, consequently applied to the measurement of places, astronomy, and mechanics; however, there is no reference

---

[4] In 1986, this representation caught the attention of Lucio Saffaro (1970), who chose it as the symbol for the Venice Biennale [12, p. 123–125]. Moreover, the apparent contour of the drawing highlights the characteristics of this polyhedron as a three-dimensional interpretation of the five-pointed star.

[5] According to Gavazza [2, p. 13] this could prove that a collaborator of Valerio Castello participated in the decoration work.

[6] Ms. VI 6, Biblioteca Universitaria di Genova.

to stellated dodecahedra. It is relevant to observe that the manuscript does not mention regular polyhedra, so one can assume those notes must be missing, because this chapter would have been a standard topic in any course of geometry. The College community was frequented by other mathematicians who were Jesuits, such as Orazio Grassi (1583–1654), rector in Genoa since 1646.

It was useful to consult the original collection of the Jesuit College library in Genoa in order to find what printed texts were actually available at the time. The library of the Jesuits has a complex history, which is interconnected with the transformation of the adjacent church of Saint Gerolamo and Saint Francesco Saverio. The construction work of the church started in 1650, but from 1930 onwards, it was used as a library with the construction of an upstairs reading room and a storehouse below, thanks to the installation of a metal structure which was connected to the original Jesuit library (or room III) [18]. Currently, the church and library complex are closed for restoration, but the fact that the original nucleus is still partially located in the same space, allowed us to identify a series of texts that actually belonged to the original Jesuit storage space. In verifying that these texts were part of the original Jesuit library, the *Catalogue of Gasparo Luigi Olderico* (1785–87),[7] proved to be a useful tool. After the suppression of the Society of Jesus (1773), the administration board designated by the Ligurian Republic appointed the former Jesuit Olderico as librarian and he worked to enlarge the spaces in order to hold the substantial body of material [19, 20].

Following our research, it was evident that during the Jesuit period, no copy of the *Harmonices mundi* by Kepler was available in the library, even though Kepler's famous astronomical tables (T*abulæ Rudolphinæ, quibus astronomicæ scientiæ, temporum longinquitate*, 1627) were carefully stored there.[8] A source for the generically elevated dodecahedron can be found in the text already mentioned in this paper, by Daniele Barbaro[9] [8] in which, as previously observed, one may also find the perspective representation of geometrical solids.

The *Catalogue* by Oderico mentions an encyclopaedic text on mathematics by Mario Bettini (1582–1637), a Jesuit mathematician from Bologna. His text, which is still available today at the library, is the *Aerarium Philosophiae Mathematiicae*[10] [21] printed in 1648. In the third and last tome of the text, it was possible to see a novel representation of a stellated or generically elevated dodecahedron developed as a dodecahedron with pyramids built on each face [21, p. tomo III, Sect. 3, 1-9, Fig. VII] (Fig. 2.5). Its three-dimensional representation is evident in the form shadows of the pyramids constructed on its faces, the height of which, however, is not specified.[11]

---

[7] Bibliothece Universitatis Genuensis Catalogus secundum auctorum Cognomina Ordine Alphabeticus dispositus, 1785-87 (Biblioteca Universitaria di Genova, Atrio Rari Ms. C. 33 1 4).

[8] Biblioteca Universitaria di Genova, 3 B 7 61.

[9] Biblioteca Universitaria di Genova, 3 LL V 43

[10] Biblioteca Universitaria di Genova, 3 X III 63-65

[11] The description by Bettini mentioned the internal pyramids of the dodecahedron. He then referred to another section of his text on the half-diameter of the circumscribed sphere, coinciding with the side of the pyramids, which is different from Kepler's pyramids.
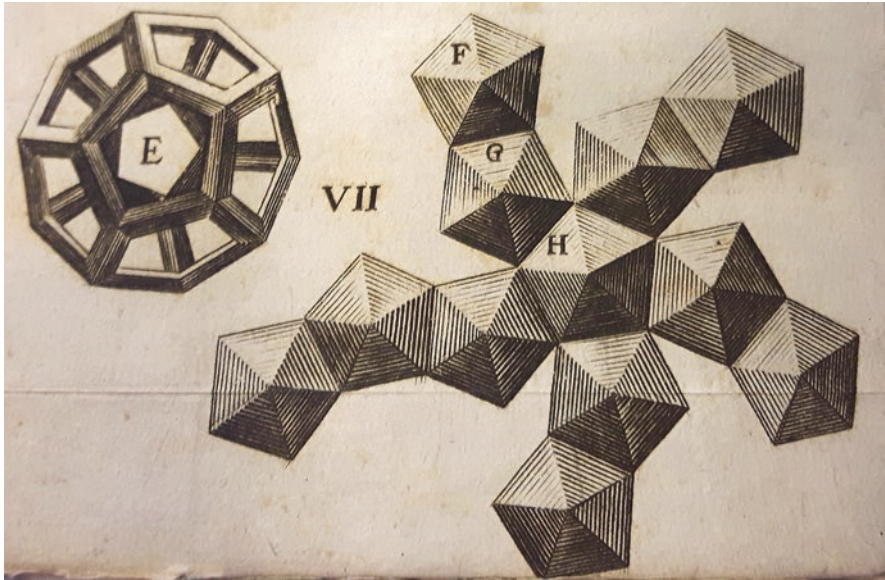
Fig. 2.5 M. Bettini 1648, tome III, Figure VII. 010

Mario Bettini also wrote theatrical pieces, that showed his specific interests in astronomy and mathematics and were performed in Bologna and other European cities. For example, the *Tragicum sylviludium* (performed for the first time in Parma, 1612) contains a description of the planet Venus that draws on classical knowledge, but also on the recent observations of that time by Tycho Brahe (1546–1601) [22], p. 210], with whom Kepler collaborated since 1600. Bettini worked in stagecraft, as demonstrated by the optical illusions (projections and anamorphosis) documented in tome I of his cited text. Seghizzi also worked as an architect for theatres as can be seen by his innovative projects in the Formagliari theatre and the Malvezzi theatre in Bologna, respectively, dating 1641 and 1651 [15, p. 2].

A more specific aspect connecting Bettini and Seghizzi, besides sharing the city of Bologna and the interest for theatre and perspective, is the allegoric representation of the title page of Bettini's book, accomplished by Girolamo Curti [22, p. 236] who, as previously stated, had been the teacher of Seghizzi himself. Although there are a number of possible references, one cannot identify with certainty the source used by Seghizzi but, whatever its origin, the polyhedron in the *Room of Leda* is the regular small stellated dodecahedron, as it was explained, that only Kepler described and illustrated correctly 36 years before the representation of the fresco. Comparing the six polyhedra, oriented in different directions, shows that the images can be superimposed, as it is here illustrated for polyhedra 1 and 2 (Fig. 2.6, at the top), thus confirming that they belong to the same drawing transposed six times to the surface of the vault.
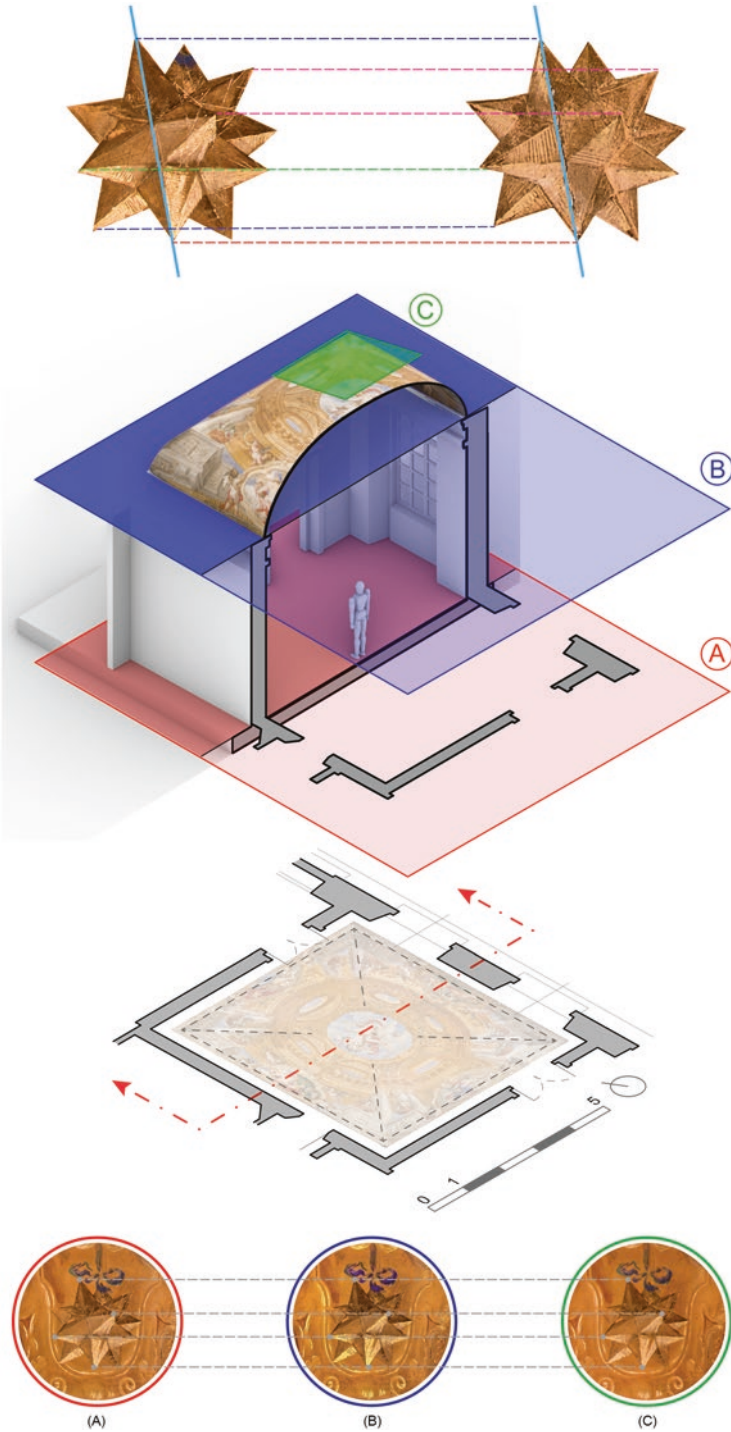
Fig. 2.6 At the top: a comparison of two of the six solids showing the superimposition originated by the same drawing. In the centre: axonometry with identification of the projection plans of the results obtained at the bottom. (**a**) Orthophoto. (**b**) Rectilinear projection. (**c**) Tangent projection

Before analysing the characteristics of the Genoese stellated polyhedra, it is useful to compare the different survey and representation materials that we used for the present research.[12] The high-resolution rectilinear projection of the vault was extrapolated from a nodal panoramic photo, i.e., a perspective projection that is closer to the natural sight of the observer. An orthophoto, a high-resolution orthogonal projection, was obtained thanks to photo-modelling survey. By applying the texture of photo-modelling, we obtained a virtual model, and the projection was drawn through a plane tangent to the vault near to the dodecahedron that was taken into consideration.

As it can be observed by comparing the representations described (Fig. 2.6a–c), once they are all brought back to the same dimension, their differences cannot be perceived, especially because they are positioned close to the centre of the vault, which additionally does not have a steep curvature—for this reason, the representation of the orthophoto was chosen.

The graphic elaboration in Fig. 2.7, a superimposition of the outline of one of the perspective images of the small stellated dodecahedron, highlights certain features of the painted polyhedron. One can see that two of the added pyramids should not be visible in a frontal view (highlighted in green, in Fig. 2.7), but we can also observe the modified position of other pyramids (the most evident of which is depicted in orange in Fig. 2.7). Despite these modifications, it is still possible to recognise the continuity between the lateral faces of the pyramids with the pentagon of the adjoining base (blue line in Fig. 2.7), derived from the construction previously described (Fig. 2.3).

Fig. 2.7 On the left: the stellated dodecahedron in the *Room of Leda*. On the right: its superimposition with a perspective view of the virtual model

The present paper argues that some aspects were wilfully altered to obtain a perspective image that was closer to an ideal shape of the polyhedron; in fact, these distortions cannot be explained solely by the slight curvature of the cylindrical surface onto which they are projected.

Thanks to this geometric construction, it is possible to visualise the five-pointed star and the apparent decagonal contour of the solid. This aspect prompted further research into the possible meaning of the polyhedra represented in the *Room of Leda*. Generally, regular solids are connected with the concept of geometric perfection, as in *Mysterium Cosmographicum* (Tübingen 1596), where Kepler used regular polyhedra as the basis of a fascinating—yet not fully convincing—interpretation on the orbit of planets, associating them to the cosmos and its creation.

In ancient times, the five-pointed star symbolised health and harmony, after Pythagoras identified its golden ratios. This figure is associated particularly with Venus, the symbol of beauty [23, p. II, 427]. As we have seen, Venus was also painted in one of the allegoric representations on the vault; perhaps a homage to the beauty of the future guest of the room, Barbara Airolo.

The reference to Leda, queen of Sparta, and her heroic sons, such as Castor and Pollux, can be seen as a celebration of the family lineage residing in this building. The reference to Barbara as Leda, mother of Helen of Troy, is dubious in any case, because Leda is mostly remembered for her extramarital affair with Zeus, which is the scene represented in Barbara's bedroom.

Many symbolic and mythological interpretations can be put forward; however, there is a clear intention in the representation in association with the polyhedron recently discovered by Kepler. The oval frame could also be a reference to the elliptical orbit of planets, known as the first law of Kepler (*Astronomia Nova*, Prague 1609). The ellipsis, which was common in the seventeenth century, especially in Baroque architecture, can also be explained with the intention of uniformly covering the rectangular surface of the room.

The numeric theme can also be taken into account: why six polyhedra? Is it a reference to the six known planets (including the Earth)? Or the six days of creation? Or simply because six is a perfect number, i.e. equal to the sum of its divisors? In some cases, the number 6 is assimilated to marital love, as it is the product of the first feminine number (2) and the first masculine number (3) [23, p. II, 395]. Moreover, a different projection of the stellated dodecahedron generates an apparent contour coinciding with a six-pointed star (Fig. 2.3).

Considering all previous observations, the only certainty is the strong connection between the arts and science of that period, that surely stimulated the vanity of certain patrons. In the present paper, we hypothesised that Francesco Maria Balbi might have indulged his interests, or those of his wife Barbara Airolo, in new scientific discoveries and, therefore, asked Valerio Castello and Andrea Seghizzi to reach out to local academics, perhaps Jesuits, who could collaborate with them to define a decorative system that made reference to Kepler's geometry, its symbolic meaning or its connection to cosmology.

Maria Barbara Airolo was the daughter of the wealthy Giovanni Tomaso Airolo. She married Francesco Maria Balbi in 1640, but there is no further information

about her, the person that inspired this decorative structure, as usually occurs with women in history. The only form of recognition she received for her artistic inclination came from her father's will (1644), who left her a painting of her choosing from his collection [24].

It is important to remember that, during that time in Genoa, there were other libraries with texts on cosmology and geometry, as demonstrated by an inventory in 1651[13] from the library of a granduncle of Francesco Maria, Gerolamo Balbi (1546–1627).[14] There were many treatises on mathematics, astronomy, and cosmography (Tolomeus, Euclid, Regiomontano, Finè, Gallucci, Brahe, Clavio and Apiano, Gemma Frisius and Magini). Even if it was not possible to trace back the direct source of the stellated polyhedra in the frescoes, Kepler's previous work may well have found its way to several different sources, which eventually brought it to end up on the ceiling of the *Room of Leda*.

Observations on Shadows

Further interesting aspects come to light when analysing the shadows of polyhedra, the importance of which has already been explained by Magnani [13, p. 73]. The first distinct characteristic is the presence of form shadows alone, because cast shadows are observed only in rare cases. The direction of the light that generated these form shadows is compatible with the orientation of the windows, as it can be noted in some sections of the painted vault as, for example, in the pedestal of the painted columns (Fig. 2.8a) or the brackets of the impost cornice (Fig. 2.8b).

Comparing the different polyhedra could end up being quite difficult. In order to observe the shadows on the small stellated polyhedra represented on the fresco of the vault, the single solids were enlarged, and their position and orientation maintained (Fig. 2.9).

Observing the six stellated dodecahedra as a whole, it is clear that the artist considered the two windows in the room as the main source of light but, in some cases, the shadows appear to be generated by the real sources of light as well as the fake openings painted in the vault. Further contradictions prompted us to reflect upon the meaning of these shadows. For example, polyhedron five mainly seems to receive a lateral light with respect to the windows while, in some faces of each polyhedron, shadows and light appear to have been placed at random.

A potential reason for this distribution might be that the painter assigned shadows and light on the basis of a better tonal contrast with the background, with the aim of giving better visibility to the painted shape, taking into account the relative distance of the observer in relation to the dimension of the painted subject.

---

[13] ASG, Notai Antichi, Notaio Calvi Carpenini, 26.8.1649. Per la trascrizione: Montanari 2015

[14] Gerolamo is a son of Nicolò, brother of Pantaleone, father of Giacomo, father of Francesco Maria.

Fig. 2.8 The *Room of Leda*: detail of the shadows on the vault (see Fig. 2.1). (**a**) The pedestal at east. (**b**) The brackets of the opening at north

These polyhedra rarely have cast shadows, as can be observed in dodecahedron 1 (Fig. 2.10c). In fact, the addition of cast shadows to the dodecahedra would have required drawing more projected pyramids, thus generating a superimposition of lines that would have compromised the artist's search for clarity, as demonstrated by the alteration of the perspective image [25]. One particular shadow drawn on polyhedron 4 (circled in red in Fig. 2.9) is somehow difficult to interpret, but it seems to be compatible with the shadow cast by the band holding the solid, which is projected onto its top faces.

If we draw a comparison between the fifteenth century Venetian stellated dodecahedron (Fig. 2.10a), Kepler's dodecahedron (Fig. 2.10b), and those in the *Room of Leda* (Fig. 2.10c), we observe that the form shadows are correctly represented by Kepler, while the other two examples do not attribute the same luminosity to the faces belonging to the same plane. Only in Kepler's polyhedron does each face have uniform shading; it is an ideal representation with one single source of light and without cast shadows. In the Genoese polyhedron, the faces do not have uniform shading, which might reflect the artist' intention of highlighting a clearer contrast with the background. Moreover, shadows could also be influenced by the context in the fresco, in the attempt to simulate the complexity of a real space.

Conclusions

The painted vault in the *Room of Leda* shows various interesting features, such as the first appearance in Genoa of the small stellated dodecahedron, the new geometric element introduced by Kepler in 1619. For this reason, the present study
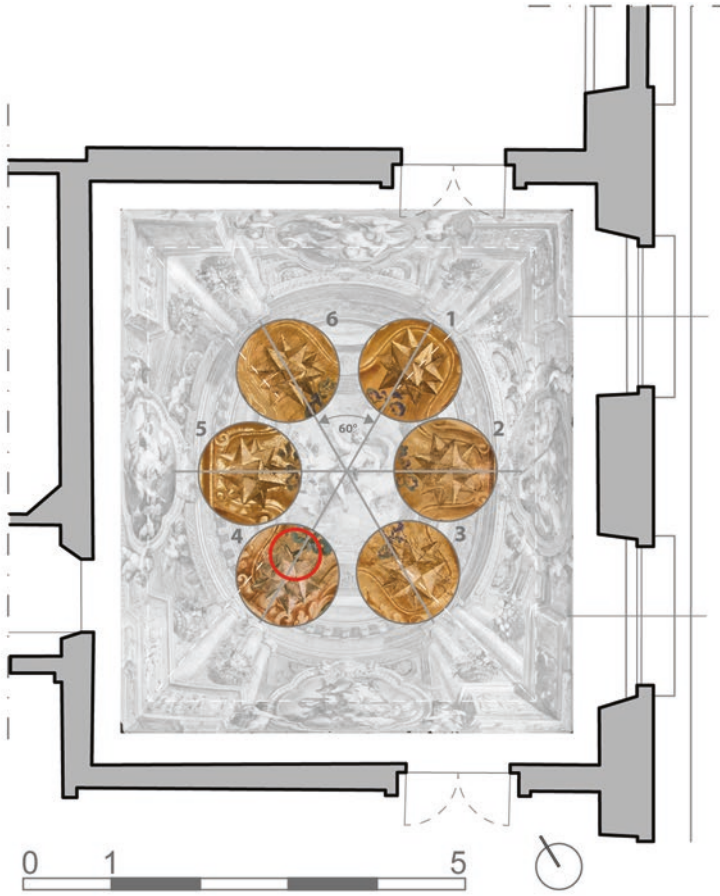
Fig. 2.9 Orthophoto with enlargement of the six polyhedra. Verification of compatibility of the shadows with real and illusory lights. Circled in red a probable cast shadow
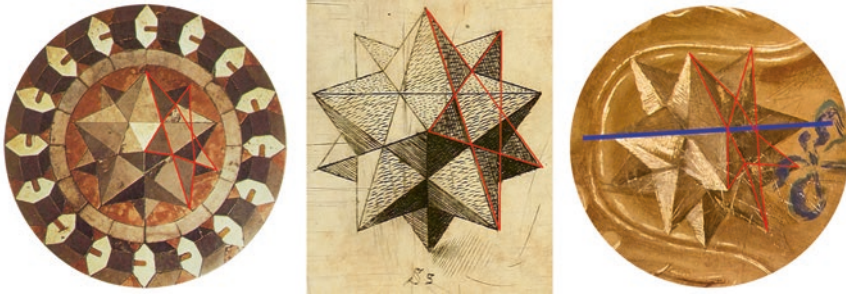
Fig. 2.10 Comparison between three representations of the small stellated dodecahedron. (**a**) Venetian representation. (**b**) Kepler's representation. (**c**) Genoa's representation and analysis of its form shadows

investigated a series of possible iconographic and scientific sources, as well as the symbolic meaning of this polyhedron and its method of representation. It is here hypothesised that the distortions applied to the representation of the geometric solid in the *Room of Leda* were executed in order to come closer to its ideal form and allegorical meaning.

In fact, the perspective layout of the dodecahedron was altered by adding parts that should not be visible in a frontal view and by eliminating cast shadows. This signals the intention to place attention on the five-pointed star that strengthens the allegoric structure of the represented myths, and is a symbol of harmony and beauty, as a possible homage to Barbara Airolo, the future guest of the room.

References

1. Magnani, L., & Rotondi, T. G. (2003). La Sala di Apollo e le Muse nel Palazzo Balbi Senarega. In *Domenico Piola: frammenti di un barocco ricostruito* (pp. 57–69). Genova.
2. Gavazza, E. (1989). *Lo spazio dipinto. Il grande affresco genovese nel Seicento*. Sagep.
3. Brigaglia, A., Palladino, N., & Vaccaro, M. A. (2018). Historical notes on star geometry in mathematics, art and nature. In M. Emmer & M. Abate (Eds.), *Imagine math 6: between culture and mathematics*. Springer. https://doi.org/10.1007/978-3-319-93949-0
4. Dalai, E. M. (1984). Figure rinascimentali dei poliedri platonici. Qualche problema di storia e autografia. In C. Marani (Ed.), *Fra Rinascimento, Manierismo e Realtà* (pp. 7–16). Giunti.
5. Di Teodoro, F. P. (2014). ad vocem Luca Pacioli. In *Dizionario Biografico degli Italiani* (p. 80). Istituto della Enciclopedia italiana.
6. Camerota, F., Di Teodoro, F. P., & Grasselli, L. (2015). *Piero della Francesca. Il disegno tra arte e scienza*. Skira.

7. Hayashi, S. (2009). I Poliedri nelle Tarsie di fra Giovanni da Verona: l'Influenza delle Illustrazioni nel De Divina Proportione (1509) di Luca Pacioli. *Studi Italici, 59*, 97–117.
8. Barbaro, D. (1569). *La pratica della perspettiva*. Borgominieri.
9. Kepler, J. (1619). *Harmonices Mundi*. Linz.
10. Cromwell, P. (1995). Keplers work on polyhedra. *Mathematical Intelligencer, 17*(3), 23–33.
11. Field, J. V. (1979). Kepler's star polyhedra. *Vistas in Astronomy, 23*(2), 109–141.
12. Emmer, M. (2008). Il Mazzocchio da Paolo Uccello a Saffaro. In *Matematica e cultura 2008* (pp. 112–126). Springer.
13. Magnani, L. (2008). Il ciclo di Valerio Castello nel palazzo di Francesco Maria Balbi. In M. Cataldi Gallo, L. Leoncini, C. Manzitti, & D. Sanguineti (Eds.), *Valerio Castello 1624-1659. Genio Moderno* (pp. 65–77). Skira.
14. Pigozzi, M. (2006). Ferdinando Galli Bibiena: le esperienze di Seghizzi e di Troili e la consapevolezza della teoria prospettica dei francesi. In F. Farneti & D. Lenzi (Eds.), *Realtà e illusione nell'architettura dipinta* (pp. 285–294). Alinea.
15. L'Occaso, S. (2018). ad vocem Andrea Seghizzi. In *Dizionario Biografico degli Italiani* (p. 91). Istituto della Enciclopedia italiana.
16. Garibaldi, A. C. (1992). Matematica e matematici gesuiti a Genova tra Sei e Settecento. In *I gesuiti fra impegno religioso e potere politico nella* (Vol. 2, pp. 115–126). Quaderni franzoniani, V.
17. Cosentino, G. (1987). Religione, didattica e cultura nel collegio genovese. In *Il Palazzo dell'Università di Genova. Il Collegio dei Gesuiti nella strada dei Balbi*. Università degli studi di Genova.
18. Scelsi, V. (2017). Fuselli, Labò e la nuova biblioteca di Genova (1926–1935). *Ananke, 81*, 91–96.
19. Càndito, C. (2001). *Occhio, misura e rilievo. Gli strumenti ottici e catottrici per l'architettura e il recupero del Collegio dei Gesuiti a Genova*, Genova; reprint. Alinea 2005.
20. Montanari, G. (2015). *Libri dipinti statue: rapporti e relazioni tra raccolte librarie, collezionismo e produzione artistica a Genova*. GUP.
21. Bettini, M. (1648). *Aerarium Philosophiae Mathematiicae, in quo elementa Philosophiae Geometricae de Planis, Curvis & Solidis figuris*. Ferroni.
22. Aricò, D. (1996). *Scienza, teatro e spiritualità barocca. Il gesuita Mario Bettini*. Cooperativa Libraria Universitaria.
23. Chevalier, J., & Gheerbrant, A. (1989). *Dizionario dei simboli: miti, sogni, costumi, gesti, forme, figure, colori, numeri*. Biblioteca universale Rizzoli.
24. Lercari, A. (2010). *Repertorio di fonti sul Patriziato genovese. Famiglia Airolo*. http://www.sa-liguria.beniculturali.it/images/PDF/patriziato/Airolo.pdf
25. Gombrich, E. H. (1995). *Shadows. The depiction of cast shadows in Western art*. Yale University Press.

Cristina Càndito is an Associate Professor in Drawing and Representation and member of the teaching body of the PhD program at the Architecture and Design Department, University of Genoa. She holds degree in Architecture (1991) and Modern Literature (1998) and a PhD in Drawing and Surveying (1999). She taught at the Polytechnic School of Milan, and she was Architect at the Regional Board - Ministry of Cultural Heritage in Bologna and Genoa.

Her teaching and research activity concerns Drawing, particularly Descriptive Geometry and History of Representation, through applications based on traditional and digital methods, about Architectural Perspectives and cultural accessibility.

Ilenio Celoria following his degree in Architecture at the University of Genoa (2000), he developed his interest in teaching and research in photography. He is currently Contract Professor at the Polytechnic School, University of Genoa, in the course of Photography and Digital Imagine (master's degree in Digital Humanities). His photographic projects have been exposed at the Venice Biennale, the Museum of Natural Sciences in Turin, Mu.Ma, Sant'Agostino Museum and Palazzo Ducale in Genoa, in the Instituto Italiano di Cultura in Cologne, Vienna e Prague and in other Italian and foreign cities.

Chapter 3
Polyhedral Transformation Based on Confocal Quadratic Surface Properties. Graphical Speculations

Andrés Martín-Pastor (ORCID)

Abstract Several procedures are presented that allow us to discretize a rotational quadratic surface in a simple way while fulfilling various geometric conditions. The transformations made are derived from a series of lines of graphical reasoning based on certain properties of rotational quadratic surfaces. The graphic procedures employed are analysed together with the results produced, upon which a discussion is opened regarding the relationship between these graphic procedures with the stereographic projection and 3D homology. The contribution of the article resides, not in the field of mathematical discretization, but in the presentation of graphical reasoning in order to facilitate the comprehension of the properties of rotational quadratic surfaces and their possible use in the design of polyhedral surfaces.

Introduction

We want to evince the representation of polyhedra in the history of Descriptive Geometry as pieces that, beyond being merely symbolic, enable certain complex spatial transformations to be graphically understood. The relationship of polyhedra with perspective (the first codified system of representation) has known extraordinary examples in History: Daniele Barbaro, Vignola-Danti, Lorenzo Sirigati, Jean François Niceron, Jean Dubreil, Albrecht Dürer, and Wentzel Jamnitzer, among many other geometers. The formulae initiated by Luca Paccioli and Barbaro trigger an analysis of the internal geometry of polyhedra, which substantially conditions their form of representation. Each polyhedron must therefore be known a priori in order to be represented on the basis of its internal relations. The proposed strategy always links the polyhedron with the space to be represented because, once the internal structure of the polyhedron is known, we can ascertain how space is transformed [1].

A. Martín-Pastor (✉)
Department of Graphic Engineering, ETSIE, IUACC, Universidad de Sevilla, Sevilla, Spain
e-mail: archiamp@us.es

Several centuries after the codification of perspective science, the first geometers who strove to accurately graph four-dimensional geometries were faced with new challenges: on the one hand, they had to represent invisible objects while, on the other hand, they had to define a new form of representation that was yet to be codified.[1] In these first attempts, tetra-dimensional polyhedra played a decisive role which still is in existence today [3].

Following this inherited tradition, we have also relied on polyhedra to explore the properties of a transformation arising from certain properties of rotational quadratic surfaces presented in a recent article [4].

Generalization of One Property of the Archimedes Paraboloid

Archimedes (287–212 B.C.), in his work *On Conoids and Spheroids*, Proposition XII [5], is the first to comment on the relationship between a section of the rotational paraboloid and its projection (Fig. 3.1a). This relationship is interpreted by Professor Gentil-Baldrich as follows: any section of a rotational paraboloid is orthogonally projected onto the plane perpendicular to the axis as a circumference [6, p. 26].[2]
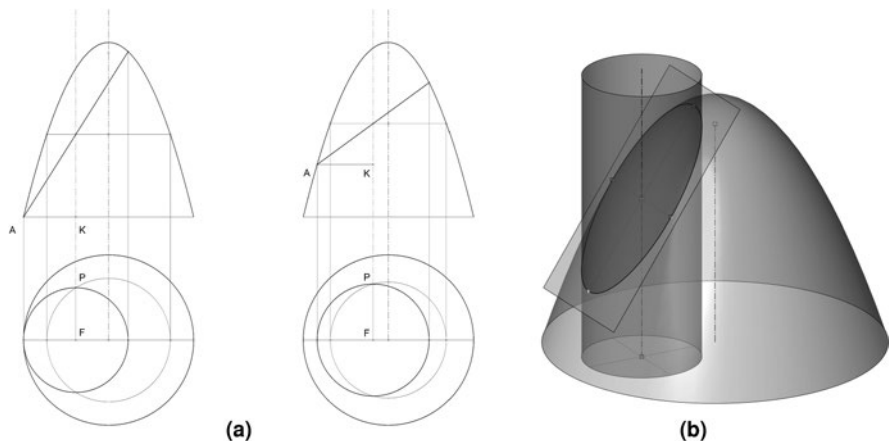
Fig. 3.1 (**a**) Proposition XII by Archimedes. (**b**) Three-dimensional extrapolation. Any right rotational cylinder, with its axis parallel to the axis of the paraboloid, produces a planar curve (ellipse) at its intersection with the paraboloid

---

[1] Llorens-Herrero, in [2], managed to systematize the tetra-dimensional Euclidean space by means of a complete Graphic System. His method consists of extrapolating the reasoning of Monge's Dihedral system to the fourth dimension.

[2] Translated by the author from "*toda sección elíptica de un paraboloide de revolución se proyecta ortogonalmente sobre el plano perpendicular a los ejes como una circunferencia*" [6, p. 26].

If this property announced by Archimedes is approached as a relationship between the paraboloid and the rotational cylinder, then the problem can be appreciated as a particular case of rotational quadratic intersections; any rotational cylinder, with its axis parallel to the axis of the paraboloid, produces a planar curve (ellipse) at its intersection with the paraboloid[3] (Fig. 3.1b).

Through purely graphic reasoning and with the help of digital graphic tools, this property between cylinders and paraboloids can be generalized to all rotational quadratic surfaces (Fig. 3.2) and summarized in

> If two rotational quadratic surfaces share the position of one of their foci at the same point, then the intersection curves between the two surfaces are always planar. [4, p. 194]

The oblate ellipsoid and one-sheeted hyperboloid are excluded from this definition.
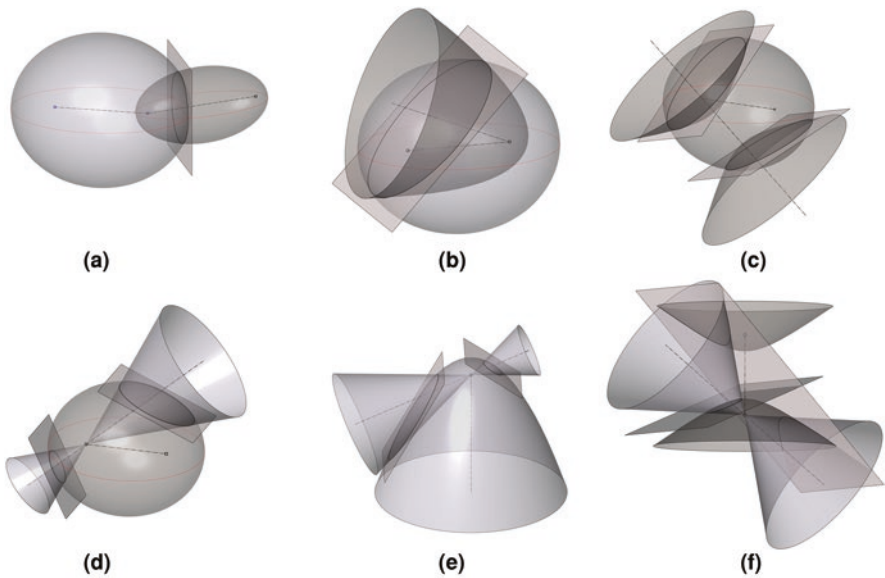
Fig. 3.2 Planar intersection of rotational quadratic surfaces that share the position of one of their foci at the same point

---

[3] The use of this property offers interesting solutions to discretize parabolic surfaces. Narvaez-Rodriguez [7] applies the Archimedes property for the discretization of rotational paraboloids using lightweight conical components.

This property, regarding confocal quadrics, was expounded by Poncelet [8] in the context of the formulation of projective geometry in the nineteenth century, in which many other authors participated.[4]

Although the property is open to many other applications, in this paper we explore its capacity to project a net of cyclic polygons onto a rotational quadratic surface, in order to preserve their planarity after the transformation.

Area of Application, Objectives, and Methodology

In this study, various graphic procedures related to the aforementioned property are shown, aimed at converting rotational quadratic surfaces into polyhedral surfaces, thanks to which polyhedra can be converted into more complex polyhedra.

In a first attempt to define the scope of this investigation, our study has been limited to polyhedra inscribed in rotational quadratic surfaces, that is, in which all vertices belong to the surface that defines the latter. The resulting polyhedron, or polyhedral network, can be understood as a discretized surface shape, now composed of flat polygons. The graphic procedure itself, shown below, rules out other discretization solutions, such as those produced by panelling tangential to the surface or other more complex solutions. However, it should be emphasized that this text is not intended to contribute with anything new to the theory of surface discretization as a general mathematical problem, nor to its practical application in the field of panelling.

As a mathematical problem, the discretization of quadratic surfaces, especially ellipsoids, constitutes a well-known topic in the field of surface discretization. Numerous methods of panelling have been studied for quadratic surfaces. We should

---

[4] In addition to the text published in [4], we consider the following references, that have been translated by us:

Chasles's *Aperçu Historique* [9] shows us two properties related to the subject of study: 324. Two surfaces of the second degree of revolution which have a common focus are homological and their centre of homology is this focus [9, p. 786]; and 361. The cone, which has a focal point of a surface of revolution for its vertex and a plane section of the surface for its base, is of revolution [9, p. 804].

The second edition of Poncelet's *Traité des Propriétés Projectives* [8] states that, as the subject in question (confocals) had, in his time, been the object of investigation by various geometers, he concluded it to be in accordance with his manuscript deposited in 1824 at the *Académie des Sciences*. Poncelet further clarifies his authorship in the discovery of these properties, when he refers that, when he read about this Memoir in the session of April 12, 1824, he concluded he had developed and highlighted several of the general applications, and, in particular, the angular and descriptive properties relating to lines and second-order surfaces that he called homofocal or confocal because they have a common focus [8:120]. Furthermore, the main property, to which we have alluded, is by him stated this way: any system of confocal second-order surfaces, which can also include spheres that have the common focus as their centre, intersect two-by-two in conical sections [8, p. 121].

It is important to stress out that Poncelet did not think highly of Chasles, whom he constantly accused of maliciously omitting work of other geometers. Regarding the study of confocals, Poncelet quotes other authors such as M. Quetelet, M. Ch. Dupin, and Bobillier [8, p. 419].

bear in mind Monge's ellipsoid, mentioned by Hachette in 1822 [10], regarding the lines of principal curvature and their relation to current panelling methods, a subject that was also studied by Jimenez and Pottmann [11]. There are many theses and research papers on surface panelling, and various panelling methods proposed are indirectly related to the present study [12, 13].

From Plane to Space. Graphic Methods

We will apply the generalized property in accordance with the following reasoning:

– The first step consists of making a parallel projection of a circumference on a rotational paraboloid in the direction of its axis. According to the property presented by Archimedes, the circumference is always projected on the paraboloid as an ellipse. Therefore, any polygon inscribed within the original circumference is contained in the plane of the ellipse after the transformation. It should be borne in mind that all the ellipses contained in the paraboloid are also contained in cones of revolution whose vertex is in the focus of the paraboloid (Fig. 3.3a).
– The second step consists of placing a rotational quadratic surface (for example, an ellipsoid) in such location that it shares one of their two foci with the paraboloid.
– The third step consists of projecting conically, from the common focus, the polygon contained in the paraboloid on the ellipsoid. According to the property, the intersection of the projecting cone (quadric) and the ellipsoid (quadric) is also a planar curve since the focus of the cone (the vertex) shares its location with the focus of the ellipsoid.

As a result of the transformation, the polygon inscribed in the initial circumference has been transformed into a plane polygon whose vertices belong to the ellipsoid (Fig. 3.3b).

(a)   (b)
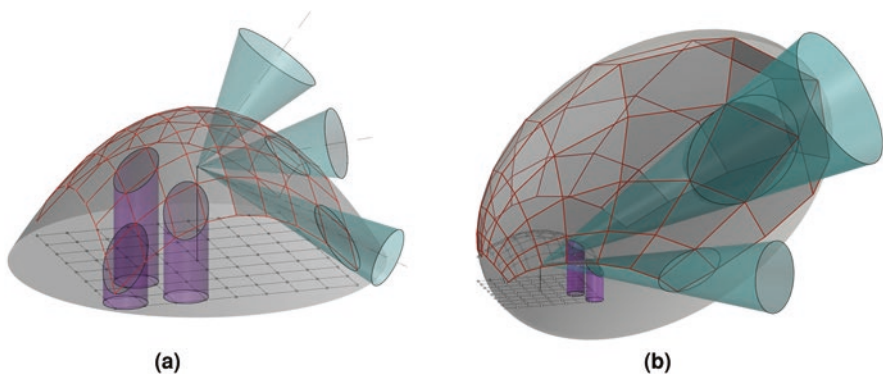
Fig. 3.3 (**a**) Parallel projection of polygons (inscribed in circumferences) on a rotational paraboloid. (**b**) Conical projection of the polygons contained in the paraboloid on the ellipsoid

This graphic reasoning, which works from the plane to the space, can be used to produce not only the transformation of one polygon, but also a network of polygons. Through this graphic reasoning, we produce a discretization in planar surfaces based on highly complex polygonal patterns, which include networks of squares, hexagons, octagons, dodecagons, etc.

The Method of the Flat Polygonal Patterns

The condition set forth by Archimedes (Fig. 3.3) requires that the first polygon must be inscribed in a circumference. Regular polygons meet this condition and their main combination in networks or patterns has also been ascertained. We have applied the procedure to the 25 patterns in order to completely fill the plane with regular polygons, so that they always share their edges (Fig. 3.4a, b). The best known are the eleven Archimedean patterns studied by Kepler (1619) that include the three regular patterns (triangles, squares, and hexagons) [14]. The remaining 14 patterns are part of the demi-regular group [15], and derive from the 2-uniform tessellations, which are a generalization of the k-uniform tessellations in their most abstract term, with infinite combinations studied by Grünbaum and Shephard [16, p. 65].

The case of the pattern based on regular pentagons, which Kepler also studied, is of major interest and is often present in Hispano-Muslim art. Kepler's proposal, studied by researchers such as E. Bindel [17], partially solves the problem of filling in the plane with a pentagonal network. The pattern includes equilateral polygons as the result of the inability to fill the plane, in its entirety, with regular pentagons. As can be observed in Fig. 3.4c, this pattern can also be successfully applied. This takes us to the irregular patterns formed, not only by regular polygons or fragments thereof, but directly by irregular polygons (Fig. 3.5a).

According to the above, the selected patterns are not the only ones that can be applied. In fact, we could panelise any rotational quadratic surface with any kind of polygon, regular or irregular, as long as the following generic condition is verified: *all the polygons of the mesh must be circumscribed and share the edges from vertex to vertex*. This ensures that all the vertices of the panelling are contained within the quadric surface and that the panelling is flat (Fig. 3.5b).

The Method of the Circumference Mesh

The general problem of projecting from the plane to space can also be developed, not from polygons, but from circles. By applying the same transformation, circles are transformed into flat ellipses in space and the planes that contain these ellipses are cut perimetrically by adjacent planes. Therefore, the function of these
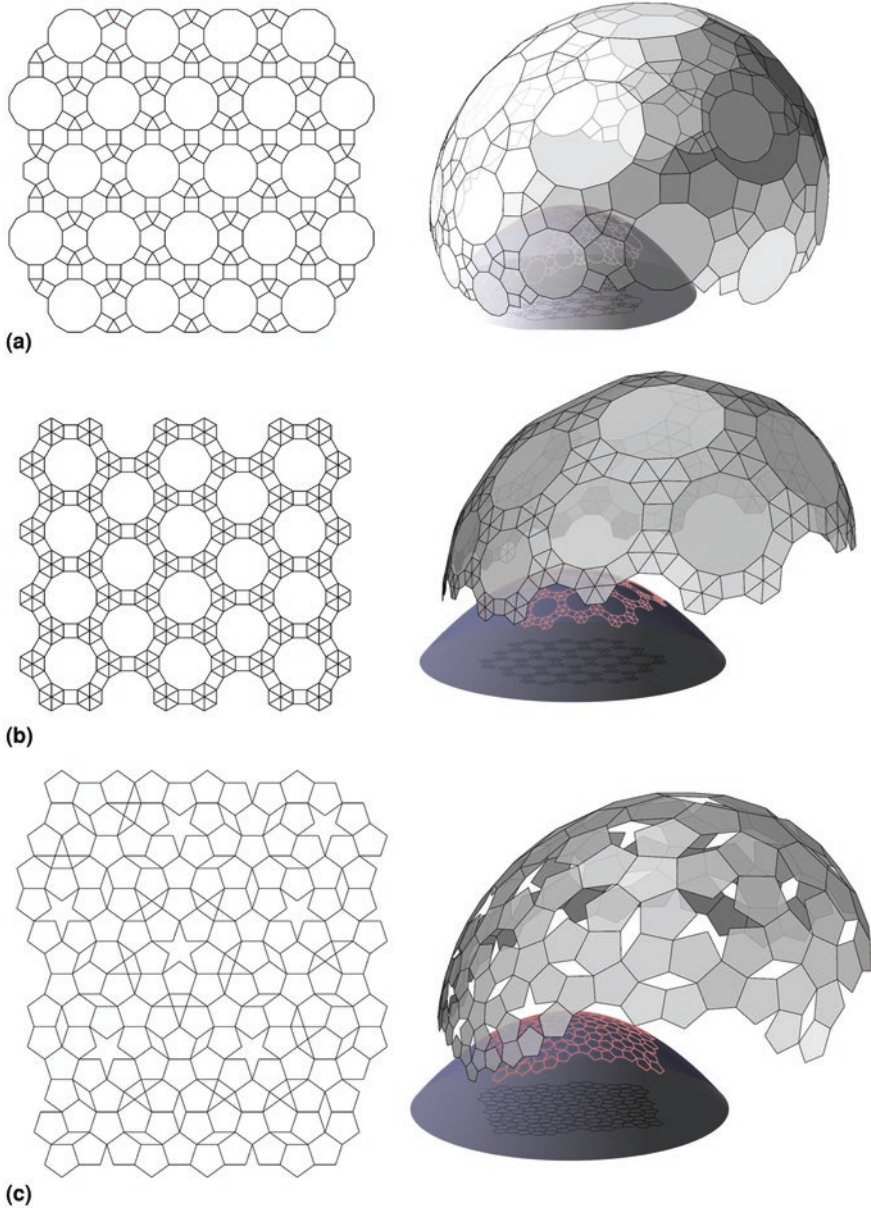
Fig. 3.4 (**a**) Pattern made by regular polygons of 3, 4, 6, and 12 edges. (**b**) Pattern made by regular polygons of 3, 4, and 12 edges. (**c**) Pattern based on regular pentagons

circumferences, which are transformed into ellipses, is to define each of the different planes in space, rather than place the vertices exactly on the surface of the paraboloid.
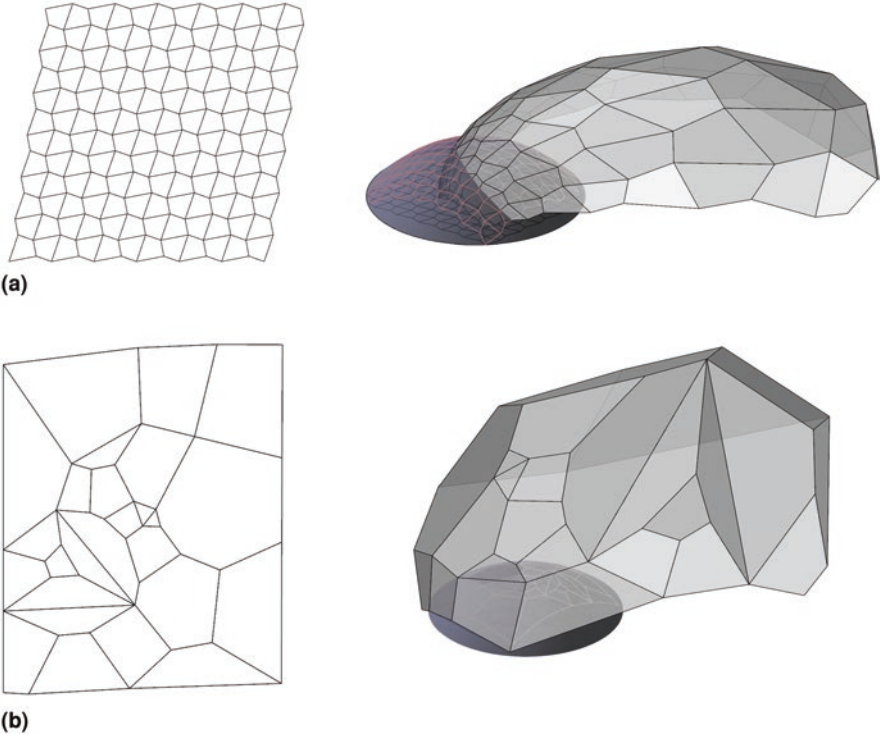
Fig. 3.5 (**a**) Pattern formed by the combination of a single irregular polygon. (**b**) Mesh formed by irregular polygons inscribed in circumferences

Circles can be tangent, secant, or even not touching each other, but each circle, when projected into space, defines a different plane in space that always intersects adjacent planes. Consequently, it can be concluded that, in the case of the paraboloid, *any random set of circumferences in the plane achieves a possible discretization of the quadratic surface.*

This problem can be analysed geometrically in depth in connection to the radical axis and the radical centre of the circumference [18]. Thanks to these concepts, we can ascertain, from the initial plane (Fig. 3.6a) to the subsequent polygonal network of the final spatial discretization (Fig. 3.6b). The radical axis defines the intersection of the planes defined by two circles, while the radical centre defines the intersection of three adjacent planes, or the vertex of the trihedron (Fig. 3.6c).

Each circumference has an associated polygon whose vertices can be located in any of three different situations: inside the circle, outside the circle, or (singularly) in the circle itself. In the first two cases, the vertices are not contained in the surface, but remain either inside the volume of the quadric (vertex inside the circle) or outside the said quadric (vertex outside the circle). Only when the vertices of the polygons are contained in the original circumference, are all of them located on the surface itself, as occurs in the method of the flat polygonal pattern. If all the
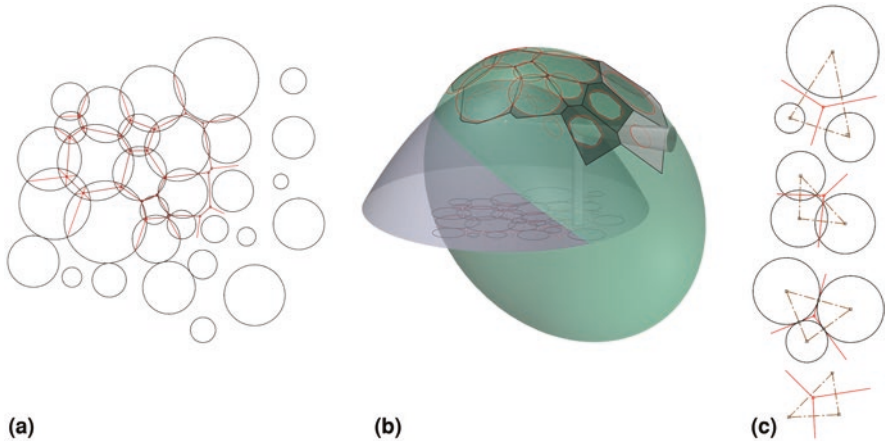
Fig. 3.6 (**a**) Random set of circumferences in the plane. (**b**) Final spatial discretization. (**c**) Radical axis and radical centre

circumferences are point circles (of zero radius), then each plane of the panelling is tangent to the quadric at those points.[5]

Therefore, for all the vertices to be contained exactly on the surface, it would be necessary to impose the previous condition that all the vertices are inscribed in a circle. A particular case of imposing this condition is to study the different ways of compacting circles tangent to each other within a closed contour: a problem studied by Stephenson [19]. Especially applicable is the case of compacting groups of three or four tangent circles.[6]

Discussion. Beyond the Stereographic Projection

If, within a certain perspective, the aforementioned methods are considered, it can be stated that we have developed a transformation that converts circumferences contained in a plane into conics (ellipses) contained in a quadric. The quadric surface could be interpreted as the initial plane that has been curved and closed at a point which represents infinity. This has a huge resemblance to stereographic projection. Spherical stereographic projection produces equivalences between circles in a plane and planar sections of a sphere. In fact, stereographic projection has traditionally

---

[5] Discretization through tangent planes is another type of discretization that has been omitted from this study. However, it is interesting to note that, in this case, the closed contour of the radical axes of the point circles would correspond to the cells of Voronoi algorithm.

[6] In a group of four circles, where each circle is tangent to two others, one circle exists that passes through the four points of tangency.

been employed to project the lines of a celestial vault, onto maps and astrolabes, as exact circles.

Interestingly enough, if the transformation based on the method of the flat polygonal patterns is applied to a sphere, then identical results are found to those produced by spherical stereographic projection. We also arrive at the same equivalence when comparing the results with stereographic projections of the same patterns made from the umbilical points of rotational quadratic surfaces (Fig. 3.7a, b).

On carrying out a more critical analysis, we observed that the procedure presented contemplates a field of solutions larger than classic stereographic projection (Fig. 3.7c). Limitations of stereography are due to the strict orientation of the pattern plane with respect to the projection centre. In stereographic projection, the centre must be an umbilical point of the surface, and the plane must be parallel to
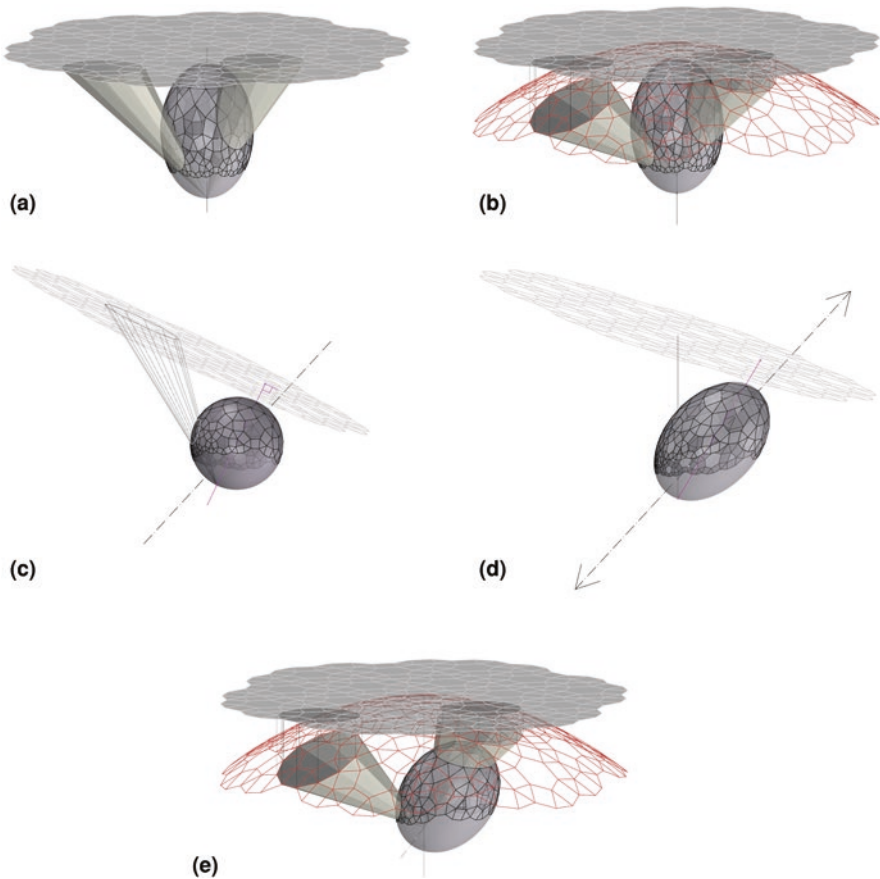
Fig. 3.7 (**a**) Stereographic projections from an umbilical point of the ellipsoid. (**b**) Transformation based on the method of the flat polygonal patterns. (**c**) Stereographic projection on a sphere. (**d**) Affine transformation of Fig. 3.7c. (**e**) Transformation based on the method of the flat polygonal patterns as a combination of stereographic and affine transformation

the tangent plane in this point. The transformation supported by the generalized property (Fig. 3.7e) allows to disorient the plane with respect to the umbilical point. It can be understood as the combination of stereographic projection on a sphere (Fig. 3.7c) and affine transformation (Fig. 3.7d).

From Spheres to Other Quadrics. Projecting by Cones

According to the described generalized property, any cone of revolution whose vertex is located in the focus of a rotational quadratic surface cuts this surface in accordance with a planar curve. Therefore, any family of revolution cones, whose vertex is located in the centre of any uniform polyhedron, can project the vertices of the original polyhedron onto another rotational quadratic surfaces such as ellipsoids (Fig. 3.8a), paraboloids, and hyperboloids (Fig. 3.8b). The transformation maintains the flatness of the faces of the final projected polyhedron, which is thus inscribed in the second quadratic surface.

In general, this property is fulfilled for irregular polyhedra whose vertices are all situated on the surface of a sphere, on the condition that the vertex of the projected cone is located in the centre of the sphere and in the focus of the rotational quadratic surface (Fig. 3.8c).
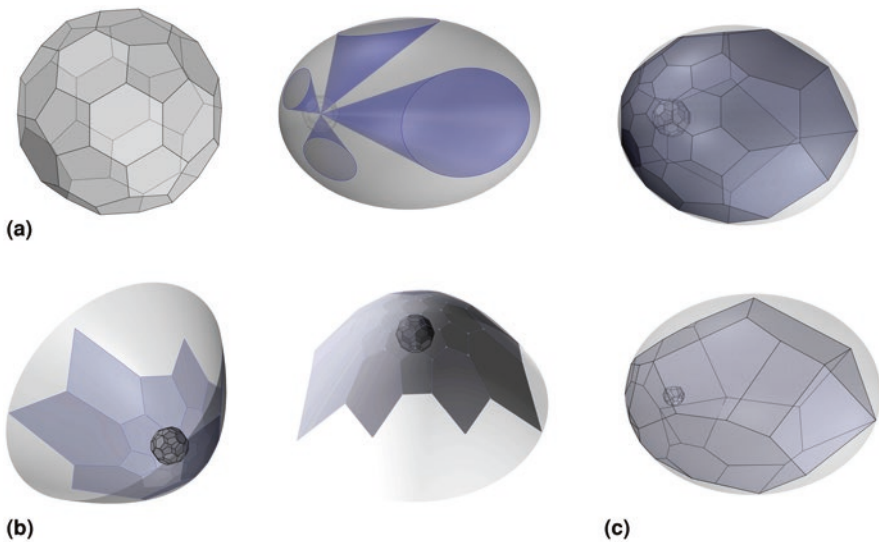
Fig. 3.8 (**a**) Projecting by cones. Example of discretization of ellipsoid based on the truncated icosahedron. (**b**) Example of discretization of the paraboloid and hyperboloid based on the truncated icosahedron. (**c**) Transformation of irregular polyhedra

Projecting by Ellipsoids, Paraboloids, or Hyperboloids

Instead of using conical projecting rays—being the generatrixes of a cone whose vertex is located at the focus of the quadric—we can also use ellipsoids, paraboloids, or hyperboloids as projecting surfaces. These quadratics surfaces must share the position of one of their foci with the quadric of reference and pass through the vertices of the polyhedron. The projections would be made, not by means of straight lines, but by conics (ellipses, parabolas, and hyperbolae) contained in a section that passes through the rotation axis of the quadric used as projecting surface. The points contained in flat sections of a sphere (the faces of the polyhedron) transform into points contained in flat sections of another rotational quadric surface, with the difference that these flat sections are separated from each other (Fig. 3.9a).

(a)

(b)   **(c)**
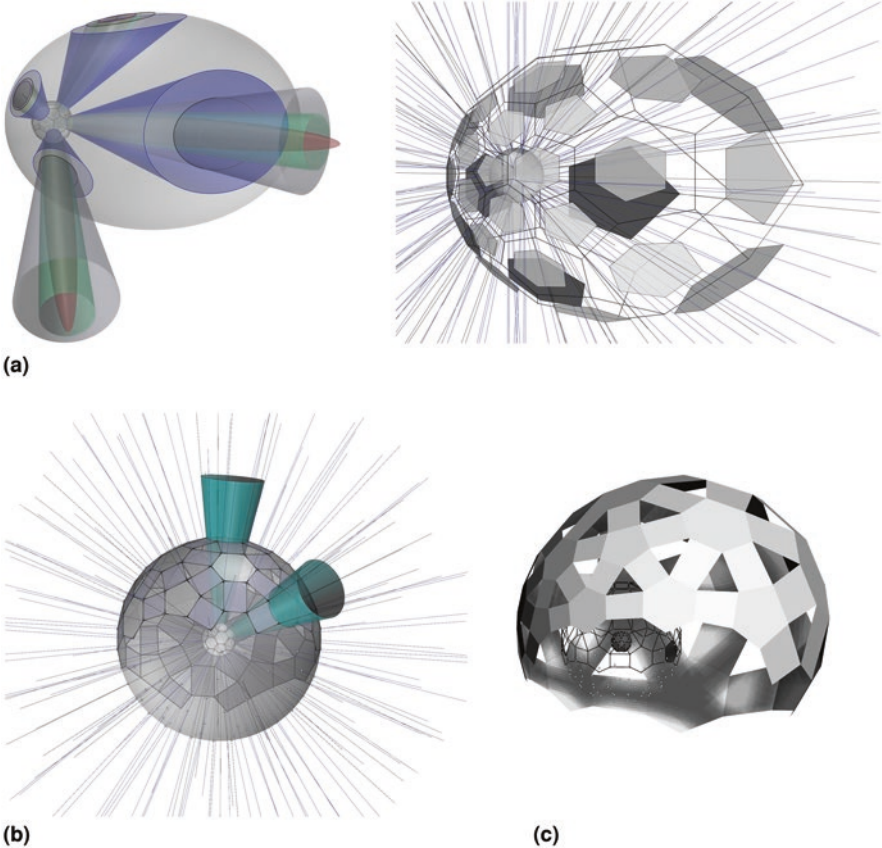
Fig. 3.9 (**a**) Projecting in ellipsoids, paraboloids, or hyperboloids. Example of discretization based on the truncated icosahedron. The vertices are projected by hyperboloids. (**b**) Graphic procedure to produce bevelled polyhedra. (**c**) Truncated icosahedron with bevelled edges

If we apply this transformation to a polyhedron inscribed in a sphere onto another concentric sphere (for example, projecting it by hyperbolae), each edge of the first polyhedron is transformed into two different edges in the second polyhedron that is also coplanar and forms a new face. Hence, this can be considered as an operation that automatically bevels the edges of the first polyhedron, in accordance with different criteria, within the chosen projection surface, ellipsoid, paraboloid, or hyperboloid and their eccentricities.

The bevelled polyhedron inscribed in the second sphere may be conically projected onto a third rotational quadratic surface, on the condition that they share a focus with the centre of the sphere. This way, a graphic procedure is established to produce bevelled polyhedra (Fig. 3.9b, c).

Discussion. Graphical Characterization of 3D Homology

The graphic study carried out in case 1 with projecting cones, reveals that this transformation can be generalized for all points of space beyond the surface itself.

If we can perform the transformation of a polyhedron whose vertices are contained in a sphere, we can also carry out the transformation of a polyhedron with vertices contained in various spheres. This is the case of the rhombic dodecahedron in Fig. 3.10a. The two concentric spheres, which contain the vertices of the polyhedron, become two ellipsoids that share one of their foci with the centre of the two spheres. The transformed polyhedron also has planar faces, and this condition determines the transformation of the second sphere into a unique ellipsoid. The transformation is determined via the first sphere-ellipsoid set, which we call the *reference* (Fig. 3.10b).

Once this transformation is defined, the problem is generalized for any concentric sphere. Space continuum could therefore be understood as consisting of a set of spheres that are concentric to the reference sphere, where each one is transformed into a different rotational quadric surface (Fig. 3.10c). The transitions from ellipsoid to paraboloid and hyperboloid therefore carry a special importance since these determine the singular points of such a transformation.[7]

As a result of these graphical speculations, we present an intuitive method to characterize completely this transformation in graphical terms (Fig. 3.10d). While this is a basic transformation of space studied in mathematics, it has not been a popular subject in courses in Descriptive Geometry.[8]

The projective transformation might be better understood if we consider that there are two linked spaces—the initial space and the homologous space—such that

---

[7]We are currently developing a more complete and exhaustive characterization of this same topic, to be published in a near future.

[8]A rare example is described by Taibo Fernández [20, p. 273]. The graphical elements that define this homology (homology centre, homology plane, plane limit 1, and plane limit 2) remains implicit on defining the form and the position of the reference sphere and the reference ellipsoid.
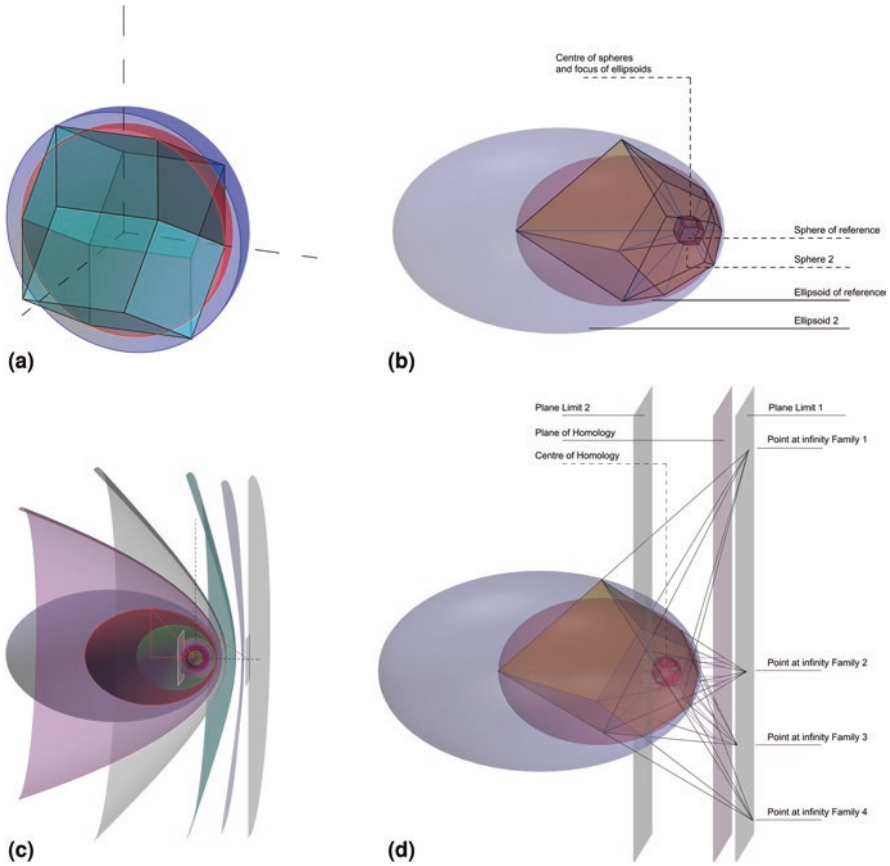
Fig. 3.10 (**a**, **b**) Transformation of the rhombic dodecahedron from two spheres (red and blue) to two ellipsoids. (**c**) Generalization for the entire space: each point in space corresponds to one sphere and each sphere is transformed into a different rotational quadratic surface. (**d**) The transformed rhombic dodecahedron shows its relationship with 3D homology

initial points are transformed into homologous points. Once a reference sphere (initial) and a reference ellipsoid (homologous) have been defined, the transformation of any other sphere into a second ellipsoid (paraboloid or hyperboloid) is determined.

A second sphere of greater radius cuts the axis at A and B. The tangents from both points to the circumference (which represents the equator of the sphere of reference) determine points M and N. Points M and N become their homologous, points M1 and N1. From these points, two tangent lines start from the ellipse itself, and determine the homologous points A1 and B1 at their intersection with the axis. These points define the major axis of the ellipsoid which is then determined by the major axis and the position of the focus (Fig. 3.11).

It can be verified that, as we increase the radius of the second sphere, its homologous ellipsoid has more eccentricity, up to a specific position where the sphere
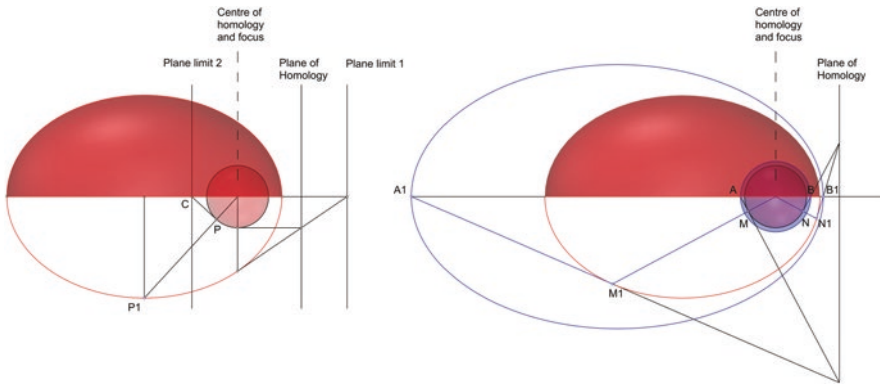
Fig. 3.11 Geometric relationships for the characterization of 3D homology

becomes a paraboloid. This position can be precisely ascertained from the homologous point P1, located on the minor axis of the reference ellipse, from which we find point P (initial), on the circumference. From here, and with the help of the tangent, we find point C which determines the radius of the sphere-paraboloid.

Spheres with a radius greater than that of the paraboloid-sphere become hyperboloids. The plane *limit 1* is tangent to the sphere-paraboloid. This plane represents the locus in initial space where all of its points are projected into the infinity of the homologous space. If a point is located behind *limit 1 plane*, it is necessarily contained on a hyperboloid-sphere in initial space and its projection, metaphorically, *crosses infinity*, so to speak, and appear just on the other side, on the second sheet of the hyperboloid.

As the initial points move further and further away from the centre of homology, they become contained in spheres of greater radius and their homologous projections are located in increasingly flattened hyperboloids and closer to the *limit 2 plane*. *Limit 2 plane* is, therefore, the place in the homologous space where the initial points are infinitely distant from the centre of homology.

Conclusions

For all the reasons outlined above, we conclude that, through a simple graphic procedure, a way for the discretization of rotational quadratic surfaces can be defined from patterns of plane polygons and circles. This provides additional solutions to other well-known discretization procedures, such as stereographic projection, and to other procedures of a mathematical nature, thereby opening a suggestive field of research. Likewise, the transformations of flat polygons inscribed in spheres towards other rotational quadratic surfaces, through conical projections (parabolic, elliptic, or hyperbolic), produce interesting ways of discretizing these surfaces.

A second conclusion is related to the way to characterize 3D homology, in accordance with the graphical procedure from which it is derived, by means of a sphere and an ellipsoid. This implies that advances in graphical control can completely redefine the way to approach a geometric problem.

As a final consideration, it should be borne in mind that it is not the digital and parametric graphic tools, by themselves, that make it possible to define, or reinterpret, inherited geometric knowledge, but rather the ability that these graphic systems provide for the generation of augmented graphic thinking [21].

References

1. Gentil Baldrich, J. M., & Martín-Pastor, A. (2015). Polyhedra as a form of geometric knowledge: The Spanish Jamnitzer or the fourth book of 'Artes Exçelençias dela Perspectiba'. *EGA, 25*, 56–65. https://doi.org/10.4995/ega.2015.3677

2. Llorens-Herrero, A. (2016). La representación gráfica del espacio tetradimensional euclídeo. La ampliación del método diédrico a cuatro dimensiones. Un-published doctoral thesis, Universidad de Sevilla. Available in full text in: https://idus.us.es/xmlui/handle/11441/52367

3. Martín-Pastor, A., & Gentil-Baldrich, J. M. (2019). Considerations regarding the representation of the invisible: Monge's method in four dimensions. *EGA, 24*(35), 118–129. https://doi.org/10.4995/ega.2019.11551

4. Martín-Pastor, A., & Narvaez-Rodriguez, R. (2019). New properties about the intersection of rotational quadratic surfaces and their applications in architecture. *Nexus Network Journal, 21*(1), 175–196. https://doi.org/10.1007/s00004-018-0420-x

5. Archimedes-Maurolico, F. (1685). *Monumenta omnia mathematica…,* Panormi [Palermo]: Apud Cyllenium Hesperium, 1685. [*De Conoidibus et Sphaeroibidus in two books*: 1° pp. 226–246; 2° pp. 247–275]. https://doi.org/10.3931/e-rara-12132.

6. Gentil-Baldrich, J. M. (1997). *Sobre la intersección de las cuádricas de revolución de ejes paralelos*. Departamento de Expresión Gráfica Arquitectónica.

7. Narvaez-Rodriguez, R., & Barrera-Vera, J. A. (2016). Lightweight conical components for rotational parabolic domes. In S. Adriaenssens, F. Gramazio, M. Kholer, A. Menges, & M. Pauly (Eds.), *Advances in architectural geometry 2016* (pp. 378–397). vdf Hochschulverlag AG an der ETH Zürich. https://doi.org/10.3218/3778-4_25

8. Poncelet, J.-V. (1866). *Traité des propriétés projectives des figures. Ouvrage utile a ceux qui s'occupent des applications de la Géométrie Descriptive et d'opérations géométriques sur le terrain. Tome Second. Deuxième edition*. Gauthier-Villars. (First Edition 1822, Paris, Bachèlier).

9. Chasles, M. (1837). *Aperçu historique sur l'origine et le développement des méthodes en géométrie particulièrement de celles qui se rapportent a la géométrie moderne suivi d'un mémoire de géométrie sur deux principes généraux de la science la dualité et l'homographie*. M. Hayez.

10. Hachette, J. N., & Pierre. (1822). *Traité de Géométrie descriptive* (2nd ed., p. 1822). Corby Libraire Éditeur.

11. Jimenez, M. R., Müller, C., & Pottmann, H. (2019). Discretizations of surfaces with constant ratio of principal curvatures. *Discrete & Computational Geometry, 2019*, 1–35. https://doi.org/10.1007/s00454-019-00098-7

12. Eigensatz, M., Kilian, M., Schiftner, A., Mitra, N. J., Pottmann, H., & Pauly, M. (2010). Paneling architectural freeform surfaces. *ACM Transactions on Graphics, 29*(4), 45. 1–10.

13. Schiftne, A., Höbinger, M., Wallner, J., & Pottmann, H. (2009). Packing circles and spheres on surfaces. *ACM Transactions on Graphics, 28*(5), 1–8. https://doi.org/10.1145/1618452.1618485

14. Kepler, J. (1619). *Harmonice mundi* … Lincii Austriae [Linz]: Sumptibus Godofredi Tampachii bibl. Francof.: Excudebat Ioannes Plancus.

15. Critchlow, K. (1970). *Order in space: A design source book*. Viking Press.

16. Grünbaum, B., & Shephard, G. C. (1986). *Tilings and patterns*. W. H. Freeman. ISBN: 0-7167-1193-1.

17. Bindel, E. (1964). *Harmonien im Reiche der Geometrie: in Anlehnung an Keplers "Weltharmonik."*. Verlag Freies Geistesleben.

18. Aurenhammer, F. (1987). Power diagrams: Properties, algorithms and applications. *SLAM Journal of Computing, 16*(1), 78–96.

19. Stephenson, K. (2005). *Introduction to circle packing: The theory of discrete analytic functions*. Cambridge University Press. ISBN: 13 978-0-521-82356-2.

20. Taibo Fernández, A. (1983). *Geometría descriptiva y sus aplicaciones. Tomo II*. Tébar Flores.

21. Martín-Pastor, A. (2019). Augmented graphic thinking in geometry. Developable architectural surfaces in experimental pavilions. In C. Marcos (Ed.), *Graphic imprints. EGA 2018* (pp. 1065–1075). Springer. https://doi.org/10.1007/978-3-319-93749-6_87

Andrés Martín-Pastor [ORCID: 000-0002-5588-2886] is an architect with a Ph.D. from the University of Seville (Spain), where he currently works as an associate professor in the Department of Graphic Engineering. His research is focused on perspective and geometry in architecture, and covers a broad range from inherited graphic traditions until the digital tools of today. His research also includes the study of developable surfaces and their applications in lightweight architecture. He has lectured at several International Universities and published books, chapters, and articles.

Chapter 4
Concave Deltahedral Rings Based on the Geometry of Concave Antiprisms of the Second Sort

Marija Obradović and Slobodan Mišić

Abstract Finding a possibility to create unique polyhedral surfaces with such specific geometric regularities as the congruence of faces, a high level of symmetry and the ability to describe an infinite polyhedron, served as a starting point for the explorations in this study. Such surfaces can be obtained through a single element, the equilateral triangle, given that they are deltahedral. Here, we will focus on deltahedral rings composed of fragments of the concave antiprisms of the second sort, type major, that we identify as *CA-II-n.M*. This paper shows not only that it is possible to close a full ring using fragments of selected *CA-II-n.M,* but also that we can predict the shape of the ring depending on the number of sides of the base-polygon {*n*} within the chosen *CA-II-n.M*. The number of solutions obtained for each *CA-II-n.M*'s representative depends on *n* and can vary from 1 to 5, out of 8 possible solutions.

Introduction

If we aim to explore a variety of polyhedral forms that do not need to satisfy the criterion of convexity, we get an infinite number of shapes that may be difficult to systematize and describe, unless we rely on previously chosen criteria. Certain regularities that usually concern the uniformity of faces of the chosen polyhedron and the symmetry of the surface itself are requested. In this paper, we examine the possibilities of defining polyhedral surfaces with the following characteristics:

M. Obradović (✉)
University of Belgrade, Belgrade, Serbia
e-mail: marijao@grf.bg.ac.rs

S. Mišić
University of Arts in Belgrade, Belgrade, Serbia
e-mail: slobodan.misic@fpu.bg.ac.rs

53

1. the faces are regular polygons;
2. the surface consists of congruent faces, i.e. it can be produced using a single shape;
3. a high level of symmetry is mandatory, and it may include radial symmetry, rotational and point symmetry;
4. the surface can be translationally repeated to infinity.

In this respect, deltahedral surfaces are particularly suitable, because they fulfil the first two conditions. Out of the deltahedral surfaces that meet the remaining conditions, ring-like surfaces were chosen as the most convenient. The lateral surfaces of uniform antiprisms and polygrammatic antiprisms [1] are those that first come to mind, but we looked further in order to explore new forms that meet the above criteria. With this research, we examine the possibility of forming concave ring-like surfaces (flower-like and star-like), which can be continuously repeated by translation (i.e. like antiprisms), thus forming infinite cylindrical polyhedra [2].

For the development of the concave deltahedral rings, we use ready-made components: fragments of concave antiprisms of the second sort that we abbreviate as *CA-II-n*[1] [3]. Why did we choose these surfaces, instead of, for example, those of convex antiprisms? Because the position of the faces of *CA-II-n* allows adjacent lateral surfaces to be joined into a whole, while the bases of the associated units remain coplanar. On the other hand, with convex antiprisms, by joining the faces of two adjacent units, we would obtain deltahedral surfaces having the bases that would not be coplanar (Fig. 4.1c) due to the dihedral angles between lateral triangular faces and bases. Hence, we choose the *CA-II-n,* i.e. fragments of its lateral surface as initial elements, not only because they meet the requirements of all the above conditions, but also because their properties, measures and all essential parameters for their generation and presentation were already known to us, from previous research.

Concave antiprisms of the second sort (*CA-II-n*, hereinafter) are polyhedra that, similarly to convex antiprisms, consist of two identical regular polygons connected by a deltahedral lateral surface. The lateral surface is generated by 2π polar array of the open hexahedral cell composed of six equilateral triangles arranged around a common vertex. The term *second sort* has its origin in the fact that two rows of equilateral triangles in the lateral surface exist. There is an infinite number of *CA-II-n*'s representatives, some of which (with base-polygons of $n \in \{3, 4, 5 \ldots 11\}$) are shown in Fig. 4.1a.[2]

In this paper, we consider one of the two types of *CA-II-n* formation, namely the one with a greater height which we name as major type (*CA-II-n.M*). We search for deltahedral rings formed by polar array of *CA-II-n.M's* fragments, thereby keeping

---

[1] The notations introduced for the concave antiprisms of the second sort: *CA-II-n*, *CA-II-n.M* and *CA-II-n.m* in the current study, are somewhat different from those introduced by the authors in [3] (*CA II-n*, *CA II-nM* and *CA II-nm*), for greater clarity.

[2] A detailed description of the genesis of *CA-II-n*, together with their geometric properties is given in [3].
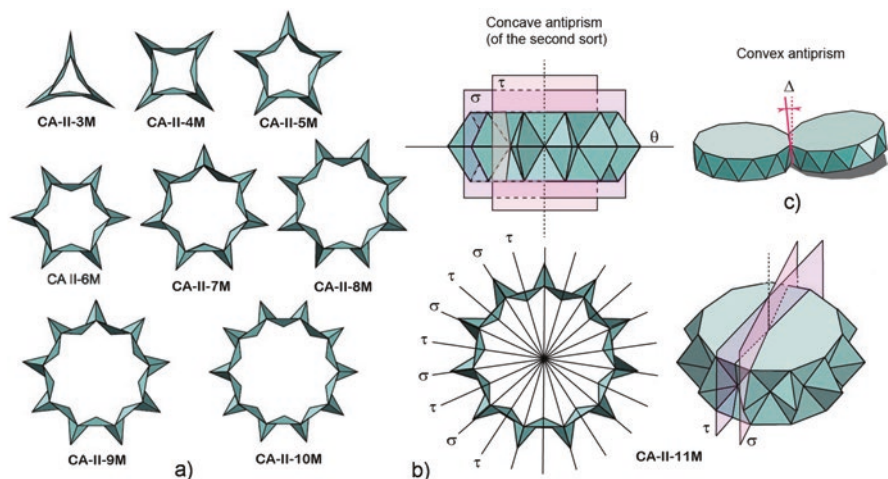
Fig. 4.1 Some representatives of *CA-II-n.M*. (**a**) Eight examples of *CA-II-n.Ms*; (**b**) Top and front view of *CA-II-11.M* with its symmetry planes σ and τ; (**c**) A deviation from the coplanarity of the bases of two convex antiprisms caused by joining of their triangular faces

the crucial linear and angular measurements of the initial solids. Our goal is to obtain highly symmetrical forms derived from a single element—the equilateral triangle.

Investigating a Possibility for the Deltahedral Rings' Formation

To explain the process of creating concave deltahedral rings (*CDR*), we will start with the *CA-II-n*'s lateral surface, whose fragments will be used in subsequent steps. When forming a *CA-II-n*, we start from the planar net of the open hexahedral cell—a regular hexagon subdivided into six equilateral triangles (Fig. 4.2). Depending on the way the net is folded, similarly to other polyhedra of the second sort (*CC-II--n.M/m* [4], *CP-II-n,M/m* [5] and *CP-II-n.B* [6]),[3] it is possible to form two types of lateral surface. If the central vertex (G) of the open hexahedral cell is protruding, we obtain a type with a lower height for the lateral deltahedral surface, which we term *minor* and abbreviate as *CA-II-n.m*. If the central vertex (G) is indented, we obtain the type with a greater height, termed *major* and abbreviated to *CA-II-n.M* that will be the focus of this paper (Fig. 4.2a).

As shown in Fig. 4.2a (see also Fig. 4.1b), the vertices A, F and E lie in the symmetry plane σ_1 and the vertices B, C and D lie in another symmetry plane σ_2. This

---

[3] The notations used in this study slightly differ from those in [4–6], due to greater clarity and continuity with the notations for concave antiprisms *CA-II-n.M/m*.
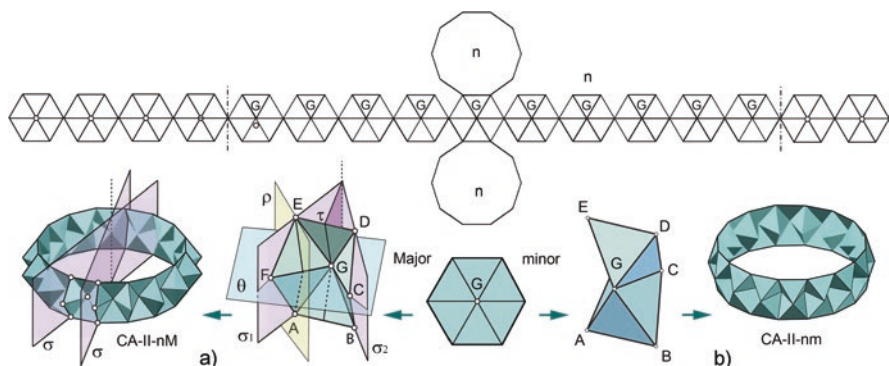
Fig. 4.2 Lateral surfaces of (**a**) *CA-II-n.M* and (**b**) *CA-II-n.m*

allows a given open hexahedral cell to be connected to its adjacent, that one to the next and so on, until they form a full circle and a closed ring for the lateral surface. The same logic will be used in this paper, except that instead of the open hexahedral cell, we will use a cell formed of two paired *CA-II-n.M*s connected by a pair of joint triangular faces. Due to the face disposition of *CA-II-n.M*, the vertices F, G and C belong to plane θ, the traverse symmetry plane of the *CA-II-n*, which is parallel to the bases planes, thus they are at the same height. Additionally, the triangles AGF and EFG are plane reflexive with respect to the plane ρ, perpendicular to the edge FG. The corresponding relations apply to the pair of triangles BCG and CDG as well, since they are plane reflexive to the former pair with respect to plane τ. We use these characteristics of the *CA-II-n.M*s to form a new unit cell of a deltahedral ring.

The key procedure for the ring's formation is to bring the two outer pairs of equi-lateral triangles (AGF, EFG and BCG, CDG) from the open hexahedral cells of the two adjacent *CA-II-n.M*s into an overlapping position (Fig. 4.3a). The planar sym-metries of the triangles AGF and EFG make this procedure possible. In this way, we get a new unit, an open decahedral cell (Fig. 4.3b), which is a building block for a new deltahedral structure. Thereby, it takes over the measurements (points' heights, angles) from the initial *CA-II-n.M*.

Then, we examine which multilateral reflection of this decahedral cell (Fig. 4.3c) may produce a closed deltahedral ring, necessarily concave and of the second sort (abbr. *CDR-II*), forming a full circle with no partial overlaps or gaps. The final result, therefore, comes down to the polar distribution of these cells, with *K* concave antiprisms[4] in the array, where *K* is a natural number (*K* ∈N).

The open decahedral cell can be positioned in such a way that the surrounded space it defines (shaded in Fig. 4.3) faces the interior of *CDR-II* forming a flower-like ring, which we named as Case A; or faces its exterior forming a star-like ring, named Case B. In both cases, open decahedral cells can be combined with one or more hexahedral cells between them that are fragments of the *CA-II-n.m*. Given that

---

[4] For the formation of *CDR-II,* we only use fragments of the same *CA-II-n.M*.
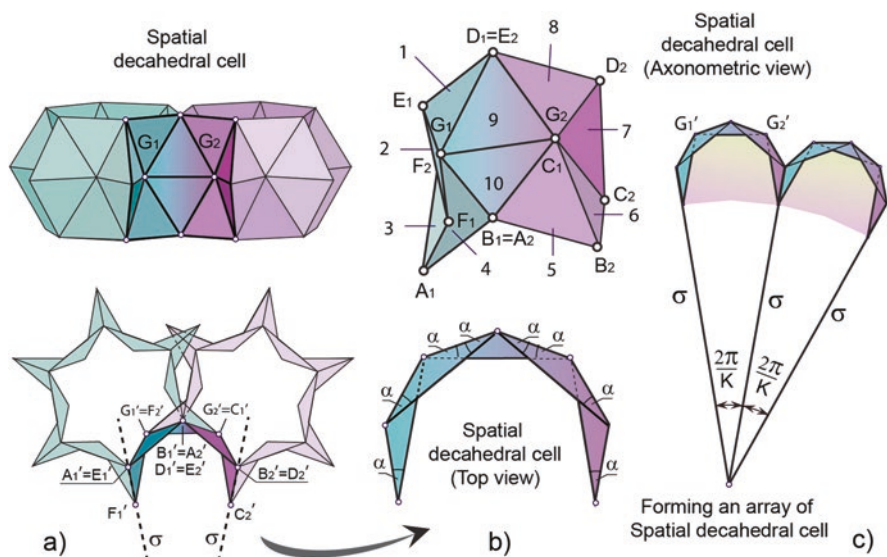
Fig. 4.3 The formation of the open decahedral cell: (**a**) Joining faces of two lateral surfaces of *CA-II-n.M*s and forming an open decahedral cell; (**b**) The open decahedral cell in isometric and top view; (**c**) Forming an array of open decahedral cells
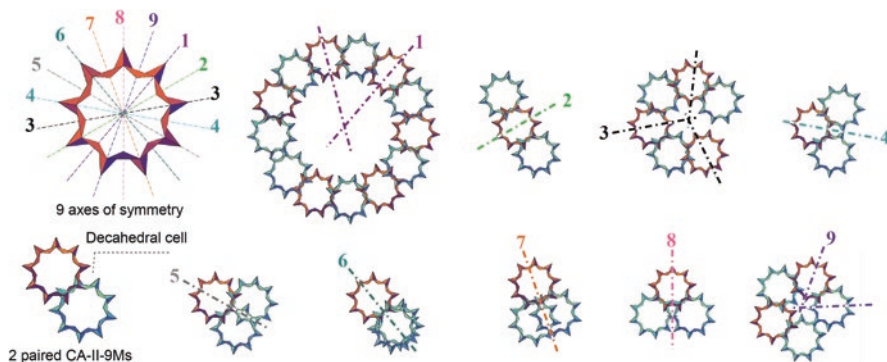
Fig. 4.4 Experiments with rings formation depending on the symmetry axis of the initial *CA-II-9.M*

the two different units are involved in the ring's construction, such cases of *CDR-II* are denoted by A_f and B_f.

*CA-II-n.M*s themselves are characterized by radial symmetry and rotational symmetry, while in the cases in which the bases have an even number of sides, we also encounter point symmetry. Each base-polygon of *CA-II-n* has *n* axes of rotational symmetry (Fig. 4.4). To solve the task, we take two paired *CA-II-n.M*s with a

common open decagonal cell. Observing these in orthogonal projection, we apply successive reflexive symmetries across the corresponding symmetry axes of their polygons until we close the full circle. The solutions differ depending on the selected axes of reflection.

Figure 4.4 shows some of the results we get with the example *CA-II-9.M*, if we run the experiment graphically. The basis of the observed concave antiprism is nonagonal, so it has 9 axes of symmetry (1–9). When observed in orthogonal projection, we can adopt each of them as an axis of reflection, i.e. each symmetry plane being projected as a line. Across the chosen axis, we transform the adjacent *CA-II-9.M*, the one that shares the common decahedral cell. By successive repetition of this procedure, we examine whether there will be a complete and precise closure of the full circle. We can observe that each symmetry axis produces a different result. Most of them will result in overlaps or gaps between adjacent cells, and only some of them will provide a closed ring, according to the initial conditions. We note that the hexahedral fragments of the *CA-II-9.M* regularly occur between the open decahedral surfaces. This does not affect the validity of the solution and we will adopt such cases if they close the ring (as mentioned above, those are Cases A_f and Cases B_f). Hence, considering them as valid, we adopt those solutions with an integer number (*K*) of the *CA-II-n.M*s in the circle.

In the first steps of the research, it is difficult to predict how many solutions will be obtained and how they will look like. The clear interdependence between numbers *n* and *K*, or the very number of solutions we get for an individual representative *CA-II-n* is not immediately noticeable. For instance, for certain representatives, we will only get one solution, while for others, we will have as many as five solutions. Instead of testing each individual axis in order to determine number *K*, we use a mathematical calculation based on trigonometry of the decahedral cell's orthogonal projections.

In Fig. 4.5, we see the positions of the open decahedral cells after successive reflections across the symmetry planes σ and τ of the decahedral cell and the angles that these planes determine for the array. The planes (seen as lines σ' and τ' in the orthogonal projection) are also symmetry planes of the *CDR-II* formed out of *K* decahedral cells. Each chosen pair of symmetry axes intersects in the same point (A or B) and defines the angles of the polar array between them. The angles determine the number *K* of petals in Case A, or the star points in Case B.

We worked on the following formulas that define:

– the base angle in the congruent isosceles triangles—orthogonal projections of the *CA II-n.M*'s faces, denoted by α (see Fig. 4.3b);
– the largest angle between two symmetry planes τ' and τ' of the *CA-II-n.M*s in the ring (Fig. 4.5b), denoted by φ;
– the angle between planes $σ_1$' and $σ_2$' defined by the outer vertices of the open decahedral cells (Fig. 4.5a), denoted by ω.

$$\alpha = \pi \frac{n-2}{6n} \tag{4.1}$$
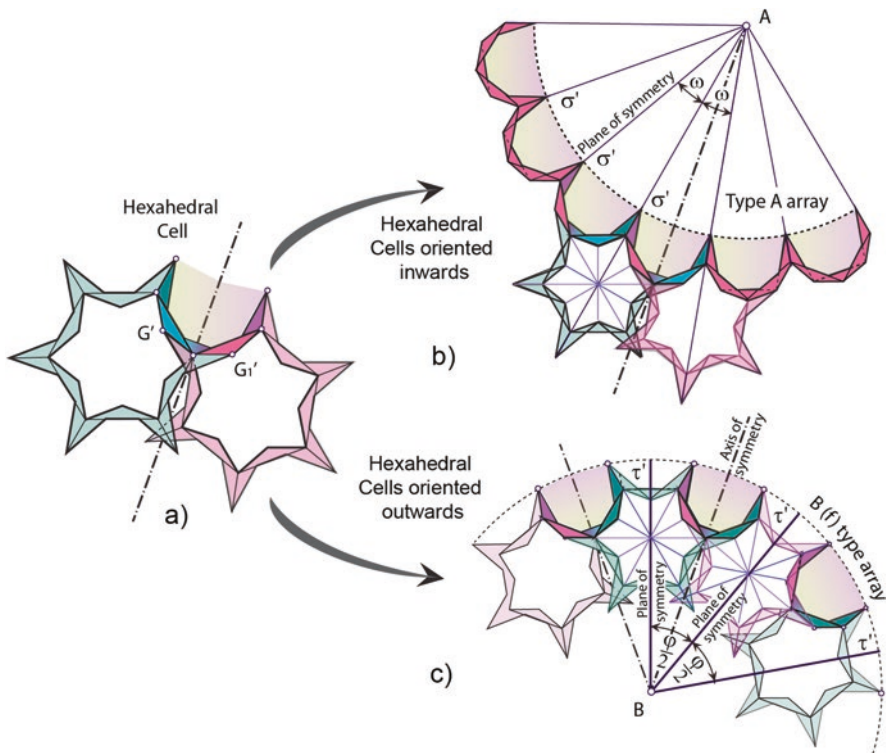
Fig. 4.5 (**a**) Formation of a hexahedral cell by joining the lateral surfaces of two *CA-II-n.Ms*: (**b**) Case A, with open decahedral cells oriented towards the interior of the ring; (**c**) Case B, with open decahedral cells oriented towards the exterior of the ring

$$\varphi = 4\alpha \tag{4.2}$$

$$\omega = |10\alpha - \pi| \tag{4.3}$$

It follows that the amplitude for angles φ and ω can be expressed as $f(n)$, such as

$$\alpha = \frac{\pi}{6n}(n-2) \tag{4.4}$$

$$\varphi = \frac{2\pi}{3n}(n-2) \tag{4.5}$$

$$\omega = \frac{2\pi}{3n}(n-5) \tag{4.6}$$

Once angles φ and ω have been calculated, we determine which number k, as their multiplier, produces a full circle creating either Case A or Case B, having that

Table 4.1 The number of petals/star points in the CDR-II depending on the n of CA-II-n.M

n	$\propto$	φ	ω	$k=\dfrac{2\pi}{\varphi}$		j	$K_{A,B}$	$k=\dfrac{2\pi}{\omega}$		j	$K_{B,A}$	$H=f(a)$ a = edge length
3	10°	40°	80°	A_a	9	1	9	B	4.5	2	9	1723052a
4	15°	60°	30°	A_a	6	1	6	B	12	1	12	1711992a
								B_{f3}			3	
5	18°	72°	0°	A_a	5	1	5	C	∞	1	∞	1701302a
				B_f	5	1	5					
6	20°	80°	20°	B	4.5	2	9	A	18	1	18	1693377a
7	21.428°	85.715°	34.286°	B_f	4.2	5	21	A_f	10.5	/	10.5	1686999a
				B_{f3}			3					
8	22.5°	90°	45°	A_a	4	1	4	A	8	1	8	1681793a
				B_f	4	1	4	B_f	8	1	8	
9	23.333°	93.333°	53.333°	A_f	3.857	7	27	B_f	6.75	/	6.75	1677478a
10	24°	96°	60°	B_f	3.75	8	30	A	6	1	6	1673849a
				B_{f3}			3					
11	24.545°	98.182°	65.454°	B_f	3.667	3	11	A_f	5.5	2	11	167076a

$$k = \frac{2\pi}{\varphi \vee \omega} \quad \text{(see Table 4.1).}$$

Note: if $n = 3t + 2$, we have a third Case, C (C_f), when the angles between all symmetry planes equal 0. The amplitude of this angle, ψ, is expressed by the formula(s):

$$\psi = n\varphi = 2\pi t = 0° \tag{4.7}$$

Case C, in which $K = \infty$ and an infinite linear ring appears, unites Cases A and B because, viewed from different sides of the *ring*, the open decahedral cell can be oriented outward or inward. However, if k is not an integer, we additionally multiply it by a minimal integer j that results in the integer K. In fact, if we express the value of k as a fraction, j is the reciprocal of its denominator. Thus:

$$k \cdot j = K \tag{4.8}$$

where $K \in N$. This way, we get solutions even when it is not possible to close the circle solely from open decahedral cells and we have to combine them with open hexahedral cells. As we can see from Table 4.1, the resulting solution Cases are denoted by A, A_f, B_f, B_{f3} and A_a, with additional Cases C and C_f. The above simple formulas (4.1)–(4.8) help us to obtain swift solutions, regardless of the case in question, where factor j in formula (4.8) is applied to adjust the value of K up to

an integer. Therefore, cases in which $j > 1$ are those with the additional hexahedral fragments of *CA-II-n.M*, the ones we have denoted by A_f and B_f. Accordingly, in the general setting, the maximum number of possible cases/solutions is 8. Yet, we can never get all 8 of them within the same n, because some of the Cases (i.e. A and B, A and A_f, B and B_f, C and C_f) cannot exist simultaneously for the same *CA-II-n.M*. The maximum number of solutions is thus 5, as can be seen in the example of *CA-II-8.M*.

To complete all the data needed for the definition of the ring itself, we need the heights, i.e. the distance between the parallel planes of the bases. We take them as the known value $H = f(a)$, the height of the *CA-II-n.M* that generated it, where a is the length of the polyhedron's edge. The overview of values k, j, K and H (height) for the observed $n \in \{3, 4, 5 \dots 11\}$ is given in Table 4.1.

To obtain what we name as true deltahedral forms, we remove all redundant faces, such as the ones that penetrate each other or do not participate in the formation of the ring. Thus, we obtain concave deltahedral rings (of the second sort) with K petals or star points, abbreviated as: *CDR-II-K*.

Findings of the Research

Validating the above results using an AutoCAD application, through the gallery of 3D models within the observed sample of *CA-II-n.M*'s representatives, we came up with interesting observations, which may not be noticeable when relying solely on formulas.

For the *CA-II-n.M*s with $n \in \{3, 4, 5\}$, a special type of Case A occurs, so we denoted it as Case A_a. When we place two adjacent *CA-II-n.M*s in such a position that two pairs of triangles in their lateral surfaces (e.g. $A_1G_1F_1$, and $E_1F_1G_1$ of the observed *CA-II-n.M*) overlap with the corresponding pair of the adjacent one (Fig. 4.6a), we place the next *CA-II-n.M* in a position that another pair of triangles ($B_1C_1G_1$ and $C_1D_1G_1$) overlap as well and we then continue the sequence of *CA-II-n.M*s according to the same scheme. With the K number of *CA-II-n.M*s in a row, the ring will be closed completely. Therefore, instead of forming just an open decahedral cell, we get a fully enclosed deltahedral cell, which forms a ring structure for itself.

Such a structure is nothing but a lateral surface of a double convex p-sided antiprism (Fig. 4.6b), which, being duplicated, now becomes concave. It follows that $p = K$.

The dihedral angles between adjacent faces of two base-joined antiprismatic surfaces are greater than π, so this property also qualifies such a case as a concave deltahedral ring of the second sort (*CDR-II-p*), because:

– a concave deltahedral surface is obtained,
– it consists of a double row of equilateral triangles,
– it has a radial symmetry,
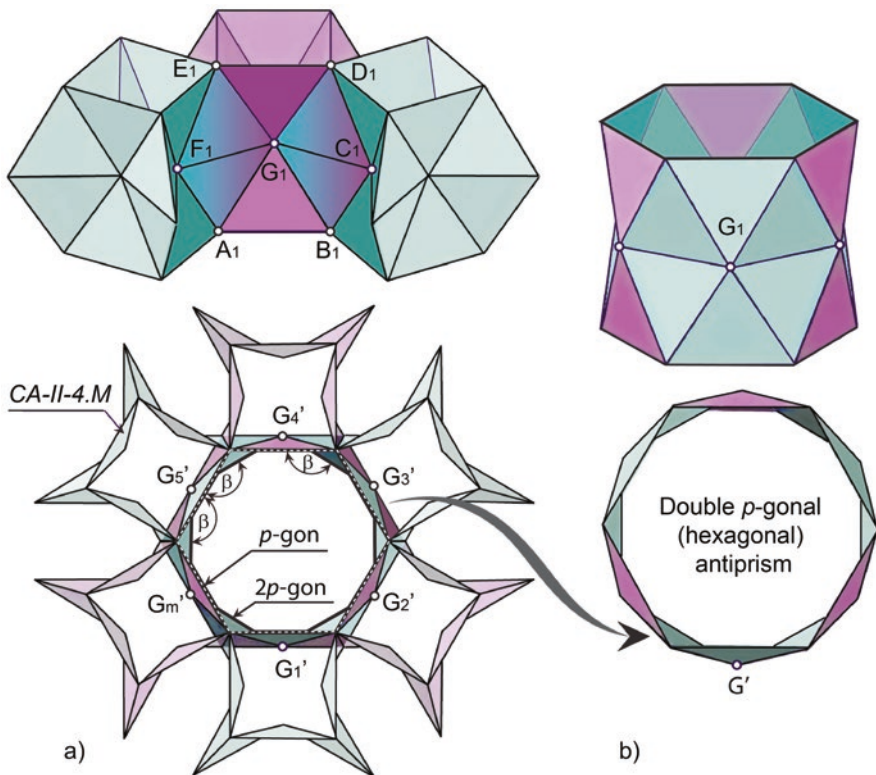
Fig. 4.6 Formation of *CDR-II* of type A_a: (**a**) Six *CA-II-4.M*s joined by pairs of triangular faces; (**b**) *CDR-II* of type A_a

which are all the characteristic of concave polyhedra of the second sort.

Let us now consider why Case A_a occurs for the *CA-II-n.M*s where $n \in \{3, 4, 5\}$ and if there is any other n that satisfies the conditions of forming a lateral surface of a (double) convex antiprism.

If we observe the angles β found in a $2p$-sided polygon that emerges as the inner one in the orthogonal projection of a *CDR-II* of type A_a (Fig. 4.6a), after trigonometric calculations, we find that:

$$\beta = 2\pi \frac{n+1}{3n} \tag{4.9}$$

Consequently, the number $p = K$ of the base sides of the newly obtained double antiprism is:

$$p = \frac{3n}{n-2} \tag{4.10}$$

Table 4.2 The occurrence of Case Aa in CDR-II for the observed range of $3 \le n \le 200$

$p = \dfrac{3n}{n-2}$																	
n	3	4	5	6	7	8	9	10	11	12	13	14	15	16	17	18	19	20
p	9	6	5	4.5	4.2	4	3.857	3.75	3.667	3.6	3.545	3.5	3.461	3.428	3.4	3.375	3.353	3.333

Now, if we analyse which n satisfies the condition that p is an integer and positive, i.e. $p \in \mathbb{N}$, we come to the result that $n \in \{3, 4, 5, 8\}$. No other number satisfies this formula, because if n tends to infinity, p tends to 3 (Table 4.2).

$$\lim_{n\to\infty} \frac{3n}{n-2} = 3 \tag{4.11}$$

Therefore, only fragments of *CA-II-3.M*, *CA-II-4.M*, *CA-II-5.M* and *CA-II-8.M* can produce a *CDR-II-p* which corresponds to a double convex antiprism of *p*-sided basis.

In Table 4.2, we can see the value p representing the number of double antiprism's sides, as a $f(n)$ of the initial *CA-II-n.M*, where $p = K$, the number of *CA-II-n.M*s needed to close the ring.

Still, by using the decahedral cells formed from *CA-II-n.M*'s fragments, it is possible to obtain a star-like deltahedral ring as Case B (see Table 4.1 and Fig. 4.4), exactly as we would for any other case.

Here, we can see a pattern of geometric limitation similar to the one observed in the formation of convex regular-faced pyramids and cupolas, i.e. as Johnson solids J1 – J5 [7], where polygons with number of sides $n \ge 6$ will not participate in their formation, but now with the exception of $n = 8$. However, although lateral surfaces of double convex antiprisms are no longer regularly found as in Case A$_a$ of the *CDR-II-K*s (except the square antiprism found as the core-ring within one of the arrays of *CA-II-8.M*s, as will be shown below), the deltahedral rings of A$_{(f)}$ or/and B$_{(f)}$ variants can still be formed for any n.

Out of the gallery of *CDR-II-K*s obtained from *CA-II-n.M* fragments, we have selected a couple, as most typical examples for the observed sample of $n \in \{3, 4, 5, …, 11\}$. Figs. 4.7, 4.8, 4.9 and 4.10 show the *CDR-II-K*s formed from *CA-II-n.M*s for $n = 3$, $n = 5$, $n = 7$ and $n = 8$, together with the process of their formation.

Through visual insight, by creation of models and comparison of the obtained shapes, we noticed that certain regularities in the formation of the rings are groupable in dependence to number n of the original concave antiprism.

We have noticed that trilateral symmetry appears not only in the array of the *CA-II-n.M* fragments with n divisible by *3* ($n = 3t$), but also in the array of those in which $n = 4$, $n = 7$, $n = 10$, etc. ($n = 3t + 1$), as shown in Fig. 4.9. For such cases, we have discovered the existence of a trefoil deltahedral ring which appears as the second solution for Case B$_f$. The number K_B of *CA-II-n.M*s needed to close the ring is:
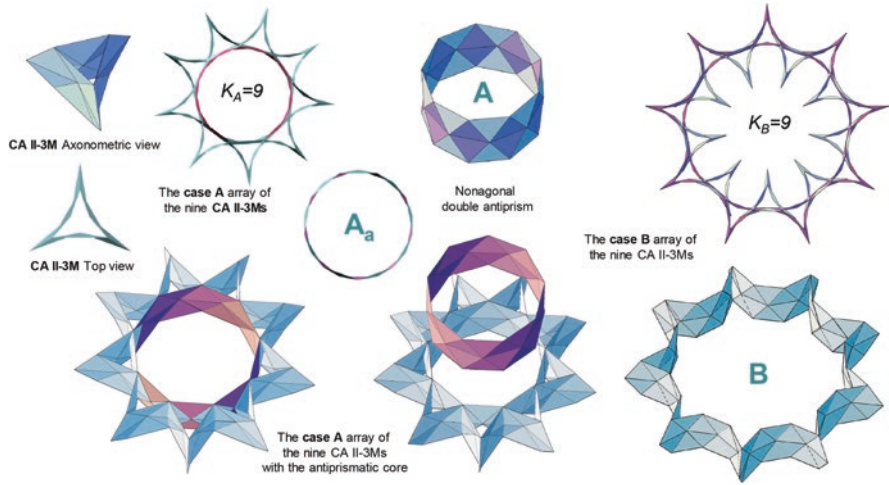
Fig. 4.7 *CA-II-3.M* with *CDR-II-9.A$_a$* and the *CDR-II-9.B* it forms
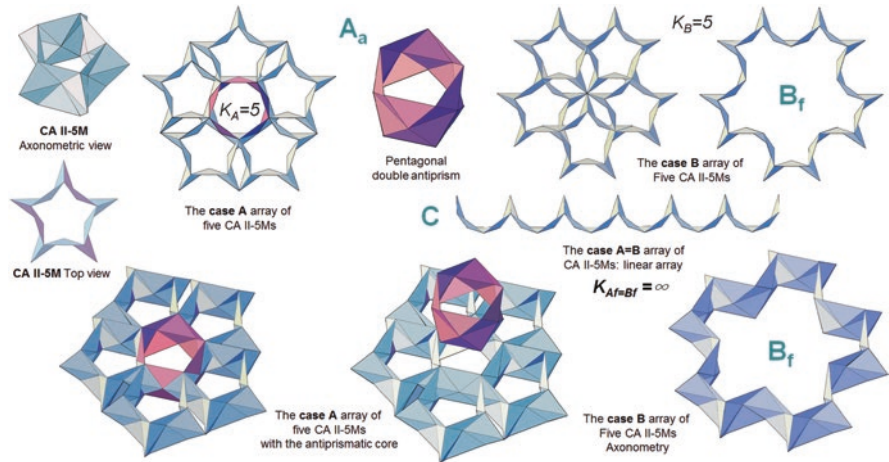
Fig. 4.8 CA-II-5.M with CDR-II-5.A$_a$, CDR-II-5.B$_f$ and the CDR-II-C it forms

$$K_B = 3n \text{ or } K_B = \frac{3n}{n} = 3 \tag{4.12}$$

On the other hand, for *n*-sided bases where $n = 3t + 2$, we find even more versatile results, because the most diverse solutions appear within these representatives. In such an instance, numbers $K_A = K_B$, so we get *CDR-II-K* variants with an equal number of petals and star points. Additionally, besides Cases A($_f$) and B($_f$), here we regularly find Case C, a *ring* with infinitely large radius. Therefore, for some *n*-sided bases, by assembling these infinite linear series of *CA-II-n.M*s', both in x, y and z
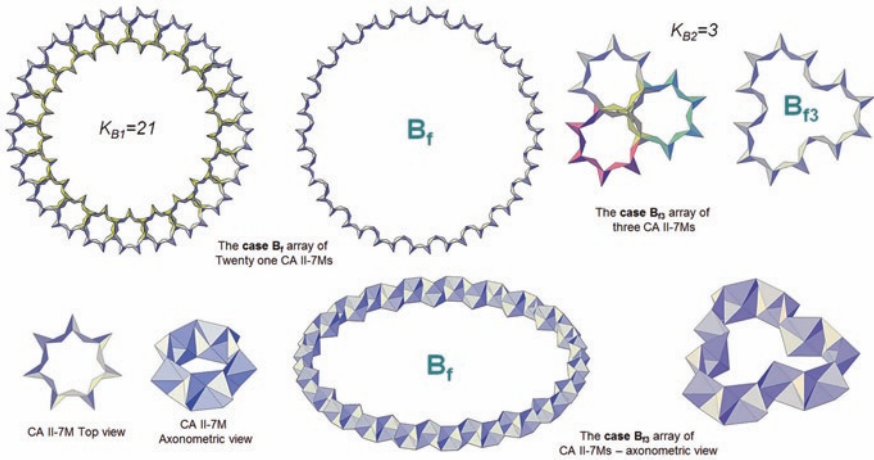
Fig. 4.9 *CA-II-7.M* with *CDR-II-21.B$_f$* and the *CDR-II-3.B$_{f3-7}$* it forms

direction, a formation of 3D tilings can be considered (Fig. 4.10). This problem is closely related to Euclidean tilings with star polygons [8], because if we are to close *CDR-II-K* so to form the solid, it would be possible by using star polygons, regular compound polygons or semi-uniform polygons [9]. The determination of these polygons and the solids formation will be the subject of future research.

The most interesting results in this regard are obtained with the *CA-II-8.M*, where Cases A and B$_f$ are found within the same structure of arrayed *CA-II-n.M*s, for the same axes of symmetry and thus with identical angles, $\varphi_A = \varphi_B$ and $\omega_A = \omega_B$, for both cases. Furthermore, two different solutions occur in Cases A$_{(a)}$ and B$_f$; those with 4 and those with 8 *CA-II-8.M*s in the ring (Fig. 4.10). In this manner, four different concentric solutions are obtained:

(a) two of Case A,

- flower-like *CDR-II* (A), formed of 8 *CA-II-8.M*s (Fig. 4.10a);
- double square antiprism (A$_a$), formed of 4 *CA-II-8.M*s (Fig. 4.10b);

(b) two of Case B$_f$:

- star-like deltahedral ring (B$_f$) formed of 8 fragments of *CA-II-8.M* (Fig. 4.10a);
- star-like deltahedral ring (B$_f$) formed of four fragments of *CA-II-8.M* (Fig. 4.10b);

- supplemented by the fifth case:

(c) the Case C$_f$ with the infinite series of *CA-II-8.M*s' fragments (Fig. 4.10b).

In situation (b) which involves eight *CA-II-8.M*s, another, ninth (double) *CA-II-8.M* can be inserted inside the *CDR-II-8.A*, playing the *core* role which convex antiprisms had in the examples of *CA-II-8.M*s with $n \in \{3, 4, 5\}$. Within this
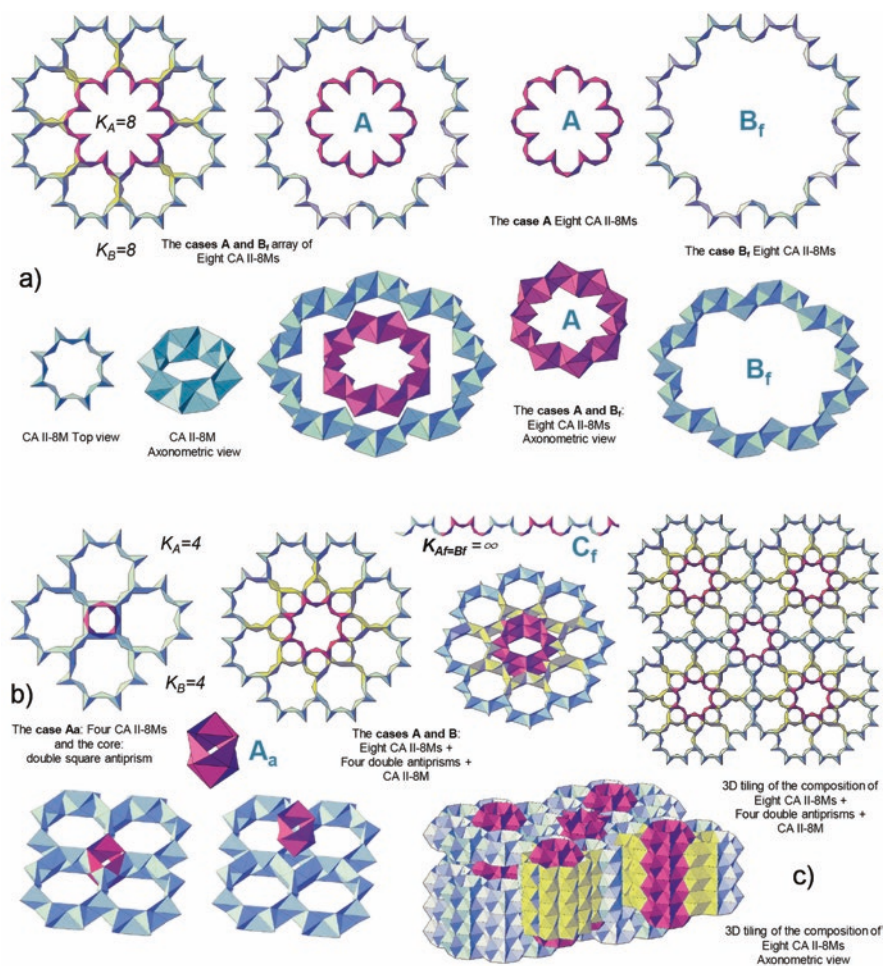
Fig. 4.10 *CA-II-8.M* with five cases of *CDR-II-K* it forms: (**a**) Flower-like *CDR-II-8.A* and star-like *CDR-II-8.B_f*, formed of 8 *CA-II-8.M*s; (**b**) Double square antiprism *CDR-II-4.A_a* and star-like deltahedral ring *CDR-II-4.B_f* formed of 4 *CA-II-8.M*s; (**c**) The Case C₁: *CDR-II-Cf-8* with the infinite series of *CA-II-8.M*s' fragments

structure, we can then identify eight double square antiprisms surrounding the *core* that double *CA-II-8.M* makes. The obtained composition can be arrayed in space infinitely, creating a 3D tessellation (Fig. 4.10c).

Finally, we look at the representatives of concave antiprisms whose bases are polygons with $n = 3t$ sides. Having in mind the immanent trilateral symmetry of the *CDR-II-Ks*, it might seem that they should provide the most special solutions, but it is not really so. These examples are limited only to A$_{(f)}$ and B$_{(f)}$ Cases, where $K = 3n$. Often, when it comes to odd values of n, Case B may be completely absent. A summary of the research findings is given in Table 4.3.

Table 4.3 Review of the research findings and predictability of number and form of solutions depending on n

n	K_{Aa}	K_A	K_B	$K_{B3} = K_B/n$	$K_C = \infty$
$3\,t$	$\dfrac{3n}{n-2}$	$3n$	Even: $\dfrac{3n}{2}$ Odd: /	/	/
$3\,t+1$	$\dfrac{3n}{n-2}$	Even: 6 Odd: /	$3n$	3	/
$3\,t+2$	$\dfrac{3n}{n-2}$	n	n	/	∞

So, from the initial situation where we could not have predicted either the existence or the number of possible solutions when using certain *CA-II-n.M*'s fragments in forming the ring, we arrive not only to the predictability of their number, but to the certainty of their shape.

Conclusions

With this paper we have shown that:

An integer number (K) of *CA-II-n.M*'s fragments can be used to form a closed, radially symmetrical ring with a concave deltahedral surface. It can be flower-like (Cases A and A_f), or star-like (Cases B and B_f) and be obtained for any $\in N$. In instances where $n=3t + 1$ it is possible to create an additional form of Case B, a trefoil ring (B_{f3}), while in instances with $n = 3t + 2$, a ring of infinite diameter (Cases C and C_f) can be made.

There is a link between the geometry of the *CA-II-nM*s with $n\in\{3, 4, 5, 8\}$ and that of the convex antiprisms with the number of base sides $p \in \{9, 6, 5, 4\}$, respectively. Now, as a form of Case A, a duplicated lateral surface of a convex antiprism appears, which is named Case A_a.

In total, eight different ring shapes can be formed: Cases: A, A_f, A_a, B, B_f, B_{f3}, C and C_f.

The obtained rings can also be termed *of the second sort* (denoted by *CDR-II-K*) as they inherit the following from the given *CA-II-n.M*:

- the linear and angular measurements, H and α, needed for their graphic and mathematical elaboration,
- two rows of equilateral triangles in the lateral surface,
- radial multilateral symmetry.

Out of the rings thus obtained, it is possible to form infinite cylindrical deltahedra, and in some cases even 3D tessellations. Formation of *CDR-II-K*s whose shapes belong to the Cases A and B alone (i.e. excluding Cases A_f, B_f and C_f), with the number of petals/star points that can be any integer $K \geq 2$, may be further

investigated. Also, the analysis of the base polygons that would enclose the *CDR-II-K*s into solids may serve as a possible direction for future research.

References

1. Huybers, P. (2001). Prism based structural forms. *Engineering Structures, 23*(1), 12–21.
2. Wachman, A., Burt, M., & Kleinmann, M. (1974). *Infinite polyhedra*. Technion.
3. Obradović, M., Popkonstantinović, B., & Mišić, S. (2013). On the properties of the concave antiprisms of second Sort. *FME Transactions, 41*(3), 256–263.
4. Obradović, M., Mišić, S. (2008). Concave regular faced Cupolae of second sort, In: *Proceedings of 13th ICGG* (ICGG 2008, Dresden, August 2008), ed. Gunter Weiss, Dresden: ISGG/ Technische Universität Dresden El. Book: 1–10.
5. Obradović, M., Mišić, S., Popkonstantinović, B. (2014). Concave pyramids of second sort -the occurrence, types, variations, In: *Proceedings of the 4th International Scientific Conference on Geometry and Graphics*, 2. moNGeometrija 2014, June 20–22. Vlasina, Serbia, ed. Sonja Krasić, Faculty of Civil Engineering and Architecture in Niš and Serbian Society for geometry and graphics (SUGIG), 157–168.
6. Obradović, M., Mišić, S., & Popkonstantinović, B. (2015). Variations of concave pyramids of second sort with an even number of base sides. *Journal of Industrial Design and Engineering Graphics (JIDEG) – The SORGING Journal, 10*(Special Issue, 1), 45–50.
7. Johnson, N. W. (1966). Convex polyhedra with regular faces. *Canadian Journal of Mathematics, 18*(1), 169–200.
8. Myers, J. (2012). Tiling with regular star polygons. Polyomino.org.uk https://www.polyomino.org.uk/publications/2004/star-polygon-tiling.pdf.
9. Bowers, J. (2012). Regular polygons and other two-dimensional shapes, Page created by, 2012. Polytope.net http://www.polytope.net/hedrondude/polygons.htm

Marija Obradović, architect, is an Associate Professor of Faculty Civil Engineering at the University of Belgrade, Serbia. She is teaching Descriptive Geometry, Computational Geometry and Visualization and presentation of 3D model in geodesy. She has participated in several national projects dealing with the development of technology and digitizing of national heritage, including the application and visualization of geometric contents. She authored two books, and over 70 scientific papers published in national and international journals and proceedings of scientific conferences. Her main interest concerns concave polyhedra of the second sort, introduced in her Ph.D. thesis: Toroidal Deltahedra with Regular Polygonal Bases.

Slobodan Mišić, Associate Professor, graduated in architecture from the University of Belgrade and has been employed in the Faculty of Applied Arts in Belgrade. He took his Ph.D. in 2013 with a thesis entitled Constructive – geometric Generating of Cupolae with Concave polyhedral Surfaces. In his scientific research, he is engaged mostly in general collinear planes, constructive geometry and polyhedral structures in architecture, engineering and arts.

Chapter 5
Filling Space with Gyroid Symmetry

Ulrich Reitebuch, Henriette-Sophie Lipschütz, and Konrad Polthier

Abstract The gyroid is a triply periodic minimal surface that belongs to the associate family of the Schwarz P and D surfaces, and has several point reflection, rotational and translational symmetries. A discrete gyroid can be built from triangles—it is a discrete surface with the same symmetries as the smooth gyroid surface, and it is discrete minimal. Each, the gyroid and the discrete gyroid, splits 3D space into two interlinked half-spaces, which are symmetric to each other. We present a pair of solid building blocks that, together, fill space, and each of them fills one of the half-spaces created by the discrete gyroid.

Minimal Surfaces

In differential geometry, a surface that locally minimizes the surface area is called a minimal surface. Many minimal surfaces are highly symmetric and have rotational, translational, mirror reflection, and point reflection symmetries. According to the Weierstrass representation, minimal surfaces can be computed as:

$$x_k(\zeta) = \Re\left(\int_0^\zeta \varphi_k(z)\,dz\right) + c_k, \quad k = 1,2,3$$

$$\varphi_1 = \frac{1}{2}f\left(1 - g^2\right)$$

$$\varphi_2 = \frac{1}{2}f\left(1 + g^2\right)$$

U. Reitebuch (✉) · H.-S. Lipschütz · K. Polthier
Freie Universität, Berlin, Germany
e-mail: ulrich.reitebuch@fu-berlin.de; Henriette.Lipschuetz@fu-berlin.de;
konrad.polthier@fu-berlin.de

$$\varphi_3 = fg$$

with suitable complex functions f and g and complex constants c_k. If a curvature line of the minimal surface is entirely contained in a plane, the surface is mirror symmetric at that plane; if the surface contains a straight asymptotic line, this line is an axis of 180° rotational symmetry for the surface.

By a factor $e^{i\vartheta}$ we get a 1-parameter family of minimal surfaces

$$x_k\left(\zeta,\theta\right) = \Re\left(e^{i\vartheta}\int_0^{\zeta}\varphi_k\left(z\right)dz\right)+c_k, \quad k=1,2,3,$$

called the associate family, and the angle θ is called the Bonnet angle. Changing the Bonnet angle by pi/2 transforms planar curvature lines into straight asymptotic lines and vice versa [1]. Any rotational symmetry of a minimal surface with rotation axis perpendicular to the surface is kept during the Bonnet transformation.

Discrete Minimal Surface

A discrete surface consists of vertices, straight edges, and planar polygonal faces. We call a discrete surface *minimal*, if the surface area cannot be decreased by moving a single interior vertex, keeping all the other vertices fixed [2].

The Gyroid Surface

The gyroid is a triply periodic minimal surface that belongs to the associate family of the Schwarz P and D surfaces. It was found by Alan Schoen [1] and proved to be embedded in 3D by Karsten Große-Brauckmann and Meinhard Wohlgemuth [3]. The gyroid has several point reflection, rotational and translational symmetries but, in contrast to the Schwarz P and D surfaces, it does not have any mirror reflection symmetries and does not contain any straight lines. However, the gyroid does have four-fold and six-fold rotary reflection symmetries with rotational axes perpendicular to the surface. The gyroid splits 3D space into two halves that are mirror symmetric to each other.

A Discrete Gyroid Surface

A discrete gyroid surface can be constructed from triangles in such a way that it is a discrete minimal surface and has exactly the same symmetries as the smooth gyroid surface [4]. Translational units of the smooth and discrete gyroid surface are shown in Fig. 5.1. If the translational unit is a cube with edge length 1 and has integer coordinates at the corners, all vertex coordinates of the discrete gyroid are integer multiples of $\frac{1}{8}$.

Space-Filling Solids

We present a pair of solids that, together, fill 3D space. We start with a truncated octahedron. We select a pair of opposite hexagons, and then select a set of short diagonals in the remaining six hexagons such that none of these has a common vertex with the first two hexagons and the six diagonals form a cycle. There are two possible choices of short diagonals fulfilling these conditions. Now we connect each of these six diagonals to the centre of gravity of the truncated octahedron, building six triangles. The surface given by these six triangles cuts the truncated octahedron into two solids. Each of the two solids is bounded by the six cut triangles, one complete original hexagon and three complete squares from the truncated octahedron, and three big and three small parts of hexagons, cut by the selected short diagonals. Neither of the two solids has any mirror symmetry, but they are symmetric to each other. The cut triangles are shown in Fig. 5.2 as white triangles, the remaining surface of the truncated octahedron is shown in blue.
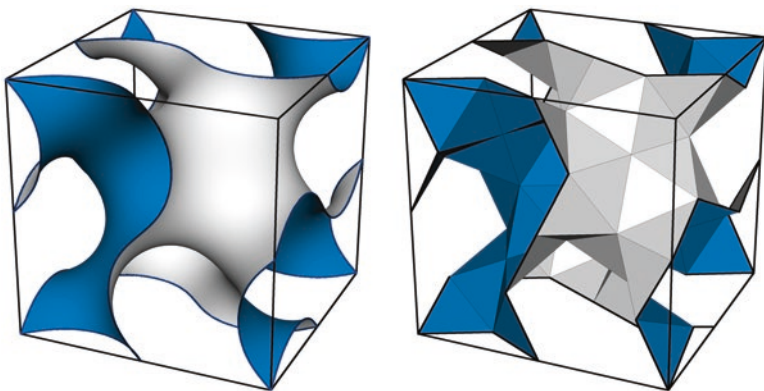
Fig. 5.1 Translational unit of smooth and discrete gyroid surface

Fig. 5.2 Cutting the
truncated octahedron into
two solids
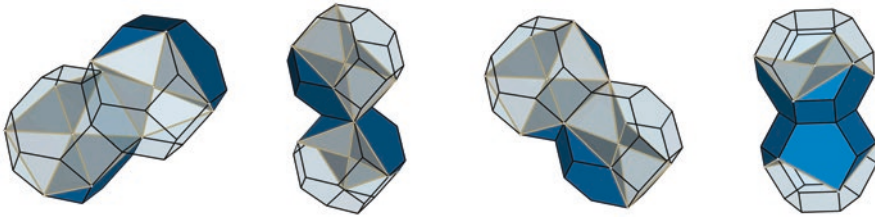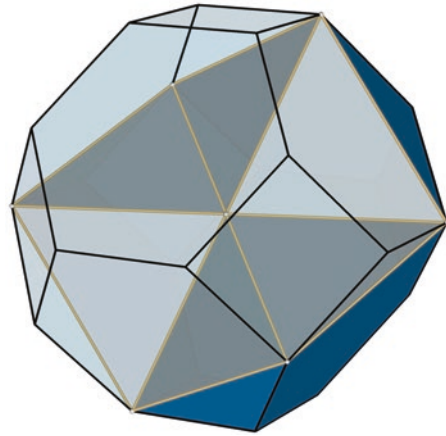
Fig. 5.3 Four ways of attaching solids: at triangles, squares, pentagons, and hexagons

Filling Half-Space

Using copies of just one of two solids, half of 3D space can be filled. Since all the
parts of the original faces of the truncated octahedron have mirror symmetry, the
solids can be attached to each other at these faces in different ways, as shown in
Fig. 5.3: attaching small (triangular) parts of hexagons, attaching squares, attaching
big (pentagonal) parts of hexagons, or attaching complete hexagons. When attach-
ing solids at squares, there are four possibilities; for hexagons there are two possi-
bilities up to symmetry. Here we have to take care that all edges show combinations
of faces, where a third copy of the solid can be attached to both solids. For the
square, the vertex at the cut-triangle surface has to be aligned; for the hexagon the
squares of the two solids must not share an edge. For the triangular and pentagonal
faces at the original truncated octahedron faces, there is only one possible way of
attaching a neighbouring solid face to face.

By these gluing rules, solids of the same type can be glued to all the faces that
are not incident to the point at the centre of gravity of the complete octahedron, in
such a way that only these cut triangles remain unglued. In this way, the cut trian-
gles form a discrete gyroid surface and one type of solid fills one of the two half-
spaces bounded by the discrete gyroid; the other type fills the other half-space. A set

of glued solids is shown in Fig. 5.4; the blue faces of the solids are glued, and the white faces build the discrete gyroid surface.

A. H. Schoen's M6 Surface

During his search for the gyroid surface, A. H. Schoen found a surface he called M6 [5], constructed from a minimal surface spanned by a skew hexahedron. The skew hexagon used for this construction has exactly the same boundary as the six-triangle patch of our discrete gyroid inside the truncated octahedron. A skew hexagon patch of the M6 surface is shown in Fig. 5.5. The gyroid symmetries build an infinite non-self-intersecting surface from the M6 minimal surface patch; this M6 surface is not differentiable at the boundaries of the hexagon patches, but it has the full symmetries of the gyroid surface.
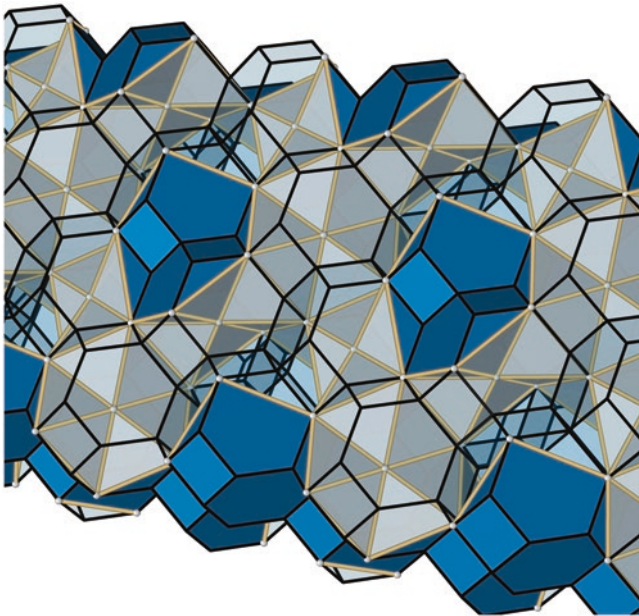
Fig. 5.4   Gluing solids fills half the space; the white surface becomes a discrete gyroid

Fig. 5.5 A
patch of A. H. Schoen's
M6 surface
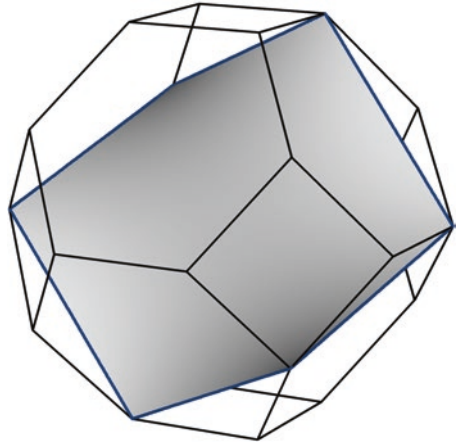
Fig. 5.6 The smooth
gyroid splits the truncated
octahedron into two solids
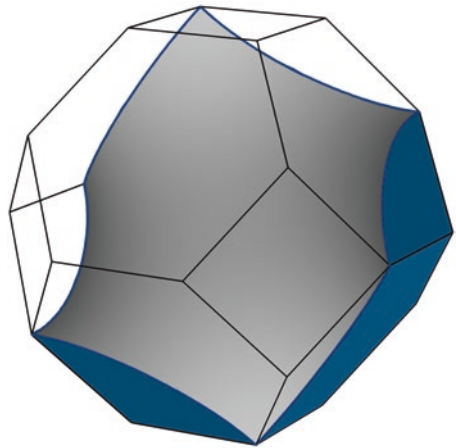
Cutting at Smooth Gyroid Surface

The same construction can be done with a curved cut surface through the truncated octahedron; if the truncated octahedron is placed with its centre of gravity in one of the points with point reflection symmetry of the smooth gyroid surface, the gyroid surface cuts the truncated octahedron into two parts that do not have any mirror symmetry but are symmetric to each other. If the truncated octahedron has the correct scale in relation to the gyroid surface, some of the gyroid's axes of 180° rotational symmetry coincide with face diagonals of the truncated octahedron and the solids can thus be used in the same way to fill one half of 3D space, building a smooth gyroid surface at the volume boundary. The other solid type again fills the remaining half-space. One solid with the smooth gyroid cut is shown in Fig. 5.6.

A.H. Schoen also experimented with hexagonal patches of the smooth gyroid surface and symmetries of the tessellation of 3D space by truncated octahedra [5]. He describes a hexagonal surface patch called *hex90*. This patch is obtained by the Bonnet transformation from a hexagonal patch of the Schwarz P surface bounded by planar symmetry lines. The same patch is bounded by straight asymptotic lines in the Schwarz D surface. The six boundaries of his hexagonal gyroid patch are geodesic lines of the gyroid surface, which connect six vertices of the truncated octahedron, but they are not contained in the hexagonal faces of the truncated octahedron—some parts of these boundary curves of the patch are inside the truncated octahedron, some parts are outside. This patch looks very similar to the patch shown in Fig. 5.6, but it is not the same. The boundaries of our patch, which is cut out of the gyroid surface by the faces of the truncated octahedron, are not geodesic lines of the gyroid surface. The surface is not perpendicular to the hexagonal faces of the truncated octahedron except for the midpoint of each hexagonal boundary curve.

Our patch boundary curve is contained in a hexagon of the truncated octahedron, and due to the gyroid's 180° rotational symmetry at certain diagonals of hexagons of the truncated octahedron, the curve has a mirror symmetry in the plane of the hexagon, so the solids with curved cut surface fit together in the same way as the solids cut by the discrete gyroid.

Conclusions

The truncated octahedron is a space-filling solid and if a tessellation of 3D space by truncated octahedra is scaled and positioned appropriately in relation to a discrete gyroid surface, the latter splits each of the truncated octahedra in the same way into two parts, which are symmetric to each other. Thus, each of the half-spaces bounded by the discrete gyroid surface is tessellated by one of the two half truncated octahedron solids.

If the same tessellation of 3D space by truncated octahedra is cut by the smooth gyroid surface, it also cuts each truncated octahedron in the same way into two solids, which are symmetric to each other. In this case, the cut surface is curved, and each of the two types of solids tessellates one of the half-spaces bounded by the smooth gyroid surface.

References

1. Schoen, A. H. (1970). *Infinite periodic minimal surfaces without self-intersections*. NASA TN D. National Aeronautics and Space Administration.
2. Pinkall, U., & Polthier, K. (1993). Computing discrete minimal surfaces and their conjugates. *Experimental Mathematics, 2*, 15–36.
3. Große-Brauckmann, K., & Wohlgemuth, M. (1996). The gyroid is embedded and has constant mean curvature companions. *Calculus of Variations and Partial Differential Equations, 4*, 6.

4. Reitebuch, U, Skrodzki, M. and Polthier, K (2019). Discrete gyroid surface. In: *Proceedings of Bridges 2019: Mathematics, Art, Music, Architecture, Education.*
5. Retrieved in November 2019 from https://schoengeometry.com/e-tpms.html.

Ulrich Reitebuch has a diploma in mathematics from Technische Universität Berlin. He works at the department of mathematics and computer science at Freie Universität Berlin and is interested in differential geometry, discrete geometry, tessellations, symmetries, and connections between mathematics and arts.

Henriette-Sophie Lipschütz received in 2016 a master's degree in mathematics and is now working as a scientific researcher at the institute of mathematics and computer science at Freie Universiät, Berlin, Germany, and is currently working on her thesis. Next to discrete differential geometry and its applications, she is interested in differential geometry, Euclidean geometry as well as the theory of polytopes, and graph theory.

Konrad Polthier is full professor of mathematics at Freie Universität Berlin since 2005. His research focuses on discrete differential geometry, applied geometry, geometry processing, and mathematical visualization.

Chapter 6
Odd or Even, Jitterbug Versus Grünbaum's Double Polyhedra

Rinus Roelofs

Abstract Coxeter, Longuet-Higgins & Miller (Coxeter et al. Uniform polyhedra. Philosophical Transactions of the Royal Society London 401–450, 1954) define uniform polyhedra to be vertex-transitive polyhedra with regular faces. They define a polyhedron to be a finite set of polygons such that each side of a polygon is a side of just one other polygon, such that no non-empty proper subset of the polygons has the same property. By a polygon they implicitly mean a polygon in 3-dimensional Euclidean space; these are allowed to be non-convex and to intersect each other. The Jitterbug transformation is a transformation that can be applied on uniform polyhedra in which the number of faces that meet in each vertex is even. Face-doubling, a method to generate new uniform polyhedra by doubling the faces of a known uniform polyhedron, can only be applied if there is at least one vertex in which an odd number of faces come together. This is what Grünbaum stated in his paper *"New" Uniform Polyhedra* (Grünbaum, *Discrete Geometry: In Honor of W. Kuperberg's 60th Birthday*. Marcel Dekker, New York, 2003). So, for each uniform polyhedron, it seems that either the Jitterbug transformation or face-doubling applies. In this paper, I show that this is not always true. And that this fact leads to the discovery of a new uniform polyhedron.

Introduction

The Jitterbug transformation was discovered by Buckminster Fuller in 1948 [1, p. 460.00]. In Fig. 6.1, we see how the octahedron transforms into the cuboctahedron by rotating and moving the triangular faces. Each triangular face is connected to three other triangular faces, meeting vertex to vertex. The movement of each of the triangular faces is a translation along the line that connects the midpoint of the face with the centre of the polyhedron, together with a rotation for which this line is the axis. The Jitterbug transformation needs two different rotation directions. If one triangle rotates clockwise, then all its neighbours rotate counterclockwise. The complete Jitterbug transformation transforms an octahedron back to an octahedron.

R. Roelofs (✉)
Independent Sculptor, Hengelo, The Netherlands
e-mail: rinus@rinusroelofs.nl
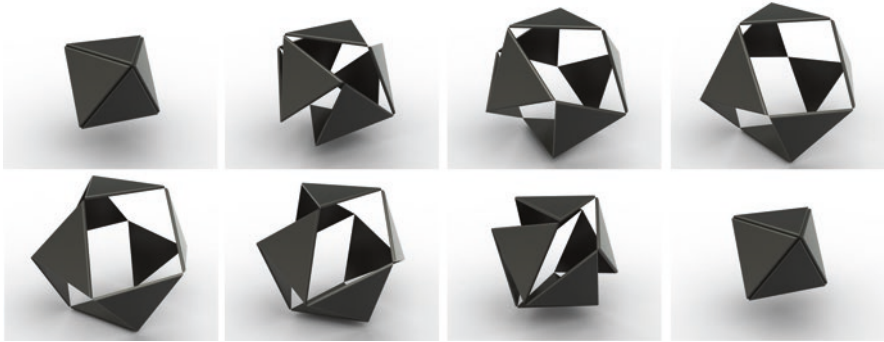
Fig. 6.1 Jitterbug transformation of the octahedron. Sequence of stills of the animation
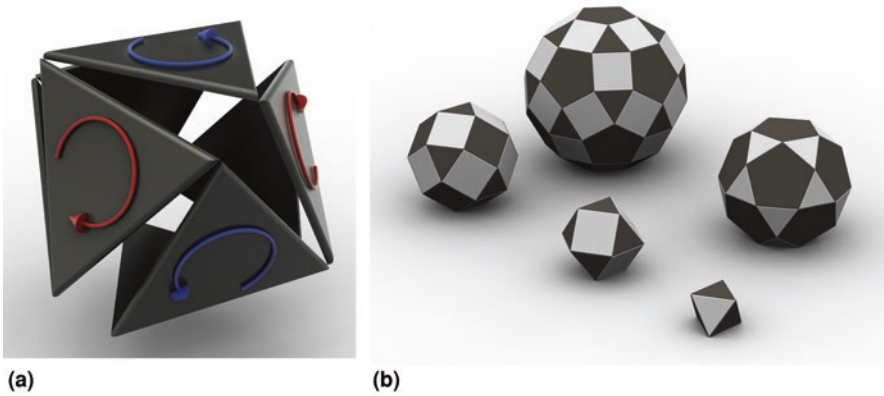
Fig. 6.2 (**a**) Rotation of the faces: clockwise and counterclockwise. (**b**) The five convex regular and semiregular polyhedra with an even number of faces meeting at each vertex

Halfway through this process, the cuboctahedron can be recognized, but the square faces are only suggested by the empty spaces in between the triangular faces.

The Jitterbug transformation connects pairs of faces with opposite rotational directions at their vertices (Fig. 6.2a). Thus, for the Jitterbug transformation to be applicable on a polyhedron, the number of faces meeting at each of the vertices must be even. When we restrict ourselves to the convex uniform polyhedra, the following polyhedra meet this requirement: the octahedron, the cuboctahedron, the rhombic cuboctahedron, the icosidodecahedron and the rhombicosidodecahedron (see Fig. 6.2b) and besides the octahedron also the other antiprisms. Through the Jitterbug transformation, each face is subject to a translation along the axis connecting the centre of the face with the centre of the polyhedron. These are helical movements, and the path described by the movements of the vertices of a face lies on the cylinder that is an extrusion of the circle determined by the vertices of the face. In

the Jitterbug transformation, neighbouring faces always rotate in opposite directions and stay connected at a vertex.

H.F. Verheyen has described the mathematical construction of the Jitterbug movement [2, pp. 203–204]. In Fig. 6.3, the construction of the movement of the Jitterbug transformation is worked out for the cuboctahedron shown in Fig. 6.3a. Figure 6.3b shows one axis for a square face, and another, for a triangular face, as well as the cylindrical surfaces deriving from the extrusion of the circumcircle of each face. The square face and the triangular face stay connected at a vertex during the movement, and thus this vertex lies on both of these cylinders. Thus, the line of intersection of these cylinders (Fig. 6.3c) represents the path the vertex follows during the movement. Consequently, the position of both the square face and the triangular face is defined at each step of the Jitterbug transformation (Fig. 6.3c, d). Accordingly, we can show each step of the cuboctahedron's transformation.

This method can be applied to the each of the five convex regular and semiregular polyhedra mentioned before. In Fig. 6.4, the process of the Jitterbug transformation is shown for the icosidodecahedron.
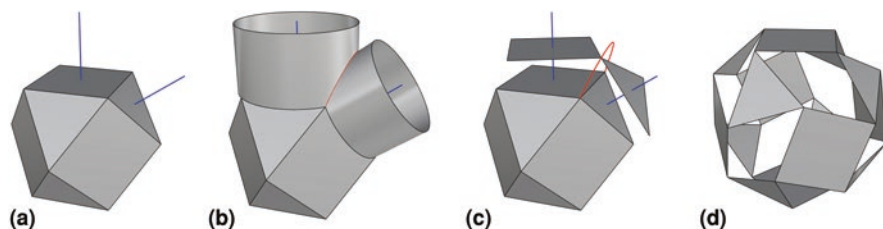
Fig. 6.3 Constructing the movement of the Jitterbug transformation
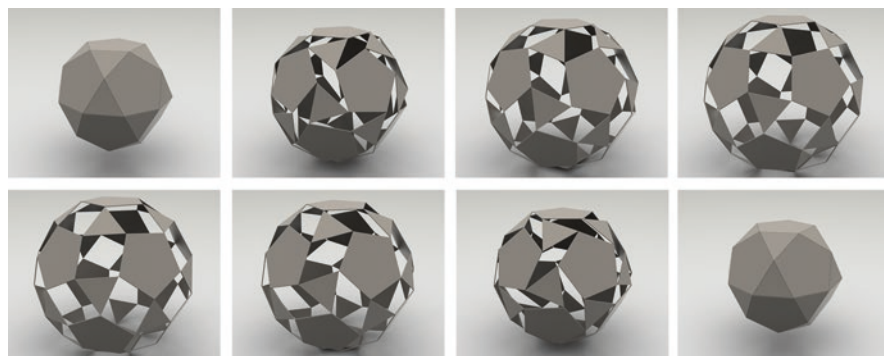
Fig. 6.4 Jitterbug transformation of the icosidodecahedron. Sequence of stills of the animation

Jitterbug Transformations Applied to Non-Convex Polyhedra

The Jitterbug movement can also be applied to non-convex uniform polyhedra, pro-viding the starting polyhedron has an even number of faces that meet at each vertex. As an example, we will take the great ditrigonal icosidodecahedron. It is possible to apply the Jitterbug transformation to the great ditrigonal icosidodecahedron, fol-lowing the construction rules as described by H. F. Verheyen. The resulting anima-tion is presented by eight stills in Fig. 6.5. Remarkably, halfway through the transformation the red pentagonal faces seem to disappear inside the icosahedron formed by the triangular faces.

   Looking more closely at the situation (Fig. 6.6), halfway through the transforma-tion we see that the pentagonal faces are arranged inside the icosahedron in such a way that they form Poinsot's great dodecahedron. The Jitterbug transformation is a loop, and so we could also have used this polyhedron as the starting point for the Jitterbug transformation.
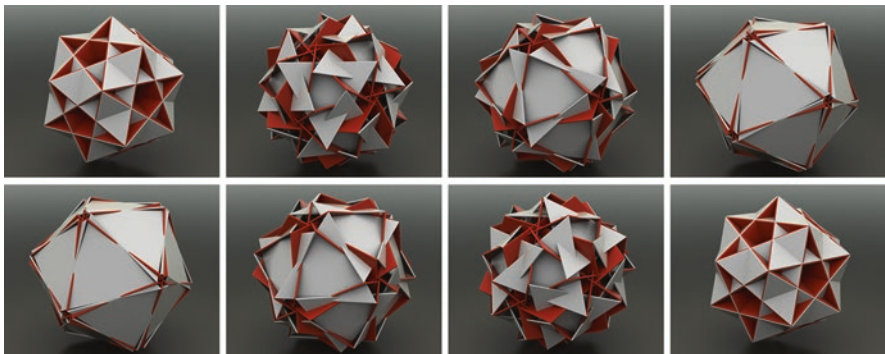
Fig. 6.5 Jitterbug transformation of the great ditrigonal icosidodecahedron
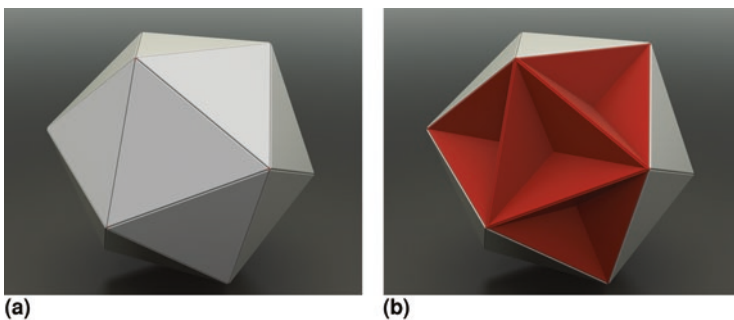
Fig. 6.6 The (**a**) outside and (**b**) inside of the new polyhedron, icosahedron, and great dodecahe-dron combined
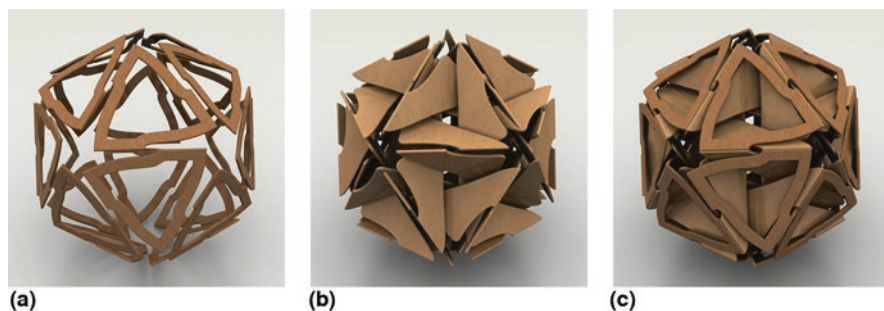
Fig. 6.7 (**a–c**) Icosahedron and great dodecahedron combined. (**a**) Triangular faces. (**b**) Pentagonal faces. (**c**) The complete polyhedron
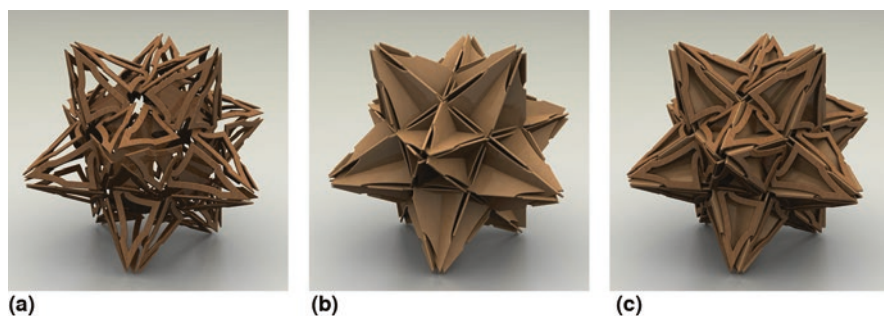
Fig. 6.8 Kepler's stellated dodecahedron and Poinsot's great icosahedron combined. (**a**) Pentagonal star faces. (**b**) Triangular faces. (**c**) The complete polyhedron

Indeed, the total configuration of 12 pentagonal and 20 triangular faces can be seen as a uniform polyhedron, according to Grünbaum's ideas for new polyhedra (Fig. 6.7). The icosahedron and the great dodecahedron have the same edge configuration. Therefore, we can combine them to this new uniform polyhedron. There is another pair of polyhedra with the same edge configuration; Poinsot's great icosahedron and Kepler's small stellated dodecahedron. These two polyhedra can combine to make another new uniform polyhedron (Fig. 6.8).

It turns out that the Jitterbug transformation can also be applied to this new polyhedron (see Fig. 6.9). The animation in Fig. 6.9 may seem to show the complete loop but in fact it is only the first half.

Face-Doubling

As we have seen, the octahedron is the only Platonic solid on which the Jitterbug transformation can be applied, because it is the only Platonic solid with an even number of faces coming together at each vertex. In 1965 Joseph D. Clinton, a
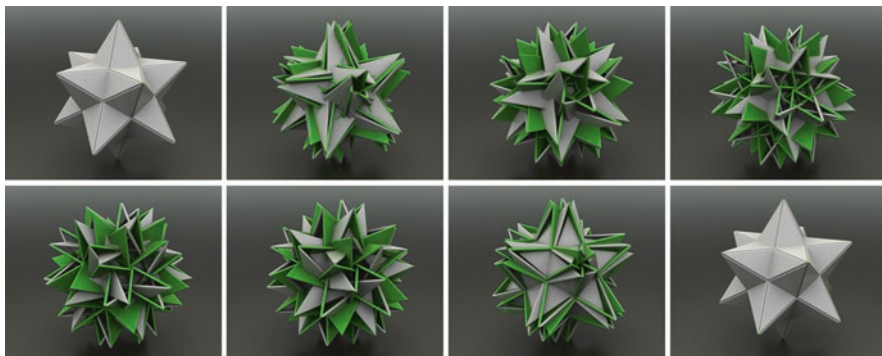
Fig. 6.9 Jitterbug transformation of the Grünbaum-combination of Kepler's small stellated dodecahedron and Poinsot's great icosahedron. Sequence of stills of the animation

Fig. 6.10 (**a**) Clinton's model of the dual face dodecahedron. (**b**) My interpretation of Grünbaum's double dodecahedron

student of Buckminster Fuller, made the first dual face polyhedral transformation model. He doubled the faces of the 'odd' Platonic solids (the tetrahedron, cube, dodecahedron and icosahedron) to become polyhedra in which each vertex has even-valence (meaning that an even number of faces come together at each vertex), and then connected, alternately, each vertex of an outer face to a vertex of an inner face [3, 4]. Clinton's construction, as can be seen in Fig. 6.10a, is now suitable for the Jitterbug transformation.

There is a great similarity between Clinton's double face concept and the face-doubling of Grünbaum where he says:

> Face-doubling replaces each face by one red and one green face, with edges joining only faces of different colours; hence the number of edges is also doubled. Face-doubling doubles the valence of odd-valent vertices, replaces even-valent vertices by two vertices each. Face-doubling results in a polyhedron if and only if the starting polyhedron has at least one odd-valent vertex. Since all vertices of a uniform polyhedron have the same valence, face-doubling is applicable only to uniform polyhedra of odd valence. [5, p. 334]

So, in summary, face-doubling can only be applied on the odd-valent uniform polyhedra and will result in even-valence uniform polyhedra. Then it is possible to apply the Jitterbug transformation.

Jitterbug Transformation Applied to Infinite Uniform Polyhedra

The vertices of the cube have odd valence. So we first double the faces and after that the resulting double-face cube is now ready for the Jitterbug transformation (Fig. 6.11).

Grünbaum remarks in his paper that some generalizations are possible: '*First, one may admit infinite polyhedra, provided they are discrete*'. [5, p. 339]. Clinton too makes use of this generalization in his dual-face models of Archimedean tilings. There are two infinite regular tilings with vertices of even valence and thus can be considered for the Jitterbug transformation. The even valence verified by the fact that these tilings are two-colourable, that is, every white tile is surrounded by black tiles and vice versa (Fig. 6.12a). The two colours, black and white, are translated into two different rotational directions by the Jitterbug transformation, clockwise and anticlockwise. In Fig. 6.12b, the different colours of the tiles are represented by the two different coloured arrows. The arrows now show the rotation direction of the Jitterbug transformation.

There are more ways to build infinite regular structures with only square faces. The column shown in Fig. 6.12c can be seen as a part of an infinite uniform polyhedron. The valence of all vertices is even and thus the Jitterbug transformation can be applied (Fig. 6.13). Note that the square faces of this infinite column can be
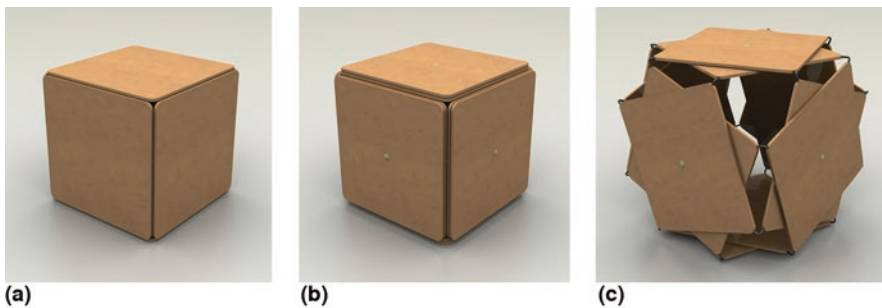
Fig. 6.11 (**a**–**c**) Cube and Dual-face cube, on which the Jitterbug transformation can be applied
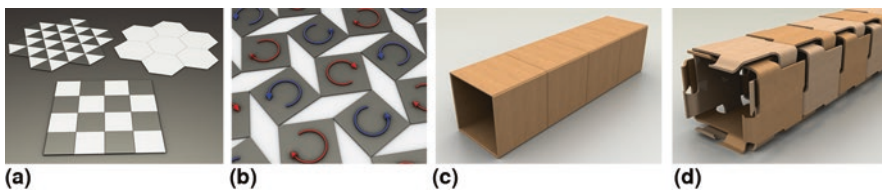
Fig. 6.12 (**a**) The three regular infinite tilings. (**b**) A step in the Jitterbug transformation applied on the 4.4.4.4-tiling. (**c**) Square column with square faces. (**d**) Doubling the square faces of the column of Fig. c
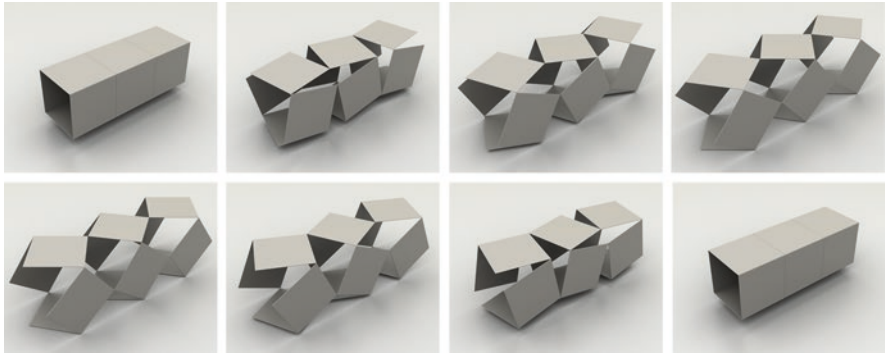
Fig. 6.13 Jitterbug transformation applied on a regular infinite column with square faces
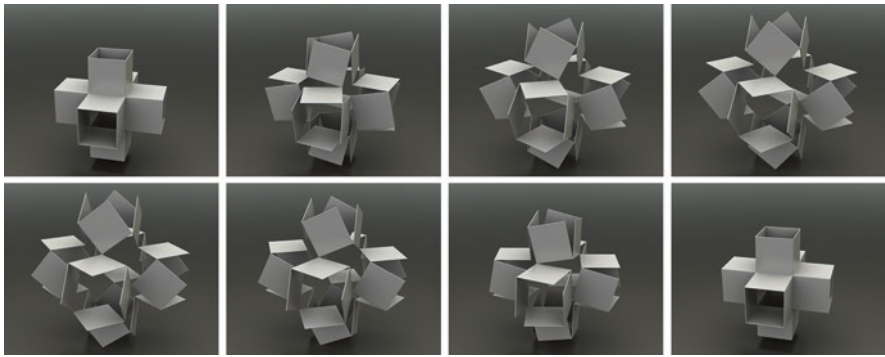
Fig. 6.14 Jitterbug transformation of a fragment of the infinite Petrie-Coxeter 4.4.4.4.4.4 polyhedron

2-coloured like the checkerboard colouring of the planar tiling by squares. Applying Grünbaum's method of doubling the faces, to this column, will not result in a new uniform polyhedron because there is no odd valence vertex. The result will be a compound of two entwined polyhedra. On the other hand, the Jitterbug transformation works as expected, as can be seen in the stills of the animation (Fig. 6.13).

A next step brings us to the infinite Petrie-Coxeter polyhedron 4.4.4.4.4.4 in which all vertices have even valence. The Jitterbug transformation should be applicable because all vertices have even valence. Indeed, this is the case, as shown in Fig. 6.14, in which we can see a sequence of stills of the animation of the Jitterbug transformation of a fragment of the Petrie-Coxeter 4.4.4.4.4.4 polyhedron.

Here too, because there are no odd valence vertices, Grünbaum's face-doubling results in a compound of two entwined polyhedra, shown in Fig. 6.15b [6]. Another infinite polyhedron worth investigating is the infinite Petrie-Coxeter polyhedron 6.6.6.6 (Fig. 6.15c) that is the dual of the infinite Petrie-Coxeter 4.4.4.4.4.4. Here too, face-doubling doesn't result in a new polyhedron because all vertices are even
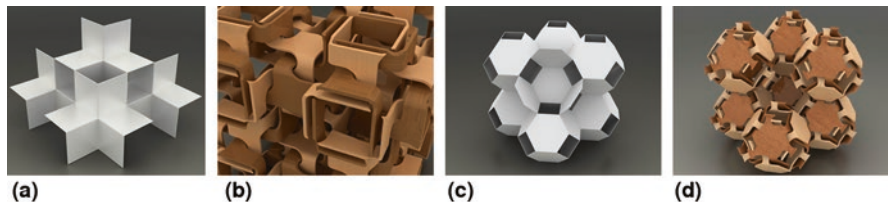
Fig. 6.15 (**a**) Fragment of the infinite Petrie-Coxeter polyhedron 4.4.4.4.4.4. (**b**) Compound after face-doubling. (**c**) Fragment of infinite Petrie-Coxeter 6.6.6.6 polyhedron. (**d**) Compound as a result of face-doubling of the infinite Petrie-Coxeter 6.6.6.6 polyhedron
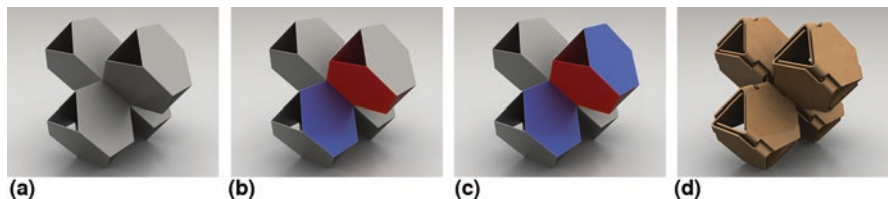
Fig. 6.16 (**a**) Fragment of the infinite Petrie-Coxeter 6.6.6.6.6.6. (**a–c**) Colouring the faces to investigate if and how the Jitterbug transformation can be applied. (**d**) Doubling the infinite Petrie-Coxeter 6.6.6.6.6.6

valence, but in a compound, a pair of two entwined polyhedra. Again, though face-doubling doesn't work because of the even-valent vertices, the Jitterbug transformation is possible.

The last infinite regular polyhedron we have to examine is the infinite Petrie-Coxeter 6.6.6.6.6.6, shown in Fig. 6.16a. We know that the Jitterbug transformation gives each face a rotational direction; if one face rotates clockwise, then its neighbouring faces have to rotate anticlockwise.

In order to assign a rotational direction to the faces of the polyhedron, we begin to colour the faces, blue for clockwise, red for anticlockwise (Fig. 6.16b). When we continue colouring the faces, we can colour the next hexagon blue again (Fig. 6.16c), but then we have a problem. The hexagon that adjoins that face has both a blue and a red coloured neighbour. The conclusion is that this polyhedron is not two-colourable, so that the Jitterbug transformation cannot be applied to this polyhedron, despite the fact that all its vertices have even valence.

Conclusion

This example shows that even valence of all vertices is a necessary condition for a polyhedron to be able to have the Jitterbug condition applied but is not a sufficient condition. The ability for faces to be 2-coloured is also necessary. For the Petrie-Coxeter 6.6.6.6.6.6, we now have to analyse face-doubling. The result is a real

"*new*" uniform polyhedron (see Fig. 6.16d). This example shows that when face-doubling applied to infinite uniform polyhedra, Grünbaum's requirement that in order to produce a new polyhedron at least one vertex has to be of odd valence [5, p. 4] is thus not necessary. It should be replaced by the polyhedron which is not two-colourable [5]. For the Jitterbug transformation to be possible, we should replace the requirement that all vertices have even valence by the requirement that the polyhedron is two-colourable. This is a stronger requirement.

References

1. Buckminster Fuller, R. (1975). *Synergetics*. MacMillan Publishing, inc..
2. Verheyen, H. (1989). The complete set of jitterbug transformers and the analysis of their motion. *Computers Mathematics Application, 17*(1–3), 203–250.
3. Clinton, J. (1971). *A geometric transformation concept for expanding rigid structures*. NASA.
4. Clinton, J. Intersecting cylinders and the Jitterbug, *Bridges Conference Proceedings, Winfield*, 2004. pp. 345–346.
5. Grünbaum, B. (2003). "New" uniform polyhedra. In *Discrete geometry in honor of W. Kuperberg's 60th Birthday* (pp. 331–350). Marcel Dekker.
6. Roelofs, R. The elevation of Coxeter's Infinite Regular Polyhedron 444444, *Bridges Conference Proceedings, Jyväskylä*, 2016. pp. 33–40.

Rinus Roelofs, After studying Applied Mathematics at the University of Twente, Rinus decided switching to the School of Arts and start a career as a sculptor. Inspired by the works of M. C. Escher and Leonardo da Vinci, the main subject of his artistic explorations are mathematical structures.

The computer is Rinus' main sketchbook and each of his ideas begins with a picture on the screen, later materialized as a rendered picture, an animation or a 3D physical model using laser cutting or rapid prototyping. In 2020, he got a PhD at the University of Leuven, Belgium, with a thesis on new uniform polyhedra.

Chapter 7
From Geometry to Reality: Designing Geodesic Structures

Gianluca Stasi

Abstract In order to adequately address the design and construction of geodesic structures, it is necessary to analyze the multiplicity of factors that so far have been considered as unequivocal. These start with the subdivision methods by which geodetic meshes can be generated, through the configuration of sets of specific tools to work on their definition and finally their adaptation to specific construction methods.

A given geodesic geometry cannot, in fact, be applied to different construction methods without adapting it to their characteristics and peculiarities; each of them configures its own specific geometry. For this reason, many of the data and concepts necessary for the definition of specific construction methods are not found in the existing bibliography.

The approach we propose in our research not only allows for a new reading of the existing methods of designing geodesic structures that addresses and tackles the source of their recurrent problems, but also allows the configuration of new construction methods that avoid these problems.

Introduction

In the first part of the twentieth century, Walther Bauersfeld and Richard Buckminster Fuller introduced geodesic technology for dome construction. Geodesic structures make it possible to cover large spans without intermediate supports, and with a high robustness, compared to the weight and characteristics of the constituent materials.

The history of the application of those technologies, however, has been plagued by recurrent pathologies due to approaches and work methods with which today,

G. Stasi (✉)
Ctrl+Z Arquitectura, Seville, Spain
e-mail: luca@ctrlz.net

they continue to be produced. Geodesic structures are based on the subdivision of a spherical surface into smaller interlocking shapes. As Popko warns, unlike the case of the circle, the division of a sphere involves difficulties that are not easily solved despite the use of computers [1, p. XIV]. There are, therefore, a great variety of strategies or systems of subdivision that, starting from different premises, can be used for the distribution of points on a sphere. These strategies are described and analyzed in depth by Popko and can be compared by evaluating their results with different indicators, such as the number of chord factors or the smallest, absolute or relative, variation between the largest and smallest of them, the number of different types of triangles formed by the geodesic mesh or variations in their size.

Some systems were created to facilitate calculation; others were created to meet specific objectives such as structural efficiency, compliance with technical requirements or a better adaptation to production and execution operations.[1] The systems vary widely, and the choice of a particular system influences both the efficiency and applicability of the meshes to the construction method. The measures and angles datasets obtained in the designs done during the sixties and the seventies were disseminated in a context in which there was a widespread belief that only one geodesic geometry existed that would provide fixed values for each frequency of subdivision.[2]

The presentation of different sets of data without explaining the different systems used for subdivision fostered a discussion, still active today, on the accuracy of these calculations. To this end and even today, assembly problems and recurrent construction pathologies have been attributed to these structures.[3] In fact, different datasets correspond to the application of different subdivision strategies, and the origin of inconsistencies must be sought in other factors.

Geodesic structures are generally defined as triangulated meshes. In fact, independently from the used subdivision system, three chords joining three adjacent vertexes form a triangle. The illustrations used in the existing bibliography contributed to this idea, by representing the geodesic systems from the chords, and not from the arches which define the corresponding spherical triangles. However, in the case of geodesic meshes, the measurement of the three sides is not sufficient to

---

[1] The applicability and opportunity of a subdivision method depend on the constructive system with which a structure is going to be built. This fact has stimulated the creation of a great number of different geometrical and non-geometrical subdivision systems that were categorized as Class I, Class II, and Class III, and the several methods that can be applied to them.

[2] In this regard, Prenis relates an encounter that happened during the winter of 1970 between David Kruschke, future author of the self-edited *Dome cookbook of geodesic geometry*, and the authors of the *Domebook*, in which the latter rejected the possibility of the existence of a set of chord factors capable of configuring a flat-based $v3$, thus both *Domebook* and *Domebook 2* presented conceptual inexactitudes about $v3$ and odd frequencies in general [2, p. 99].

[3] Lloyd Kahn, author of the *Domebook* [3] and *Domebook 2* [4], two of the most early and influential references for domes self-construction, included the *Domebook 3* in his book *Shelter* [5]. Lloyd dedicates the chapter *Smart but not wise* to the broken promises of the geodesic designs, reporting the nostalgia of the domes pioneers towards traditional ways of building, due to problems with domes referring specially to waterproofing, durability, and maintenance.

characterize those triangles, since they do not belong to a Euclidean plane. Although three points define a plane, the triangles defined by the chords still belong to a spherical system and, therefore, for their geometric definition, other data is necessary. Some of these data refer to the geometrical definition of a *double curvature triangulated mesh* and can be calculated from the three chords' factors and the radius of the spherical system. Others must necessarily be adapted to the specific characteristics of the construction system that will be used. Thus, it will be necessary to define other data, related to the used constructive method, in a subsequent phase of calculation and design.

A given geodesic geometry, in fact, cannot be applied to different construction methods without adapting it to their characteristics and peculiarities; each of them configures its own geometry. For this reason, many of the data and concepts necessary for specific construction methods are not found in the existing bibliography.

During the last ten years, we sought to integrate the development of theoretical research on the subject, with the creation of practical experiences of participative, real scale self-construction of proposed models.[4] Their accomplishment provided different communities with equipment and infrastructure they needed, and, at the same time, an opportunity for us to check the developed models, collect data for further improvements, and endorse the technology transferring protocols used for the inclusion of the local community in the involved processes. These experiences highlighted the need to consider and define a wide range of new concepts and refinements, for the analysis of construction methods applicable to geodesic structures and the different geodesic geometries that generate them.

The Subdivision Methods

The adaptation of the geometry of a geodesic mesh to the characteristics of the construction method that will be used for its materialization is fundamental to avoid the appearance of assembly problems and of those pathologies frequently detected in the implementation of buildings based on geodesic meshes. Therefore, it is advisable, as a first step, to choose a subdivision system for the configuration of a structure that is suitable for the chosen constructive method.

For the design of geodesic subdivision meshes, it is convenient to divide the surface in an orderly manner following a repetitive pattern to promote structural efficiency, facilitate production, and provide harmony and aesthetics to the final product. Popko indicates how, by uniformly distributing a set of points over the

---

[4] The author of this study has designed and built more than 25 experiences during the last ten years, e.g., the roofing for the *El Nodo* cultural centre (Saltillo, Mexico, 2010), the urban gardens equipment *Sorbole* (Seville, Spain, 2016) or the structure built for the *Biennale Architecture Lyon* (Lyon, France, 2017), all of which were constructed with local community members. Knowledge transfer programs were also developed, as the one for the *34th European Architecture Students Assembly Festival* (Veliko Tarnovo, Bulgaria, 2014) directed to architecture European students, etc. [6]

surface of the sphere, spherical polyhedra provide an appropriate starting point for further subdivisions [1, p. 191].

The use of spherical regular polyhedra as the basis for the configuration of geodetic meshes is not a new approach,[5] and it has been used since the beginning of the study of geodesic tessellations for various reasons, ranging from a greater repetition of the base element on the sphere, to aesthetic and even esoteric considerations. Most geodesic structures have been realized using the icosahedron as generator polyhedron.

Popko himself introduces the concept of Principal Polyhedral Triangle (PPT) as the basic unit of a geodesic mesh, proposing the use of the equilateral spherical sections configured by regular polyhedra as a workbench for subdivision and then applying the result to the rest of the sphere without any overlapping or discontinuity [1, p. 470]. Figure 7.1 shows the uniform distribution of points on the sphere and the Principal Polyhedral Triangle for the five Platonic solids.

In the report *Structural Design Concepts for future space missions* delivered to NASA in 1965 by Joseph D. Clinton [7], the number of equal parts into which the edge of the PPT is subdivided is defined as *Frequency*. This definition is maintained in case of subdivisions with different measures. In general, the frequency is indicated by the Greek letter ν (nu) followed by the number of subdivisions.

Clinton divided the subdivision systems in two families: Class I, which includes the subdivision *Alternate*, developed by Don Richter, Jeffrey Lindsay, and Duncan
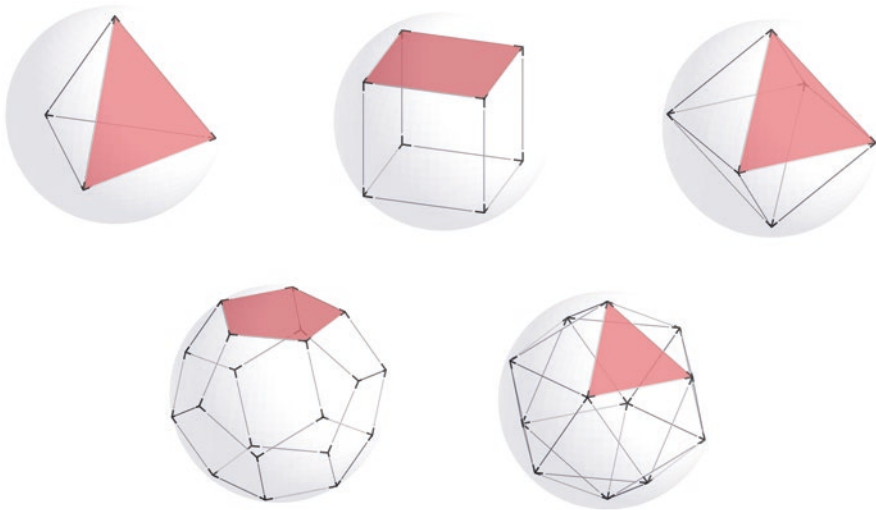
Fig. 7.1 Points' distribution and Principal Polyhedral Triangle in the five Platonic solids

---

[5] Prenis [2], Clinton [7], Kenner [8], Wenninger [9], Kahn [3–5] indicate spherical polyhedra and the platonic solids as the more appropriate base to start the regular subdivision of a spherical surface.

Stuart in the early 1950s, and Class II which includes the subdivision *Triacon*, developed in 1952 by Duncan Stuart. The *Alternate*, also known as *Ford Subdivision*, is characterized by mesh elements approximately parallel to the edges of the base polyhedron. In the *Triacon*, however, they are approximately perpendicular to it.

A Class III mesh was described in Magnus Wenninger's book *Spherical Models* [9] for those rotated meshes that form an angle with the edges of the PPT. Our study will not discuss Class II, or III subdivision meshes. Figure 7.2 shows diagrams of the Class I and Class II subdivisions and their most common frequencies.

These subdivisions may be created by the *Equal Chords Method* (Fig. 7.3a) or the *Equal Arcs Method* (Fig. 7.3b). The more diffuse subdivision method for the design of geodesic meshes is the *Equal Chords*. In this method, once the tessellation has been traced over the PPT, the new obtained vertices are projected onto the spherical surface. While on the PPT, the distance between vertexes is constant, the geometry of the model implies that the greater the distance between the spherical surface and the PPT, the greater will be the distances between the vertices and the area of the new triangular tessellation created on it. Even if all the chords and tiles are equal at the PPT level, their projection creates a very uneven geometric configuration on the spherical surface.

On the other hand, the *Equal Arcs (Three Great Circles)* subdivision system, divides into equal parts the angle defined by each chord of the PPT with the center
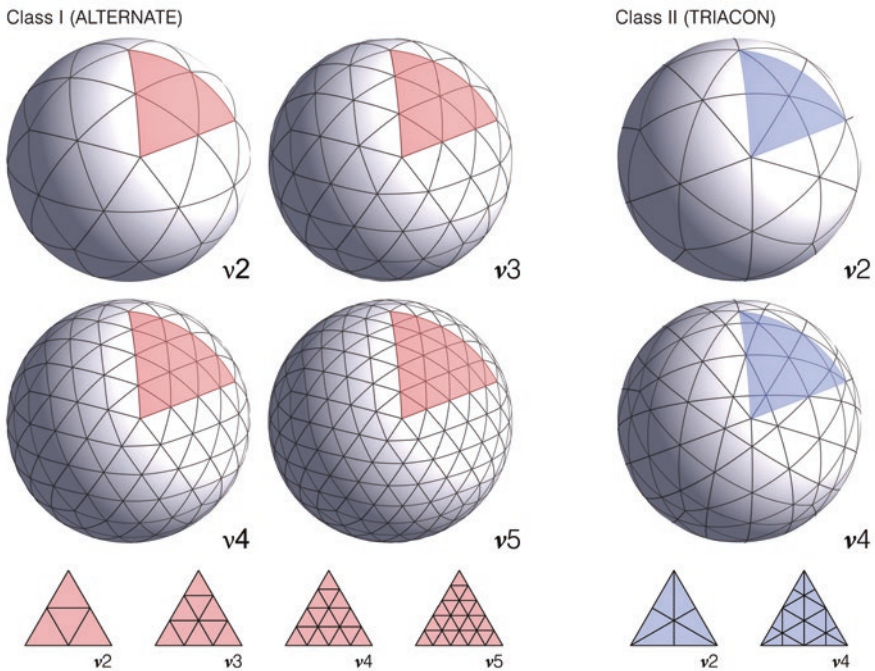
Fig. 7.2 Subdivision Class I/*Alternate* (frequencies $v2$-$v5$) y Class II/*Triacon* (frequencies $v2$ y $v4$)
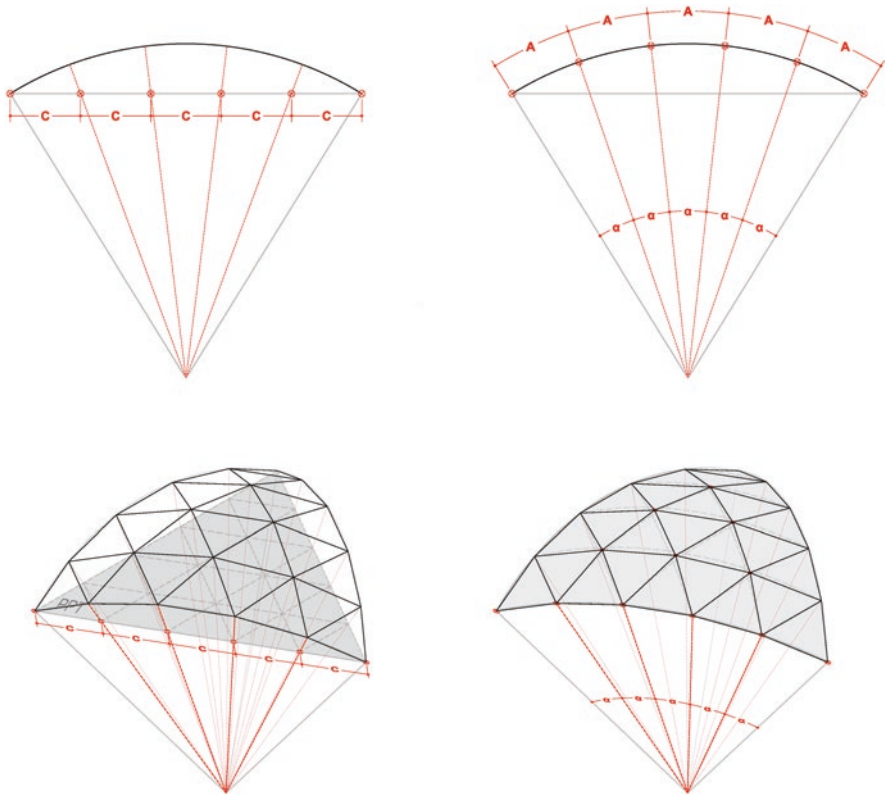
Fig. 7.3 Different subdivision methods for geodesic tessellation: for the same subdivision class and frequency each method will generate a different set of chord factors. (**a**) *Equal Chords Method.* (**b**) *Equal Arcs* (*Three Great Circles*)

of the spherical system, or the arcs of the perimeter of the spherical portion corresponding to the PPT itself. From the new points defined on the perimeter of the spherical PPT, new arcs, which are also divided into equal parts, are drawn for the definition of the new vertices of the tessellation on the spherical surface, corresponding with their intersections. Popko [1, p. 211] tells us how to proceed in the case in which the points defined by the three arcs do not coincide perfectly creating small triangular *windows*: find the centroid of each of these triangles and project it on the sphere. Working directly on the arcs formed on the spherical surface, this subdivision system promotes a more homogeneous subdivision of the surface.

As mentioned, the icosahedron is at the base of the geometry of most geodesic structures. Analyzing the results of the application of these two subdivision systems on it for frequencies from v3 to v8 (Class I), it can be noticed how the results of the subdivision with the *Equal Arcs (Three Great Circles)* method remain almost constant or present subtle variations while, when increasing the frequency, those of the *Equal Chords* tend to present more heterogeneous values, due to the projection that

Table 7.1 Comparative analysis of subdivision systems *Equal Chords* and *Equal Arcs* (*Three Great Circles*) for frequencies from 3 to 8 (Class I)

	ν3 (E.C.)	ν3 (E.A.3)	ν4 (E.C.)	ν4 (E.A.3)	ν5 (E.C.)	ν5 (E.A.3)
Lenght	84.53%	86.53%	77.92%	85.89%	75.74%	85.59%
Surface area	79.04%	87.04%	66.42%	87.52%	65.00%	87.12%
Axial agle	84.36%	86.37%	77.79%	85.79%	75.65%	85.52%
	ν6 (E.C.)	ν6 (E.A.3)	ν7 (E.C.)	ν7 (E.A.3)	ν8 (E.C.)	ν8 (E.A.3)
Lenght	75.04%	85.43%	73.30%	85.33%	72.55%	85.27%
Surface area	61.99%	87.87%	58.94%	88.08%	57.76%	87.99%
Axial agle	74.98%	85.38%	73.25%	85.30%	72.52%	85.24%

this system implies. Table 7.1 presents the results of the application of these two subdivision systems for frequency from three to eight, returning the percentage of the smallest of the values divided by the largest of each set, analyzing the length, the area, and the axial angles.

The heterogeneity of the subdivisions directly influences not only the applicability of the produced subdivision to concrete construction systems, but also the structural efficiency and the appropriateness of materials for its implementation. It is necessary to emphasize that the subdivision system by *Equal Arcs*, presented and analyzed in all its variants in Popko's *Divides Spheres* is not a recent advance, in fact, this kind of focus was already included in the chapter *Geodesic Math* that Joseph D. Clinton prepared for *Domebook 2* published in 1971 [4]. The use of the *Equal Chords* subdivision system was preferred in the seventies because it offered, in combination with the *spherical coordinate system*, a fast, reliable, and simple method to calculate new subdivisions even for very high frequencies.

Nowadays, the development and technological accessibility, together with the understanding that the use of this method contributes to constructive pathologies related to this type of structures should discourage its use. Notwithstanding, the *Equal Chords* subdivision method continues to be used as a reference in domes' self-construction manuals and in the most important digital references. This subdivision method is often used to generate datasets for the *GoodKarma* construction that will be analyzed in the second part of this research.

One of the most common defects found in published geodesic tessellation tables [7] is that they do not clearly indicate the system used for the subdivision.[6] Besides the subdivision methods mentioned in this paper, there is a wide range of options and variations. For example, the *Equal Arcs* subdivision method has several variants such as the *Two Great Circles* [1, p. 208] or the *Mid Arcs* [1, p. 213].

It is fundamental to be aware of the existence of this multitude of classes, systems, and methods of subdivision. This is the only way to understand how different

---

[6]Today, the principal digital references are www.desertdomes.com, active since 1999 and www.simplydifferently.org, active since 2008. Some of the contemporary self-edited manuals are from D. Larrauri [10], C. Zambrano [11], or M. Acosta [12]. Although none of these references indicates their subdivision method, all of them use the *Equal Chords*.

results are developed from different procedures and the importance of the tables that report them. Much of the confusions that have characterized the beginnings of these technologies, and many of today's discussions still, lie in the lack of understanding of this multiplicity and of their underlying concepts. Having seen how the lack of knowledge on these questions has caused confusions and discussions, we will address some results of research we have developed, considering this multiplicity and its independent applications to the Class, Frequency, System and Method of subdivision for the generation of the initial geometry.

Study Case: The *GoodKarma* Constructive Method

The operations to be carried out to adapt a geodesic mesh to a specific construction method can be presented using the study case of the constructive method popularly known as *GoodKarma*. *GoodKarma* is one of the most widespread methods for the self-construction of geodesic structures, due to the existence of several informal manuals, which, starting with self-edited booklets in the seventies, are today disseminated in different formats through the Internet. They are extremely popular among dome enthusiasts. This method can be used as an example to explain the problems that arise when adapting a generic geodesic geometry to specific methods. As shown in Fig. 7.4, the *GoodKarma* method organizes wooden modules around each vertex.

This type of distribution of elements around a vertex can be configured in different ways, but each of them requires different adaptation operations. This method can be used to introduce new geometrical concepts and at the same time begin to glimpse the multiplicity of construction methods applicable to the construction of geodesic structures.

Fig. 7.4 Hemispheric structure, module, and vertex detail in the *GoodKarma* constructive system

It's necessary not to confuse the *GoodKarma* method with some of its variants such as the *Pease Method*. For the house he built in Carbondale, Illinois in 1960, Buckminster Fuller opted for this method which, like the *GoodKarma*, aligns the widest face of the section of the constructive element towards the center of the geometric system and, consequently, with the Axial Triangle of the Tetrahedron (ATT) of each edge. The ends are cut with the same compound angles used for the configuration of the *GoodKarma Method* and, in a second moment, each element is cut longitudinally according to the Tetrahedron Dihedral Angle (TDA) in its upper and lower parts. The *Pease Method* is, thus, a variation or a direct evolution of the *GoodKarma Method*.

The *Pease Manufacturing Company* of Hamilton, Ohio, which built the house, continued to use the method for years and for this reason this method of construction is known today as the *Pease Method*. Similarly, there are other variations, most of which include longitudinal cuts for design optimization.

Beyond the increase of the technological level, infrastructures, training needs, use of materials, and difficulties in the assembly that they entail, these optimizations only represent successive phases of the *GoodKarma* and the results that are presented for this method are applicable to its variants.

In our research,[7] for each triangle of a given geodesic subdivision mesh that independently form the used subdivision method, the triangle formed by the three chords is named Principal Tetrahedron Triangle (PTT), and the triangle that each one of the chords forms with the center of the spherical system to which they belong is named Axial Tetrahedron Triangle (ATT).

Figures 7.5 and 7.6 help in the visualization and definition of those new operators. The distances between the PTT vertices correspond, by definition, to the measurements of the chord factors that define each PTT. Each ATT has two edges equal to the radius of the spherical system, while the remaining are equal to the corresponding chord factor.

Unlikely other systems that are based on linear elements, the *GoodKarma* constructive method is based on triangular modules. Figure 7.6 shows how to configure each of those modules. Its components are aligned with the three ATT, so that their top faces do not belong to the PTT, but to a plane containing the chord and perpendicular to its corresponding ATT.

To execute the cuts of component's ends, compound angles are used. One of the constituent angles is the axial angle, while the other is not the Internal Angle [IA], but the Principal OrthoDihedral Angle [POA] is formed on this new plane. Figure 7.6 describes how, by definition, each PTT has three IA and six POA. A set of two of these six angles is assigned to each of the three components of each module. Being oriented towards a spherical and, thus, convex surface, the value of the POA is always higher than that of the AI that is formed by the same vertex. Using the IA instead of the POA results in the introduction of structural tensions that are, without

---

[7]As part of his professional activity between 2014 and 2018 and his doctoral studies [13], the author has been doing research on the subject since 2010. Some were included in scientific publications [14–16].
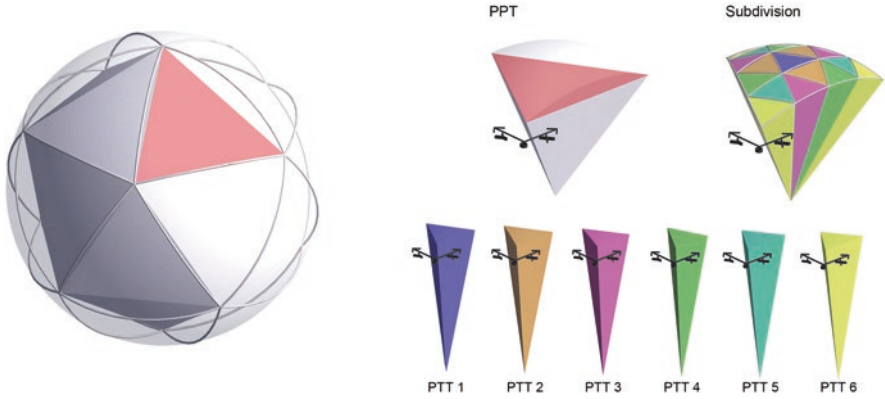
Fig. 7.5 Generation of the PTT from a PPT, Class I, $\nu 4$
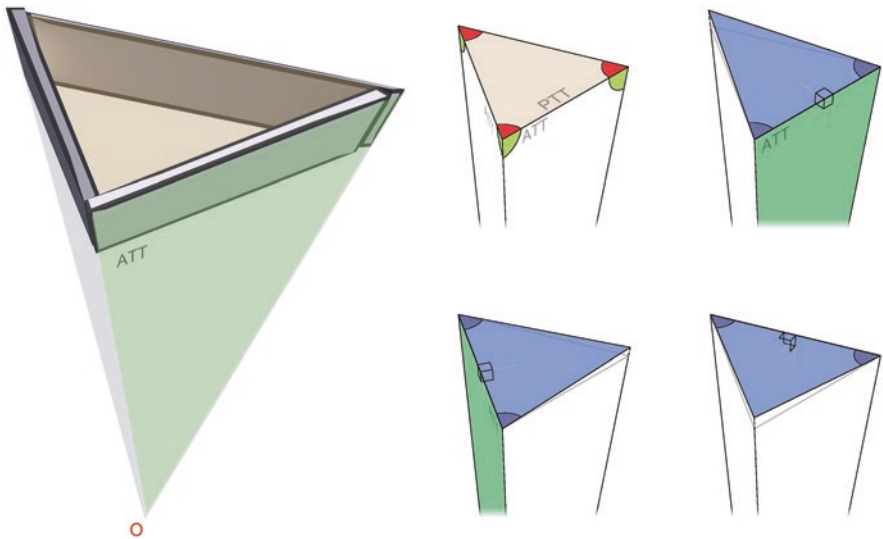
Fig. 7.6 Internal Angles (red), Axial Angles (green), and Principal OrthoDihedral Angles (blue)

any doubt, the main cause of the building and maintenance problems imputed to this construction system.

As the preparation of each triangular module requires six compound angles and, in each vertex of the system, converges five to six modules, the introduced deviations may have significant consequences on the geometry of the whole structure. The rotation of the components upper face, with respect to the PTT, depends on another angle that we have not found in the bibliography we investigated. The Dihedral Angle formed between the PTT under analysis, and those with which it shares one side, isn't, in fact, a functional data to this calculation. It must be noted that the ATT plane that each chord forms with the center of the spherical system
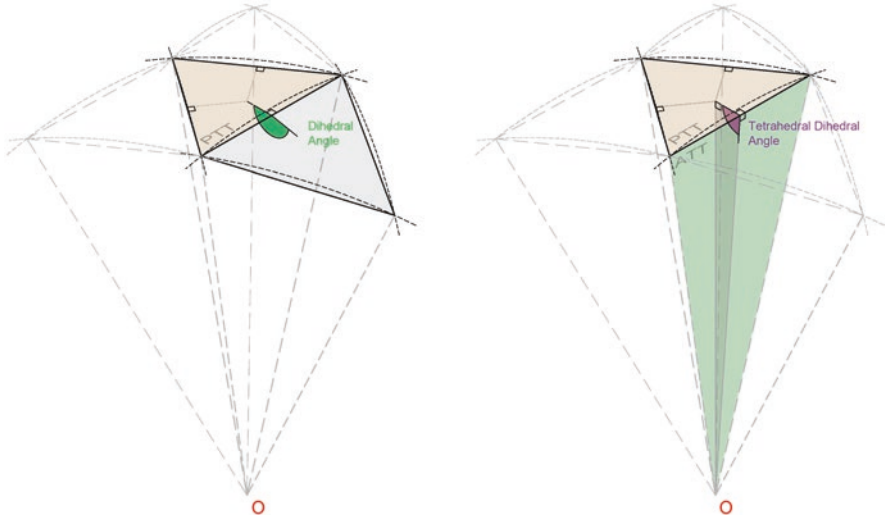
Fig. 7.7 Dihedral Angle (green) and Tetrahedral Dihedral Angle (violet)

does not divide the corresponding Dihedral Angle in equal parts; the Dihedral is not symmetrical with respect to the ATT plane. Figure 7.7 illustrates the definition of the Tetrahedral Dihedral Angle [TDA] as the angle between a PTT and each one of its three ATT.

Comparing the Results

A common error is to work on a spherical system as if it were a planar system and apply the properties of Euclidean geometry. Unlike a triangle in a Euclidean plane, the sum of the amplitude of three POA for each vertex of a spherical triangle, either rightwards or leftwards, is always larger than 180°.

For the calculation of the POA in the three vertices and, consequently, for the design of the three-dimensional modules of the *GoodKarma Method*, one doesn't work in the same plane, but in three different planes, because, despite representing a geodesic system as a series of plane facets, we continue to work on a spherical surface in which the axioms of Euclidean geometry are not valid.

The need to adapt the geometry of an initial geodesic mesh to the specific construction method is mentioned, for instance, by D. Larrauri [10], C. Zambrano [11], and M. Acosta [12]. However, the lack of comprehension of the peculiarities and specificities of spherical geometry and operating on it as if it were a set of planar triangles led them to the application of the laws of Euclidean geometry in a spherical geometric system. By forcing the sum of the angles to correspond to 180°, they fostered more deviations.

In order to present a comparative analysis of the results, the case of the $\nu 4$ of the Icosahedron (Class I), obtained with the *Equal Chords* subdivision system, will be used, since this is by far the more commonly used.

As summarized in Table 7.2, comparing the data obtained by applying the concepts and operators introduced by our investigations, with the ones proposed in the informal manuals of this construction method, we can see how 80% of the cuts would be made using different angles.

In addition, comparing the manuals' data in Table 7.3 with the IA of the corresponding PTT, the most striking result is that, not only the values do not agree but also, in an unexpected way, the values of four of the cutting angles reported in the manuals turn out to be smaller with respect to their respective AI. Being that the PTT are oriented towards the surface of the sphere, and being that surface convex, by definition, this turns out to be simply impossible. Comparing the POA with the manuals, 80% of the cuts would be made with a different angle. Comparing the POA with the IA, this deviation would fall to 53%, demonstrating that modifying the general geometry following the rules of planar geometry can lead to the creation of even more geometrical incongruities.

Conclusions

Throughout its development, this research sought to demonstrate that geodetic structures are not, and should not, be considered as governed by a single geometry and a single construction system. Several of the areas of knowledge involved in the design and construction of geodesic structures have been organized and developed, with the aim of establishing the relationships that exist between them.

There are a great variety of concepts, a multiplicity of parameters and factors applicable to each geodetic geometry that must be considered to adapt a design to the large number of constructive systems that could be used to materialize it.

The indistinct application of general geometric schemes to specific construction methods will often produce inconsistencies between the theoretical geometric design and the actual geometric configuration of what is intended. Such approaches result in incidents in the production and assembly phases and determine the occurrence of pathologies during the useful life of buildings. The design geometry must be adapted and calibrated to the construction system.

In order to adequately address the design and construction of a geodesic structure, it is necessary to understand the multiplicity of factors that have so far been considered as unequivocal, starting from the multiple subdivision methods with which geodetic meshes can be generated. Understanding the geometric peculiarities of these *double curvature triangulated meshes* is essential to configure specific tools to work on their definition and adaptation to specific constructive systems.

The development of concepts such as the Principal Tetrahedron Triangle (PTT), the Principal OrthoDihedral Angle (POA), and the Axial Tetrahedron Triangle (ATT) is the first and fundamental step towards a coherent design process for this

Table 7.2 Comparison between Principal OrthoDihedral Angles of the five PTT of an "*Icosahedron, ν4, equal chords subdivision method*" geodesic mesh (In these results, specular triangles have been omitted) in our research [13], Larrauri [10] and Zambrano [11] (Larrauri [10] and Zambrano [11] propose the angles reported in Tables 7.2 and Table 7.3. Acosta [12] has an improved proposal, but still based on the same premises, thus following the rules of planar geometry, and presenting the same types of deviations.)

Chords' Factors							
A	B	C	D	E	F		
0.25318	0.29524	0.29453	0.31287	0.32492	0.29859		
ν4	Comparison between principal OrthoDihedral angles and manuals' angles						
A	B	A	PTT 1				
0.25318	0.29524	0.25318				Chords' factors	PTT's totals
72		54		54		Manuals' angles	180
71.8645	71.8645	54.6644	54.5849	54.5849	54.6644	POA	181,1138
CA	AB	AB	BC	BC	CA		
−0.1355	−0.1355	0.6644	0.5849	0.5849	0.6644	Deviation (degrees)	
0	0	1	1	1	1	Deviation (cut angles)	
C	C	B	PTT 3				
0.29453	0.29453	0.29524				Chords' factors	PTT's totals
60		60		60		Manuals' angles	180
60.3810	60.3824	60.6248	60.6248	60.3824	60.3810	POA	181.3882
CA	AB	AB	BC	BC	CA		
0.3810	0.3824	0.6248	0.6248	0.3824	0.3810	Deviation (degrees)	
0	0	1	1	0	0	Deviation (cut angles)	
F	D	C	PTT 5				
0.29859	0.31287	0.29453				Chords' factors	PTT's totals
63		57		60		Manuals' angles	180
64.2206	64.2137	57.9925	57.9637	59.2430	59.2789	POA	181.4562
CA	AB	AB	BC	BC	CA		
12.206	12.137	0.9925	0.9637	−0.7570	−0.7211	Deviation (degrees)	
1	1	1	1	−1	−1	Deviation (cut angles)	
D	E	D	PTT 2				
0.31287	0.32492	0.31287				Chords' factors	PTT's totals
64		58		58		Manuals' angles	180
63.1498	63.1498	59.2427	59.2179	59.2179	59.2427	POA	181.6104
CA	AB	AB	BC	BC	CA		
−0.8502	−0.8502	12.427	12.179	12.179	12.427	Deviation (degrees)	
−1	−1	1	1	1	1	Deviation (cut angles)	
E	E	E	PTT 4				
0.32492	0.32492	0.32492				Chords' factors	PTT's totals
60		60		60		Manuals' angles	180
60.5660	60.5660	60.5660	60.5660	60.5660	60.5660	POA	181.6979
CA	AB	AB	BC	BC	CA		
0.5660	0.5660	0.5660	0.5660	0.5660	0.5660	Deviation (degrees)	
1	1	1	1	1	1	Deviation (cut angles)	

Table 7.3 Comparison between Internal Angles of the five PTT of an "*Icosahedron, ν4, equal chords subdivision method*" geodesic mesh (In these results, specular triangles have been omitted.) in our research [13], Larrauri [10] and Zambrano [11]

Chords' Factors							
A	B	C	D	E	F		
0.25318	0.29524	0.29453	0.31287	0.32492	0.29859		
ν4	Comparison between internal angles and manuals' angles						
A	B	A	PTT 1				
0.25318	0.29524	0.25318				Chords' factors	PTT's totals
71.3326		54.3337		54.3337		Internal angles	180
72		54		54		Manuals' angles	180
CA	AB	AB	BC	BC	CA		
0.6674		−0.3337		−0.3337		Deviation (degrees)	
1		0		0		Deviation (cut angles)	
C	C	B	PTT 3				
0.29453	0.29453	0.29524				Chords' factors	PTT's totals
59.9202		60.1595		59.9202		Internal angles	180
60		60		60		Manuals' angles	180
CA	AB	AB	BC	BC	CA		
0.0798		−0.1595		0.0798		Deviation (degrees)	
0		0		0		Deviation (cut angles)	
F	D	C	PTT 5				
0.29859	0.31287	0.29453				Chords' factors	PTT's totals
63.6689		57.5339		58.7972		Internal angles	180
63		57		60		Manuals' angles	180
CA	AB	AB	BC	BC	CA		
−0.6689		−0.5339		12.028		Deviation (degrees)	
−1		−1		1		Deviation (cut angles)	
D	E	D	PTT 2				
0.31287	0.32492	0.31287				Chords' factors	PTT's totals
62.5649		58.7176		58.7176		Internal angles	180
64		58		58		Manuals' angles	180
CA	AB	AB	BC	BC	CA		
14.351		−0.7176		−0.7176		Deviation (degrees)	
1		−1		−1		Deviation (cut angles)	
E	E	E	PTT 4				
0.32492	0.32492	0.32492				Chords' factors	PTT's totals
60.0000		60.0000		60.0000		Internal angles	180
60		60		60		Manuals' angles	180
CA	AB	AB	BC	BC	CA		
0.0000		0.0000		0.0000		Deviation (degrees)	
0		0		0		Deviation (cut angles)	

type of construction, enabling the configuration of application schemes to be executed in self-construction and low-tech environments. The involvement of local communities is an important asset since participation and social inclusion are among the main goals of our research.

At the same time, in order to define the variety of existent construction methods, it is necessary to approach geodesic geometry with a new focus and analyze the relationships established between a given geometric configuration and the specific geometric characteristics of each construction method applicable in real scale structures.

Existing methods of representation and definitions can easily lead to the error of working on geodesic structures as if they were a set of planar triangles. Generations of dome enthusiasts, from the sixties to the present day, have fallen into this error, generating constructions that, due to recurrent pathologies, have been abandoned in the late seventies by the pioneers of this technology, as reported in *Domebook 3* [4]. Nowadays, new generations are willing to rescue this construction technology,[8] but they are bound to repeat the same mistakes and face the same problems if Euclidean geometry is applied on spherical surfaces. These problems are further amplified in construction methods such as *GoodKarma*, that use three-dimensional elements as a basis for construction.

The data obtained with the application of the tools developed through the present research on the *GoodKarma* construction system, here used as a case-study, demonstrated that certain manuals are not adequate. The divergence between the geodetic geometry adapted and calculated for this specific construction method using the concepts developed in this research and the data reported in the bibliographic references is significant and determine high stresses in the elements of the structures.

The approach proposed in our research not only allows for a new reading of the existing methods addressing and tackling the source of the recurrent problems they suffer, but also, as demonstrated by numerous experiences carried out in the field, allows the configuration of new construction methods, such as *Brujodésico* or *Zdésico* [6], that may be easily explored by communities without previous knowledge of geodesic structures and are implementable in low-tech environments.

---

[8] Nowadays, we witness the sprout of a new generation of dome enthusiasts that gather and discuss worldwide in several digital forums as, e.g., www.facebook.com/groups/acidome.calc (since 2010) or www.facebook.com/groups/1455642741182382 (since 2017).

References

1. Popko, E. (2012). *Divided spheres: Geodesics and the orderly subdivision of the sphere*. A K Peters/CRC Press.
2. Prenis, J. (1973). *The dome Builder's handbook*. Running Press.
3. Kahn, L. (1970). *Domebook*. Shelter Publications.
4. Kahn, L. (1971). *Domebook 2*. Shelter Publications.
5. Kahn, L. (1973). *Shelter*. Shelter Publications.
6. Ctrl+Z [Internet]. [Updated 2019 Mar 17]. from www.ctrlz.net
7. Clinton, J. D. (1965). *Structural design concepts for future space missions*. NASA Contract, Progress Report.
8. Kenner, H. (1976). *Geodesic math and how to use it*. University of California Press.
9. Wenninger, M. (1979). *Spherical models*. Dover.
10. Larrauri, D. (2010). Como construir un domo geodésico. https://www.academia.edu/19748963/domo_v4. Accessed 1 Dec 2021.
11. Zambrano, C. (2013). Cómo construir un domo. https://domosgeodesicos.es/2013/07/28/1/. Accessed 1 Dec 2021.
12. Acosta, M. (2019). *Domos geodésicos, manual completo de construcción*. Ediciones midomo.
13. Stasi, G. (2018). *Geometrías Geodésicas y Sistemas Costructivos. Diseño e implementación de sistemas low-tech*. Doctoral Thesis. Spain: Universidad de Sevilla.
14. Stasi, G. (2020). *Physical sculptures as mental space for reflection. Reflection-in-action*. Taylor and Francis Ltd.
15. Stasi, G., Barrios-Padura, Á., & Molina- Huelva, M. (2017). *Self-built geodesic geometries. Congress proceedings, 3rd International Congress on Sustainable Construction and Eco-Efficient Solutions*. ETSA – Universidad de Sevilla. ISBN 978-84-617-8428-8.
16. Stasi, G., Barrios-Padura, Á., & Molina- Huelva, M. (2016). *Protocolos de empoderamiento y estructuras geodésicas. Congress proceedings, XXX Jornadas de Investigación. Configuraciones, Acciones y Relatos*. FADU - Universidad de Buenos Aires. ISBN 978-950-29-1637-8.

Gianluca Stasi, Graduated in Architecture at the University la Sapienza of Rome (2005), he obtained his PhD at the Universidad de Sevilla (2018). One of the main axes of his research is the relation between geodesic geometry and community empowerment, and knowledge and technology transfer. In his professional life, he has supported, contributed to, and developed participatory, self-construction and low-tech initiatives and processes in local communities in various parts of the world. These activated long-lasting social processes that have been recognized at an institutional level, such as with the Curry Stone Design Prize, and, most importantly, by the communities they serve.

Chapter 8
Vittorio Giorgini's Architectural Experimentations at the Dawn of Parametric Modelling

Denise Ulivieri, Marco Giorgio Bevilacqua, and Filippo Iardella

Abstract Vittorio Giorgini (1926–2010) grew in Florence, Italy, where he attended the School of Architecture. From the earliest years of his academic studies, Vittorio Giorgini showed interest in developing research on natural models with the aim of applying them to architecture. Starting from the 1960s, his studies focused on the analysis of membrane structures, tensile structures, and on the elaboration of tetrahedral and octahedral structural meshes. He experimented spatial meshes in an intuitive way, even if he understood, at the end of his career in the late 1990s, that only with the help of technology and electronic instruments it would be possible to obtain a mathematical control of meshes.

Based on an in-depth analysis of Giorgini's projects, drawings, and documents collected in his private archive, the aim of this paper is to demonstrate how pioneering Giorgini was anticipating several years of recent investigation in the field of parametric modelling and computational design.

Introduction

Vittorio Giorgini (1926–2010) was born in Florence. His father, Giovanni Battista, was a pioneer in promoting Italian high fashion around the world. Vittorio Giorgini grew up in Florence, where he attended the School of Architecture. After his graduation in 1957, he worked in Italy up to 1969; then moved to New York City, where he worked as a professor of Architecture and Planning at the Pratt Institute until 1996, when, going blind, he was forced to end his professional activity and return to Italy, where he died in 2010 with the age of 84.

D. Ulivieri (✉) · M. G. Bevilacqua
University of Pisa, Pisa, Italy
e-mail: denise.ulivieri@unipi.it; marco.giorgio.bevilacqua@unipi.it

F. Iardella
BIM and Digital Engineer, Milano, Italy

103

From the earliest years of his academic studies, Giorgini was fascinated by the natural world, which he considered not as a mere repertory of formal solutions, but as an enormous catalogue of building techniques and functions (Fig. 8.1). Based on the direct observation of natural structures, his intellectual and design studies focused on building systems for the design of functional houses. He showed great interest in the study of curved systems, such as shells and membranes, passing on to tensile structures and organizing his ideas in the elaboration of tetrahedral and octahedral structural meshes. He worked on symmetrical and asymmetrical shell beams, and further explored the issues dealt with by topology. At the same time, Giorgini developed a series of projects that, to use his own words, belong to those conventional techniques, diagrams of straight lines and planes, relating to polygons and polyhedra [1].

Until the first half of the nineteenth century, Euclidean geometry was the only instrument used for describing nature, but the advent of non-Euclidean geometry led to what Marcos Novak defines a fundamental re-thinking of the meaning of space-time, matter and energy, information, and noise [2], which inevitably led to the study of new ways of conceiving and materializing architecture. In this context, Giorgini fully understood, along with a few others, what Thomas S. Kuhn (1962) in his own words, defines, as a *new paradigm* [3]: the transition to a new vision of the physical universe in which instability and fluctuations are at the origin of the incredible variety and richness of forms and structures that could be seen all around us [4]. He thought about a different way of understanding architecture, based on the search for integration with nature, which, however, is not achieved by the simple imitation of the forms of the organic world, but in the design of spaces suitable to the needs of everyday life and economic viability.
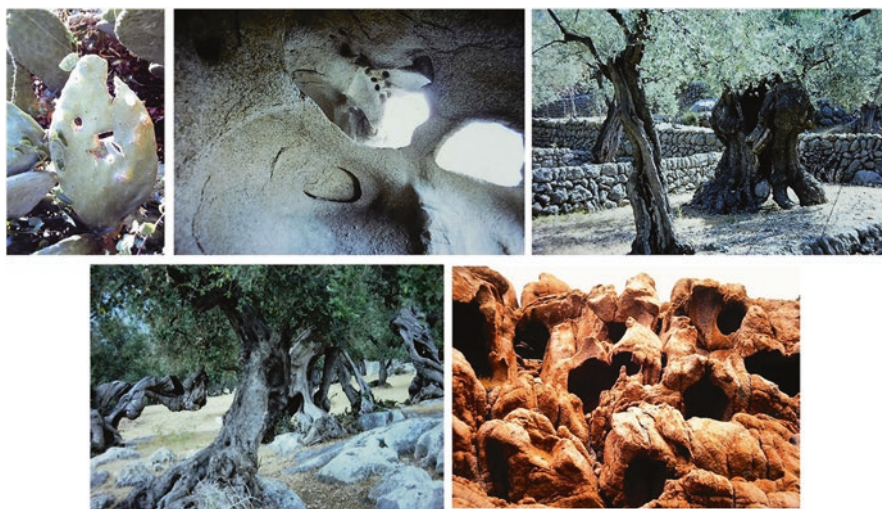
Fig. 8.1 Photos by Vittorio Giorgini of natural shapes (Courtesy B.A.Co. – *Vittorio Giorgini Archive*)

According to Giorgini, geometry is an analysis, verification, and operational tool [5, p. 193] and he considered its study as the basis of static and structure. In Giorgini's words, that we translated from the Italian, Geometry has acquired the same significance possessed by math, physics, and chemistry and has become the support of taxonomy. Like taxonomy itself, geometry can be said to have become a tool of analysis, verification, and operational methods. Geometry seems to have become a common denominator of all the above, rendering them common and inter-dependent [5, p. 19]. Giorgini continues, denoting that Geometry is the basic order from which models are developed, in his attempt to approach models of nature with efficient mechanisms of self-control. Giorgini's world is, therefore, *post-Euclidean,* within a complex and continuous reality where natural evolution proceeds, as he puts it, systematically with dynamic transformations, adaptations, and continuous retroactions [6, p. 6], a dynamic and interrelated reality that, from the 1950s onwards, he investigated through topological geometry.

Based on an in-depth analysis of Giorgini's projects, drawings, and documents collected in his private archive and in the outcome of a lecture we presented at the *Nexus Conference* in Pisa in 2018 [7], the aim of this paper is to demonstrate how pioneering Giorgini was and how he anticipated, in several years, recent investigations in the field of parametric modelling and computational design. In particular, our current research focuses on the case study of symmetrical geometric meshes, which, through dynamic transformation, change into asymmetric meshes, as it happens in nature.

Giorgini as a Morphologist-Spatiologist Architect

Giorgini defined *Spatiology* as the research he developed based on the study and observation of natural structures to achieve efficient and flexible building models similar to nature itself. In his approach, he used the morphological and geometric suggestions derived from natural elements to create a *free* design, meant as rich in formal spatial solutions, and economically convenient. Giorgini establishes that *t*he *scientificization* of design neither cramps nor sterilizes the art of which it is a part, quite the contrary, it enriches art greatly and widens art's horizons on the ground it claims. The success of the *scientificization* of design, however, depends on bravely accepting the increased difficulty of the challenge it poses. For this reason, Giorgini chose the word *spatiology* to describe the study of geometry as the mathematical discipline and *backbone* of statics, (systemic) taxonomy, and technology [5, p. 193].

As a morphologist-spatiologist architect, in 1962, Giorgini created the *Saldarini House* in the Gulf of Baratti (Tuscany), later known as *Casa Balena* (Whale House) or *Casa Dinosauro* (Dinosaur House), a *fanciful morphology,* in Del Francias's words [8, p. 26] where the topology of transformation and continuity is linked to the architectural concepts of flexibility, fluidity, and dynamism [9, p. 130].
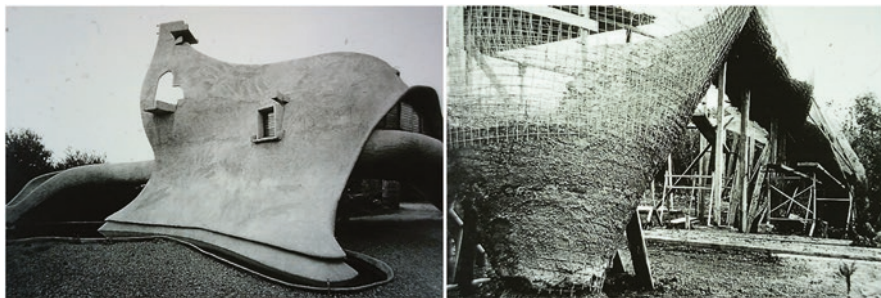
Fig. 8.2 *Casa Saldarini*, Gulf of Baratti, Livorno, 1962. On the left, view of the house; on the right, detail of a foundation plinth (Courtesy B.A.Co. – *Vittorio Giorgini Archive*)

The *Saldarini House* represents Giorgini's first real opportunity to study curved surfaces as generative elements of the space (Fig. 8.2). The project reflects Giorgini's interests in the studies of the Swiss natural scientist Hans Jenny. In those years, Jenny was involved in Cymatics: subjecting some materials, such as sand and liquids, to vibrations, which results in an infinite range of morphologies similar to natural configurations [10]. The exploration of natural geometries in the dynamics of growth and physical processes by the British biologist and mathematician D'Arcy Wentworth Thompson was also fundamental for Giorgini [11].

In the *Saldarini House*, Giorgini experimented for the first time his *isoelastic structural membrane*, that is, an asymmetrical and non-orientable *shell* beam, characterized by a double curvature, to better absorb deformations. Using common materials, such as wire meshes and concrete, he experimented with a new and personal building technology, conceiving a house characterized by topological surfaces and static efficiencies, like those of natural structures. The house lies on a continuous curvilinear foundation and on two original reinforced concrete plinths, where the 3 mm-thick galvanized electro-welded mesh with a pattern of 5 × 5 cm, covered by a layer of concrete, is fastened. The 8–10 cm thick continuous membrane makes the building profile similar to an ingenious zoomorphic morphology.

From the earliest years of his academic studies, Vittorio Giorgini showed interest in developing research on natural models with the aim of applying them to architecture, in order to obtain more efficient complex systems. He committed to the systemic vision of contemporary scientific thought, aiming to determine *the structure of a system as the order in which the elements are organized* [5, p. 211], thus developing a dynamic, articulated, sophisticated architecture, open in all the directions, where geometric principles, structural, and functional needs are perfectly integrated.

Giorgini as a Pioneer of Parametric Design

For the last several years, we have been watching, in several design practices inspired by natural phenomena and organisms, digital modelling that is based on computational logic, guides projects focused on the evolutionary aspect of the shape and on its optimization based on specific criteria. The first experiments for the parameterization of shapes and surfaces are conventionally traced back to the embryonic work of Steve Coons in 1967 [12], who was among the first to introduce a method to describe curves through parametric equations, although several scholars agree in identifying the formulation of the concept of parametric architecture in the 1940s, in the writings of the Italian architect Luigi Moretti [13, 14, p. 21, [15]]. A few years later, in 1986, Gross [16] was the first to understand the potential of the parametric approach in the elaboration of complex forms in architecture. From the 1990s to the present day, numerous experiments in parametric modelling and generative design have multiplied and spread; and among these, a few deserve special mention, the work of Serrano in 1993 [17] and certainly that of Dennis Shelden in 2002 [18], who documented in an organic and systematic way the potential of parametric design in architecture.

In the same years of Coons's research, and in advance of those of Serrano and Shelden, Giorgini started his experimental works on spatial meshes and their formal deformation under the action of forces in order to adapt them to tensions. In agreement with the statement by D'Arcy Wentworth Thompson, that the shape of an object is a diagram of forces and applying Thompson's *theory of transformations* to symmetrical and asymmetrical meshes alike [11, pp. 1026–1095], Giorgini analysed their structural behaviour and tried to quantify the forces that modify the original model, having concluded that the transitions from the linear (the straight line), to the bent (broken) up to the curved, both for lines and for surfaces and meshes, are generated by different geometries and are transformed, symmetrically and asymmetrically, according to the forces action [5, p. 199] (Fig. 8.3).

Vittorio Giorgini's studies, as much as Le Corbusier's research on hyperbolic geometry or the technological and formal solutions of Richard Buckminster Fuller and Frei Otto, coming out of the renaissance static perspective approach, moved towards Einstein's curved space, Gilles Deleuze's folded space, or the topologically deformed space theorized by René Thom [19, p. 55].

The structure of a system can be attributed to a geometrical configuration and to the action of forces. Through the transformations of the models, Giorgini investigated the structural organization of the systems, the aggregation relationships between the parts, coming to quantify the resultant forces and understand the causes of the model's transformation [7, p. 13]. In some notes and sketches, he explained that the point and the force are the first generators of systems which have a certain degree of complexity, which is developed from the dynamic interaction between the point (sign) and the forces themselves by adding to the three dimensions of geometry (space), the force—potential energy as a fourth physical dimension. The latter is understood as *the virtual* (potential) force which generates systems when applied
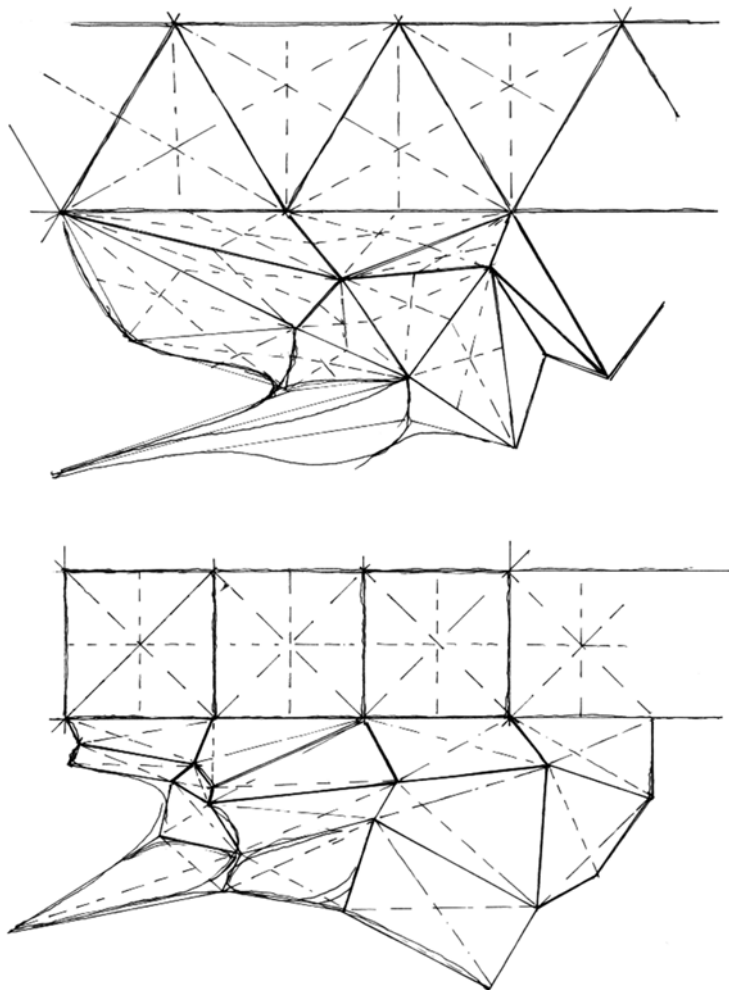
Fig. 8.3 Studies for the deformation of a mesh (Courtesy B.A.Co. – *Vittorio Giorgini Archive*)

according to a certain norm (Notebook sketches, B.A.Co. – *Vittorio Giorgini Archive*).

In a way, Giorgini seems to apply the same method illustrated in Fig. 8.4: *The Kangaroo workflow*, developed in the Grasshopper-Rhinoceros 3D plug-in software created by Daniel Piker for interactive simulation, form-finding, optimization, and constraint solving. The workflow relies on the same set of rules and operations for low-nodal models, such as single digital chains, as for high-nodal models, such as multi-supported membranes. In a digital environment, the organic forms are discretized by meshes; Giorgini used the same method in the pre-digital age. He
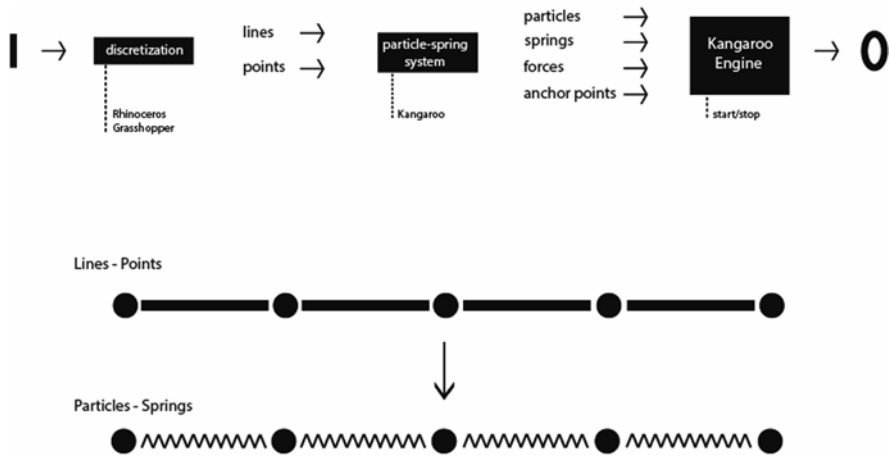
Fig. 8.4   'The Kangaroo workflow' (graphic elaboration by Filippo Iardella)

understood the *discretization technique,* but he did it in a traditional way. In a certain sense, we can say that he demonstrated to possess a *parametric mentality*.

Giorgini Parameterized

To simulate a membrane the same way as in Giorgini's meshes, a grid of springs was defined in Fig. 8.5, that shows the behaviour of two cable networks, one with a square mesh, the other with a triangular mesh, subjected to three external forces and anchored on one of the smaller sides. Giorgini modelled his meshes in an intuitive and experimental way, as in the case of *Saldarini House* or the unfinished project for the *Liberty Rural Community Centre* placed in Parksville (1976–1979), near New York City, where meshes were modelled manually, in order to obtain the desired curvature. In the same way, the wire mesh structure was moulded to the shape required with the support of wooden poles (Fig. 8.6).

Giorgini's approach to design was experimental and intuitive. During the construction of the *Saldarini House*, he confessed to not being fully aware of the topological characteristics of his creation, and that its static behaviour was a riddle to solve [5, p. 245].

Giorgini's investigations have been developed in current software of parametric modelling, in order to elaborate a critical analysis of his work, verifying, in particular, the limits induced by the lack of specific software. The experimentation focused on the modelling of double-curved asymmetric surface systems with topological morphological characteristics, such as the *Saldarini House* and the unfinished *Liberty Project*. Like Giorgini in his *Liberty Project*, we simulated, thanks to our
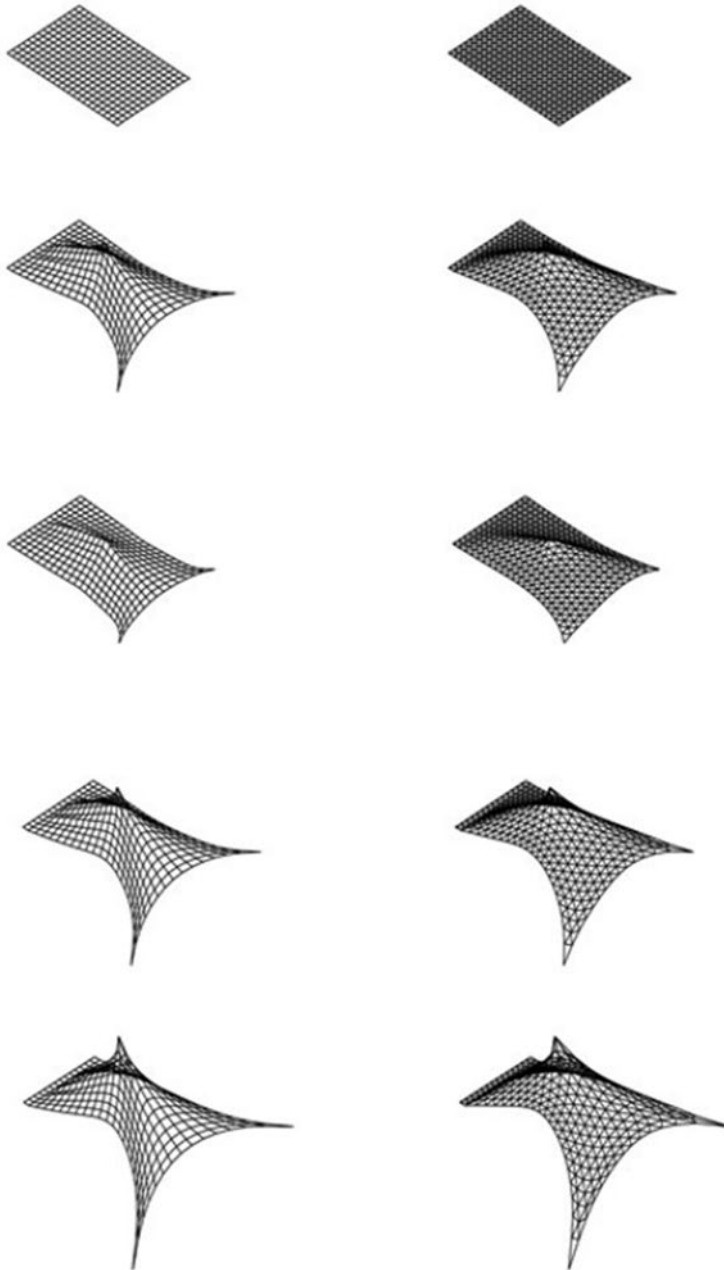
Fig. 8.5 Membranes' simulation. The figures show the behaviour of two cable networks, one with a square mesh, the other with a triangular mesh, subjected to three external forces and anchored on one of the smaller sides (graphic elaboration by F. Iardella)

Fig. 8.6 *Liberty Rural Community Centre*, Parksville (1976–1979). On the left, view of the structure; on the right, Giorgini walking on the structure for manually modelling the meshes (Courtesy B.A.Co. -*Vittorio Giorgini Archive*)
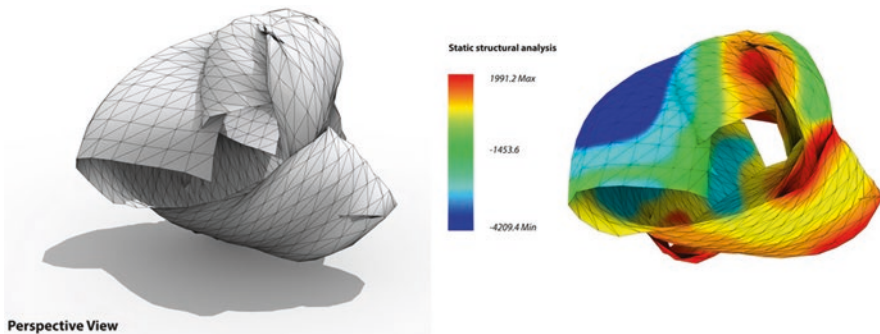
Fig. 8.7 On the left: like Giorgini in his *Liberty Project*, digital simulation of a deformed cables-net, defining the right elastic behaviour (Hooke's Law), the probable anchor points and the forces to be applied. On the right: Finite Element Method analysis of the mesh (graphic elaboration by Filippo Iardella)

digital tools, a deformed cables-net, defining the right elastic behaviour (Hooke's Law), the probable anchor points, and the forces to be applied.

Giorgini attempted to define static diagrams to quantify the forces that transformed the original symmetrical model, with the aim of investigating more efficient and economical design techniques. However, he pointed out that, while in nature, it is simple for a mesh to become asymmetrical, but that, with our techniques, it is difficult and expensive [5, p. 214]. But the most important tool that Giorgini could not use was the *Finite Element Method* analysis software. It is a numerical method for solving problems of engineering and mathematical physics, and typical problem areas of interest also included structural analysis (Fig. 8.7).

But Giorgini firmly believed in innovation and technology as tools for reducing the distance between Man and Nature. He understood that only with the help of technology and electronic instruments, it is possible to obtain a mathematical control of meshes. In 1978, during the 38th edition of the *Venice Biennale*, where Giorgini participated in the section dedicated to *Topology and Morphogenesis*, he

declared that the Euclidean geometry is not the only and most appropriate tool available, but the only one that, until then, he had been possible to exploit. He was convinced, in fact, that new tools, introduced by the developments of genetics, electronics, and information technology, would pave the way for more structurally efficient building techniques [20, p. 131] and in the 1980s, he began performing experiments with computers.

Leaving aside the orthogonality of the usual space, Giorgini developed an *ante-litteram* morphing process, based on the rectification—a sort of discretization—of curved lines. Starting in the 1970s, he developed a series of projects that belong to those conventional techniques. In his USA period (1969–1996), he began a far-reaching design phase in which the formal interpretation of natural organisms consisted of tetrahedral and octahedral meshes.

Giorgini's design is the result of a continuously generative process based on a system of parameters and relations; this process guides the result, which is almost always unknown to the architect. Giorgini's mindset is dominated by the concept of the diagram (process); the form is meant as a dynamic of transformation, in which the complex system of relations of the parts, and the internal and external forces that define the form itself must be investigated and interpreted. Giorgini realized that nature offers models set on a triangular-tetrahedral structure, such as in bone tissues, and asserts that, in nature, geometry is generally only a model and never appears as we know it or according to what we call symmetric models, such as the square or the equilateral triangle, and their transformation into rhombuses and isosceles triangles. In these transformations, Giorgini concludes that the triangle is always the basic element of such structures [1].

Natural structures, however complex, composed, and asymmetrical as they can be, are reduceable to recognizable models, in other words, to conventional systems, identified by the straight line, the flat surface, or polyhedrons. For Giorgini, a curve is a shape born under the action of multiple forces, whose conventional representation is nothing but a straight line. Applying the notions of graphic statics, he transformed curved systems into conventional systems, obtaining symmetrical geometric meshes then transformed into asymmetrical meshes through the application of forces. Giorgini's aim was to arrive at the definition of static diagrams capable of explaining forces and tensions of a given spatial conformation.

The ideational-design process of Giorgini was as parametric as the approach of Luigi Moretti or the intuitions of Sergio Musmeci; for whom, as for our architect, the concept of the diagram was central and preceded the introduction of the computer in the design practices. Giorgini's American projects represent the key to understand the application in the architecture of the models and diagrams of static forces that he studied in theory.

Our investigation focused on the modelling of the unrealized projects designed for Manhattan, like *Hydropolis* (1981–1982) and *Genesis* (1984), based on Giorgini's *Octa-Frame System*, a self-bearing octahedral-tetrahedral base-module. Giorgini explained that, given its geometric stability, the regular tetrahedron is the most statically efficient figure.

Simplification and standardization were his response to the lack of specific software. We tried to re-create a modular structure like those designed by Giorgini. When the shape was defined through the application of external forces, the closed volume was found in this step; a certain degree of approximation was taken into account to avoid calculation problems by the computer. Once found, the volume was discretized with the least number of bounding boxes with the tools of *Grasshopper* and *Pufferfish* (useful for working on Shape Changing) plug-ins. Within these boxes, the modules used by Giorgini were inserted, thus creating a modular structure (Fig. 8.8).

In 1981, Giorgini designed *Hydropolis*, an unusual neighbourhood on the East River. In *the Octa-Frame System,* the basic module defines a self-supporting structure: a bridge over the river composed of octahedral structures, displaced as interdependent modules, which form a system of self-supporting beams laid on inverted tetrahedrons that rest on truncated pyramidal plinths by means of spherical metal nodes (Fig. 8.9). Scaling the module established by the proportions of the bounding boxes, it was possible to model 3 support points—foundations, as can be seen in the Giorgini *Hydropolis* project (Fig. 8.10). The node is the most technologically complex element in which three or more metal tubular elements of variable sections converge.

Giorgini tested and revised the nodes many times during his work, before arriving to the most complex version, described as *universal connective nodes*, the *Octa-Frame System* [7].
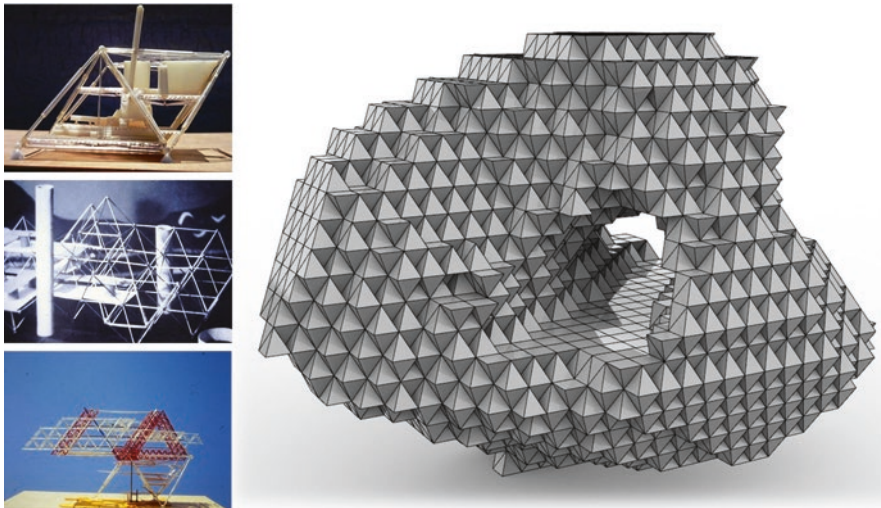
Fig. 8.8 On the left: Giorgini experimental models of structures based on the tetrahedron. On the right: digital elaboration of a modular structure like those designed by Giorgini (graphic elaboration by Filippo Iardella)
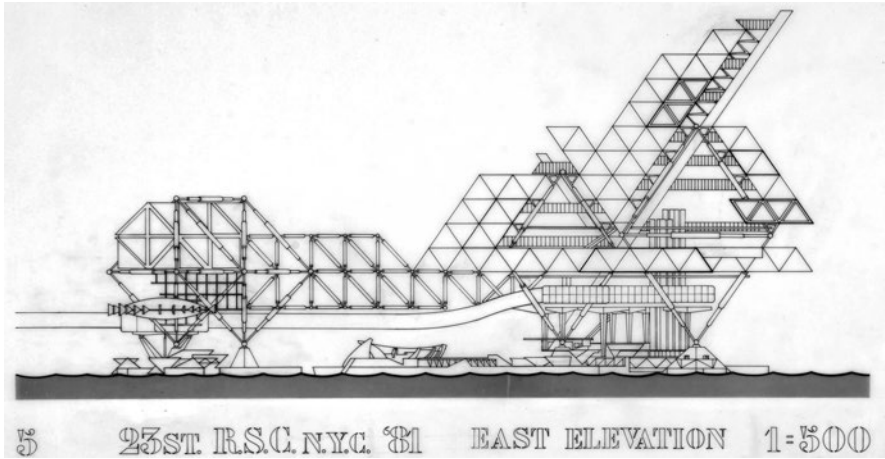
Fig. 8.9 *Hydropolis*, Manhattan, New York, 1981–1982 (Courtesy B.A.Co. – *Vittorio Giorgini Archive*)
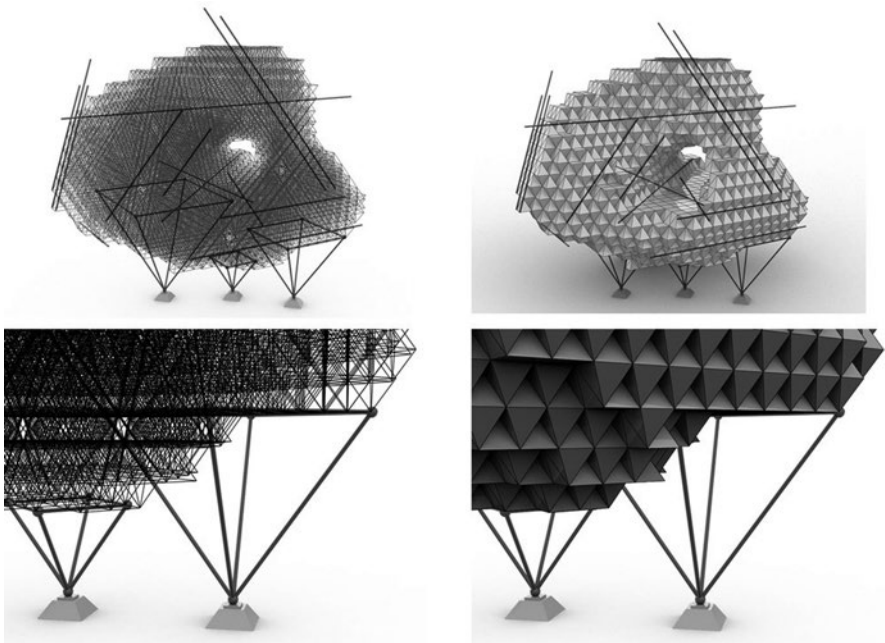
Fig. 8.10 Scaling the module defined by the proportions of the bounding boxes it was possible to model 3 support points—foundations as it can be seen in the Giorgini 's project called *Hydropolis* (graphic elaboration by Filippo Iardella)

Conclusions

In the end, Giorgini continues to surprise us for his cultural and social relationships; he was a friend of André Bloc and of the sculptor Isamu Noguchi; he knew the work of Frederick Kiesler; he met Richard Buckminster Fuller to discuss architecture; he was also a friend of Sebastián Matta, and a good friend of John M. Johansen. Giorgini met many times with Peter Eisenman at the Pratt Institute. In 1979, Giorgini took part in the exhibition *Transformations in Modern Architecture* at the Museum of Modern Art of New York, that gave rise to a book (with the same name) edited by Arthur Drexler. The *Whale House* was exposed in the section titled *Sculpture: Organic Form,* next to Frederick Kiesler's *Endless House* (1960) [21].

Giorgini foresaw the enormous creative possibilities offered by digital language, demonstrating, in a certain sense, to have a *parametric mentality*, which he could not develop due to the lack of tools and other personal reasons. In 1995, a serious eye disease affected the last part of his life.

On the one hand, Giorgini's projects related to curved systems were mostly misunderstood and labelled as informal while, on the other hand, his pioneering and unrealized projects of the American period, mostly characterized by the use of tetrahedral and octahedral meshes, were branded as utopian and absurd.

Since the beginning of the twentieth century, the observation and investigation of nature, as a resource for architecture, unite the intellectual and design paths of some of the most innovative and lively architects, engineers, and artists of the time. Certainly, Giorgini should be considered in the eminent company of other personalities, such as Nervi, Candela, Otto, Gaudí, Fuller and Wachsmann, Le Corbusier, and with the liveliest minds of that time, like Andrè Bloc and Roberto Sebastian Matta, whom Giorgini knew personally, as well as Frederick Kiesler.

During the last years of his life, he declared, with profound bitterness, that he had been left very alone and that his work had never generated great interest from critics. In his own words, that we translate from the Italian: *My research has remained fruitless to this day. What remains is only an intention, a concept, a supposition, but no confirmation* [1].

Nowadays, digital modelling has made possible rereading, analysing, and critically evaluating Vittorio Giorgini's design thinking, highlighting the modernity of his investigations full of intuitions, which, however, did not mark their time, but nevertheless persist.

Authors' Contributions   The paper shows the results of a research coordinated by Denise Ulivieri.

The contributions of Denise Ulivieri (D.U.), Marco Giorgio Bevilacqua (M.G.B.) and Filippo Iardella (F.I.) in the elaboration of the paper were: Introduction (D.U.); Giorgini as a morphologist-spatologist architect (D.U.); Giorgini as a pioneer of parametric design (D.U. and M.G.B.); Giorgini Parameterized (D.U. and M.G.B.); Conclusions (D.U. and M.G.B.).

All the digital and graphical elaborations were developed by Filippo Iardella, under the supervision of Denise Ulivieri and Marco Giorgio Bevilacqua.

All the English translations of cited texts in Italian are by the authors.

References

1. Giorgini, V. (2006). *Storia di uno stronzo*. Audio cassette tape (unpublished biography).
2. Novak, M. (2007). Babele 2000. Retrieved March 22, 2019, from http://www.trax.it/mar-cos_novak.htm.
3. Kuhn, T. (1962). *The structure of scientific revolutions*. University of Chicago Press.
4. Nicolis, G., & Prigogine, I. (1991). *La complessità. Esplorazioni dei nuovi campi della scienza*. Einaudi.
5. Giorgini, V. (1995). *Spatiology: the morphology of the natural sciences in architecture and design. Spaziologia. La morfologia delle scienze naturali nella progettazione*. L'Arca Edizioni.
6. Del Francia, M. (2006). *Vittorio Giorgini architetto. Morfologia, Topologia, Spaziologia*. Generazioni in Arte.
7. Ulivieri, D., Giorgetti, L., & Tognetti, B. (2019). Vittorio Giorgini Spatiology–morphology architect. *Nexus Network Journal, 2020*(22), 191–210. https://doi.org/10.1007/s00004-019-00453
8. Del Francia, M. (Ed.). (2000). *Vittorio Giorgini. La natura come modello*. Angelo Pontecorboli Editore.
9. Di Cristina, G. (2005). Architettura come topologia della trasformazione. In M. Emmer (Ed.), *Matematica e cultura (129–141)* (p. 4). Springer.
10. Jenny, H. (1967). *Cymatics. A study of wave phenomena and vibration*. Basileus Press.
11. Thompson, D.'. A. W. (1945). *On growth and form*. Cambridge University Press.
12. Coons, S. (1967). *Surfaces for computer-aided design of space forms*, MIT Technical Report, Cambridge.
13. Stiles, R. (2006). *Aggregation strategies (masters dissertation)*. University of Bath.
14. Bucci, F., & Mulazzani, M. (2000). *Luigi Moretti: Works and writings*. Princeton Architectural Press.
15. Palestini, C., & Basso, A. (2019). Parametric architecture and representation, the experiments of Luigi Moretti. In C. Marcos (Ed.), *Graphic imprints*. EGA 2018. Springer.
16. Gross, M. (1986). *Design as exploring constraints (doctoral dissertation)*. MIT.
17. Serrano, J.G., Coll, J., Melero, J.C., Burry, M. (1993). *The need to step beyond conventional architectural software*, eCAADe Conference Proceedings Eindhoven.
18. Shelden, D. (2002). *Digital surface representation and the constructibility of Gehry's architecture*. (Doctoral dissertation). MIT.
19. Capanna, A. (2000). *Le Corbusier. Padiglione Philips, Bruxelles*. Testo&Immagine.
20. Vinca Masini, L. (Ed.). (1978). *Topologia e Morfogenesi*. La Biennale di Venezia.
21. Drexler, A. (1979). *Transformations in modern architecture*. The Museum of Modern Art.

Denise Ulivieri   is Associate Professor of History of Architecture at the University of Pisa. Her research interests are in the field of historical-architectural heritage, with particular attention to the history of the Tuscan built environment, the analysis of vernacular architecture and local building tradition. Her research is also focused on biographical studies of architects and engineers of the nineteenth and twentieth centuries, almost forgotten by critics or only marginally studied.

Marco Giorgio Bevilacqua   is Full Professor of Architectural Representation at the University of Pisa. His research interests are in the field of valorisation of the historical architectural heritage, with particular attention to historical military architecture, architectural and urban survey and digital technologies for the communication of historical architectural heritage. He currently teaches Architectural Representation and Methodologies for Architectural surveying in the master's degree program of Architecture and Building Engineering at the University of Pisa.

Filippo Iardella   is an engineer specialized in Building Information Modelling and in programming environments for computational BIM design that allow to design workflows and automate tasks. He has a master's degree in Building Engineering and Architecture from University of Pisa and an II level master specialization in BIM Management from Polytechnic University of Milan. Currently, he works as BIM and Digital Engineer at Lendlease Italy. His tasks include BIM coordinating and assisting BIM Manager using a fully integrated BIM approach based on the digitalization of projects and data management.

Chapter 9
Architectural Inversions: The Intangible Aspect as a Form-Finding Factor in the Combined Work of Antoni Gaudí and John Pickering

Emmanouil Vermisso

Abstract This paper discusses the working methodology in the design process of architect Antoni Gaudí and artist John Pickering and identifies common principles in their theoretical and practical underpinnings. While the later work of Gaudí (*Sagrada Familia* cathedral) strictly featured ruled surfaces such as hyperbolic paraboloids and hyperboloids of revolution to derive hybrid geometrical surfaces for construction, Pickering exclusively focused on making scaffolds of geometrical deformations based on a rigorous mathematical procedure. The parallel importance of an analogue process and the aspect of the *unseen* present an opportunity for a combined exploration of their work, using the *Sagrada Familia* as a vessel of inquiry. Applying mathematical inversion to combinations of ruled surface families, we have tried to produce elements of a new architectural vocabulary which echoes these two design references and considers the celebration of design intent by describing what is not there. While we offer some insights regarding constraints and solutions for fabricating these found geometries, our interest lies in the form-finding process.

Introduction

Inspired by the extensive application of geometry in the later stage (1914–1926) of *Sagrada Familia*'s design by Antoni Gaudí, this work considers generative design processes for architecture, using mathematical rules and intersecting topology protocols (Boolean operations). Examining the rules for generating the cathedral openings, a new window variation is proposed by adopting the inherent use of mathematical thought in the work of sculptor John Pickering. Gaudí's and

E. Vermisso (✉)
Florida Atlantic University, Boca Raton, FL, USA
e-mail: evermiss@fau.edu

119

Pickering's works regard mathematics as a generative platform for design, defining layered steps for the realization of a priori unknown two-dimensional and three-dimensional outcomes. These studies originate in the work of Gaudi himself, and subsequently, Professor Mark Burry's contribution to formulating design models of the *Sagrada Familia* cathedral through parametric protocols [1–3], focusing on the use of ruled surfaces for architecture. We propose the consideration of Pickering's use of mathematical inversion to transform known geometrical surfaces to generate new topological conditions through numerical deformation. This mathematical rationale can extend Gaudí's approach by introducing a second stage of deformation in intersected ruled surfaces focusing on hyperboloids of revolution (which occur frequently in *Sagrada Familia*).

Design Process in Gaudí's Later Years: 1914–1926

Antoni Gaudí regarded nature as a model for design because he appreciated natural systems' ability to circumvent the crude tectonics of human construction by successfully resolving continuity between elements (i.e. connection between the tree trunk and branching elements). Most of his work is abundant with fluid geometries (i.e. *Casa Milà*, etc.). By contrast, during the later years of his life, Gaudí shifted towards a more austere visual expression for the *inherited* commission of the *Sagrada Familia* cathedral, adopting a rigorous geometric modulation system. Initially, this introduction of a discrete topological definition seems to move away from nature. By understanding the mathematical rules inherent in natural systems, Gaudí, in fact, further embraced the natural example. His process exploited ruled surfaces (i.e. the hyperbolic paraboloid, hyperboloid of revolution of one sheet in Fig. 9.1) because they are defined by straight lines (*rulings*), thereby facilitating
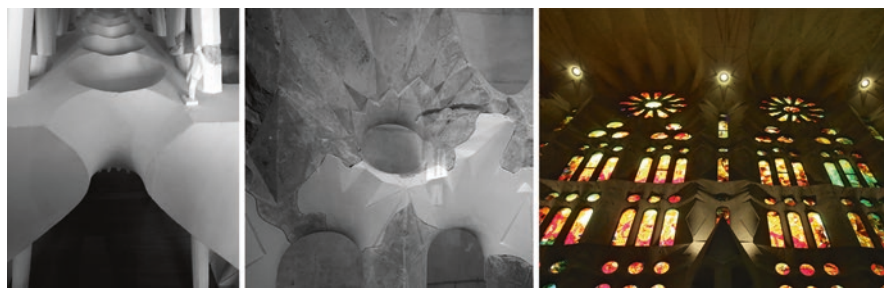
Fig. 9.1 The use of ruled surface geometry in the walls and ceiling of the *Sagrada Familia*. (**a**) Sectional model of transept vault with overlaid ruled surface (Exhibit in the Sagrada Familia crypt, Barcelona). (**b**) Reconstructed 1:10 plaster model for the Sagrada Familia transept clerestory window: the triple points from the intersecting solids and the triangulated surface patterns are visible. (**c**) Interior wall showing lateral nave windows, formed through the use of hyperboloids of revolution
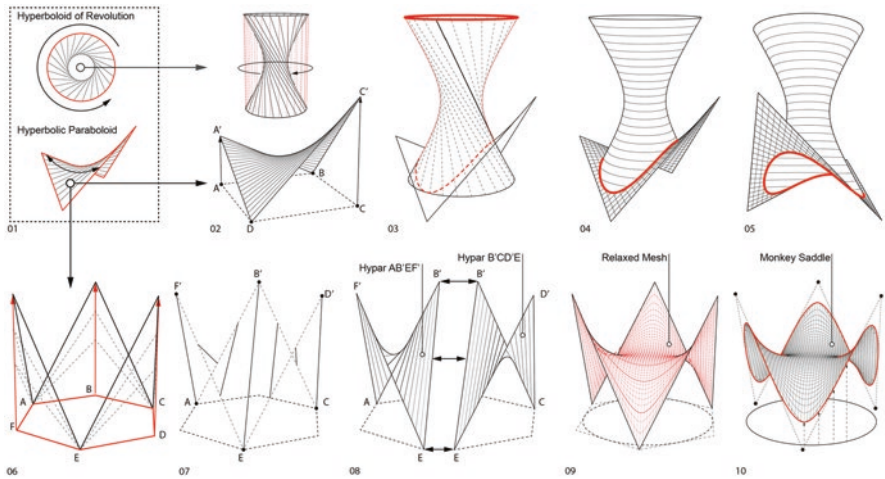
Fig. 9.2 Combined ruled surfaces: A *Hyperboloid of Revolution* (01) and a *Hyperbolic Paraboloid A'BC'D* (02) are intersected (03, 04, 05); Hexagonal boundary vertices B, D, F move to create a 3-dimensional outline (06), whose rulings define two hypar surfaces *AB'EF', CB'E D'* (07, 08), leading to a relaxed mesh (09) and a *Monkey Saddle* (10)

formwork for later full-scale construction. Gaudí followed a profoundly *layered* process for designing wall, ceiling and roof openings, which result from combined Boolean operations. Specifically, transept vaults and clerestory windows in the *Sagrada Familia* involved subtracting ruled surface volumes from a notional material solid [1, p. 114], producing doubly curved hyperboloid surface openings (Figs. 9.1 and 9.2):

> Gaudí was working in a hands-on manner with his model-makers composing walls, columns, domes, towers and vaulted ceilings predominantly by intersecting hyperboloids of revolution. [1, p. 109]

Inspiration from nature, understanding ruled surface advantages and refinement through physical prototyping, all exemplify the *Gaudian* working method which combines theory, applied scientific research and craftsmanship [3, p. 9]. This is noteworthy because the collective appreciation and *reading* of the building derive from its visual qualities, specifically its profoundly sculptural nature which most people associate with Gaudí's work; unfortunately, this engenders a partial understanding of the building—according to Burry—due to certain publications which,

> Despite their intense and concentrated examinations…fail to provide a ready interpretation of the holistic significance of his buildings beyond the sensibilities of art criticism; only one predominantly visual side of Gaudí the designer is revealed: design outcome registering often as art at the scale of inhabitable sculpture. [4, p. 13]

Ruled Surfaces in Design: Hypar & Hyperboloid of Revolution of One Sheet

Gaudí's extensive use of the *second-order* (ruled) surfaces helped their subsequent adoption in early to mid-twentieth century architecture. These types of surfaces demonstrate advantages for achieving complex surface effects and enabling full-scale construction, thanks to the possibility of a rational subdivision, separate manipulation and re-integration of the surfaces into a seamless assembly. Among the three surfaces Gaudí employed, the most apparently experienced in the *Sagrada Familia* is the hyperboloid of revolution of one sheet, which results from the rotation of a straight line around a tilted axis. This kind of *ruled* surface belongs to a geometrical class known as *second-order surfaces (quadrics),* because they are described by second degree mathematical equations [5]. Fig. 9.2 illustrates the process for generating geometrical complexity from two doubly ruled surfaces (Diagram 01). In the first example (Diagrams 02–05), a hyperbolic paraboloid intersects a hyperboloid of revolution to create a geometry that is frequently used by Gaudí in the *Sagrada Familia* ceiling vault. In the second example (Diagrams 06–10), a 3D scaffold is created from a hexagonal boundary to generate two hypar surfaces, *AB'EF'* and *CB'ED'*, which are converted to meshes, *relaxed* in *Kangaroo Physics* and trimmed with a circle to produce a topology known as *Monkey Saddle.*

The use of hyperboloids in the *Sagrada Familia* offered Gaudí some flexibility in using physical prototyping as a form-finding method, because this ruled surface preserves its overall topology after deformation. As noted by mathematicians David Hilbert and Stephan Cohn-Vossen, in their 1932 work *Geometry and the Imagination*, a physical model of rigid rulings which are attached so as to restrict sliding while allowing rotation can be manipulated to provide derivative configurations of larger or smaller height, whose topology remains a doubly ruled surface [6, p. 16] (the fixed intersection of the rulings in this configuration remains constant while changing the shape of the hyperbola it defines). Hilbert and Cohn-Vossen claim that it can be proved this surface is not a *hypar,* therefore, we must assume that is a *hyperboloid of revolution*. The consequence of this topological preservation is noteworthy, because it indicates that a physical model of this type provides an inherently *parametric* definition of the analogue process, allowing Gaudí to test various hyperboloids with the same prototype. Starting with one hyperboloid model, several window variations could have been examined, modifying their proportion before the Boolean subtraction stage. The orientation of the subtracted hyperboloid in relation to the horizontal plane (*XY*), and the positioning of the rulings in relation to the axis of revolution are also relevant, because they affect the way the light bounces off the intersected surfaces which form the walls or vaulted ceiling.

Complexity in the *Sagrada Familia*: Computational Thinking & Boolean Logic

The process of understanding Gaudí's design intent to carry forward the—unfinished during his lifetime—project of the *Sagrada Familia* was challenging according to Professor Mark Burry.[1] The absence of any theoretical writings by Gaudí bequeathed architects the forensic task of reading the geometric rules he embedded in various physical plaster prototypes at scales 1:10 and 1:25. Beyond appearances, this modulation system is typical of the building's underlying complexity and suggests that Gaudí was thinking computationally, quite ahead of his time:

> There are highly original computationally generative aspects to his decision to apply second order geometry, and the aesthetic, philosophical and practical consequences of choosing them have only become better known in recent years, many decades following his death. [1, p.106]

Figure 9.3 demonstrates the process for generating the *Sagrada Familia* clerestory windows using Gaudí's method, through Boolean operations of circular and elliptical hyperboloids (Gaudí also employed hyperbolic paraboloids elsewhere in the building). Intersections between three hyperboloids of revolution were quite common, producing what Mark Burry calls *triple points*, making an analogy of these points as the *peaks* of intersecting surfaces (*mountain ridges*, to use the words of Hilbert and Cohn-Vossen's [6]). This aspect of intersection and subtractive logic is a typical example of parametric complexity, manifested through Gaudí's application of the same geometrical modulation system for form-finding to derive ornamentation.
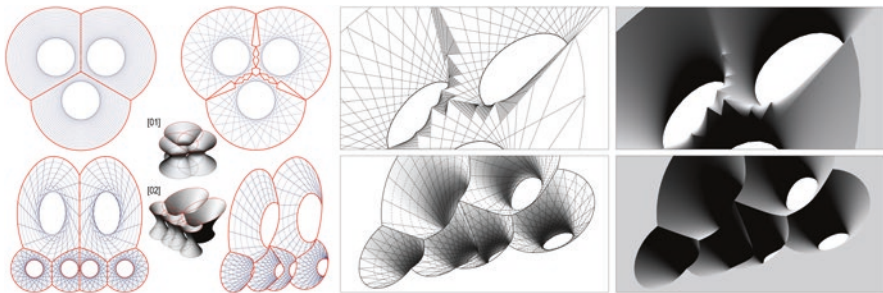
Fig. 9.3 Surface opening generation using Boolean subtraction after Gaudi's method. Top diagrams: Intersection of 3 hyperboloids of revolution (01) and resulting hyperbolic paraboloids along ridges of intersection (bold). Bottom diagrams: Intersection of 4 hyperboloids of revolution and 2 elliptical hyperboloids (02)

---

[1] Professor Mark Burry is an architect, academic and consultant to the *Sagrada Familia Foundation* since 1979, developing innovative design methods towards the building's projected completion in 2026.

Wall and ceiling surfaces demonstrate substantial decorative effects which are inherent to their geometric properties. Their sculpted-like expression is dictated by removing material from the first stage of smooth intersected hyperboloids, based on the points where the rulings intersect the aforementioned *ridges* (Fig. 9.3, top diagrams):

> …these intersected conglomerates were decoratively embellished by articulating the surface unions with triangular planes or hyperbolic paraboloids, the directrices of the hyperbolic paraboloids being designed to coincide with selected generatrixes from the hyperboloids. [1, p.109]

Overall, the resulting complexity from the three ruled surfaces Gaudí combined in the *Sagrada Familia*, as Mark Burry explains, is astonishing due to the large number of (nine) variables which individually govern each of these surfaces: x_c, y_c, z_c, x_r, y_r, z_r, a, b, c. For a typical hyperboloid—x_c, y_c, z_c are the coordinates of the hyperboloid's centroid, x_r, y_r, z_r correspond to the three axes of rotation, a and c correspond to the major and minor axes, respectively, of the hyperboloid collar ellipse (circle, if $a = c$), and c is the asymptote determining the surface slope:

> The approach that he took for major wall and ceiling vault elements, for example, is a rich one as there are nine parameters that govern the relationship between any two adjacent surfaces and the character of the intersection…there is infinite choice with nine dimensions of possibility. [1, p. 109]

Mathematical Inversion as Form-Finding Strategy: John Pickering

Mark Burry's mention of the collective regard of *Sagrada Familia* as a kind of *inhabitable sculpture* identifies peoples' limited perspective of Gaudí's work; meanwhile, the notion of inhabitable art was the ambition of an artist whose work implicitly resonates Gaudí's preoccupation for a rigorous design process, to the point it far exceeds the boundaries of art, assuming architectonic dimensions. Sculptor John Pickering experienced a shift in his work during the 1970s when—in resemblance to Gaudí—he seemingly distanced himself from nature by adopting strict numerical rules to guide his creative process. As Professor Mohsen Mostafavi observes, Pickering's application of a mathematical approach through geometry and particularly, *inversion,* in fact brought him closer to the underlying natural ordering principles (as had been the case with Gaudí) [5, p. 7]. His subsequent sculptures from this period used a mathematical process called *inversion* to introduce controlled deformation in combinations of intersected solids (Fig. 9.4). The inversion principle posits that every point in Euclidean space, has its counterpoint in the hyperbolic space, which can be calculated by the formula: $R^2 = OA \times OI$. For any given point *A*, *I* is the inverse point of *A* and *O* is the centre of inversion. Geometrically, the inverse point is referenced to as *circle of inversion*, and the inverse point is defined by the point's proximity to this circle's centre, which regulates the amount of
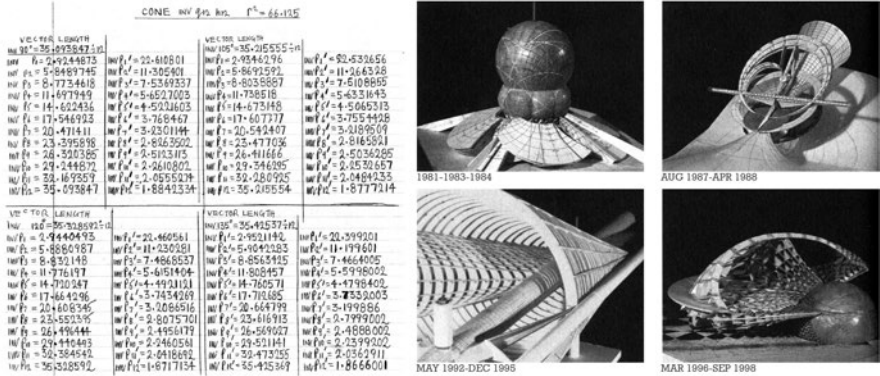
Fig. 9.4 Manual calculations of inverse point coordinates from Pickering's sketchbook. Sculptures with deformation of intersected topologies using mathematical inversion and *waffle-grid* method for fabrication (1981–84, 1987–88, 1992–95, 1996–98). (© John Pickering; © John Pickering Foundation)

distortion of the selected geometry. As we bring the centre of inversion closer to the original geometry, the distortion increases. The inversion process introduces curvature in all referenced geometries and so, orthodox Euclidean shapes like straight lines, rectangles and cubes are represented as two or three-dimensional curves, curved shapes and projective cubes in inversive geometry (Fig. 9.5). On a two-dimensional plane, inversion is relative to a centre of a circle, while in three-dimensions it refers to the centre of a sphere. This type of transformation becomes clearer in relation to non-Euclidean geometries like hyperbolic geometry, where the inverted equivalents of straight lines are represented as the arcs of a circle within the Poincaré disc model.[2]

Pickering's working process entailed manual calculations of point coordinates in space to generate guidelines for the sculptures. He often used toroidal geometries, because their inversion produced what are known as *Dupin cyclides*, a topology defined by circular curves, whose inversion also produces circles (Fig. 9.5) [6, pp. 217–218 and 7].

To employ this rule, an inversion script was developed in a parametric modelling environment and applied to transform a hyperboloid of revolution (Fig. 9.6). Examining it from various angles allows us to investigate topological curvature variation, as well as shadow patterns on the resulting topologies. The script extracts the edges from a three-dimensional surface topology, divides these into sets of points (higher values increase output accuracy), and finds their inverse points in space, by calculating the distance of the original points from the centre of the *inversion sphere* with the inversion formula: $R^2 = OA \times OI$. In the inversion of ruled

---

[2] For further information on matters of hyperbolic and inversive geometry, the reader may refer to relevant online resources like Wolfram's Math World: https://mathworld.wolfram.com/Inversion.html
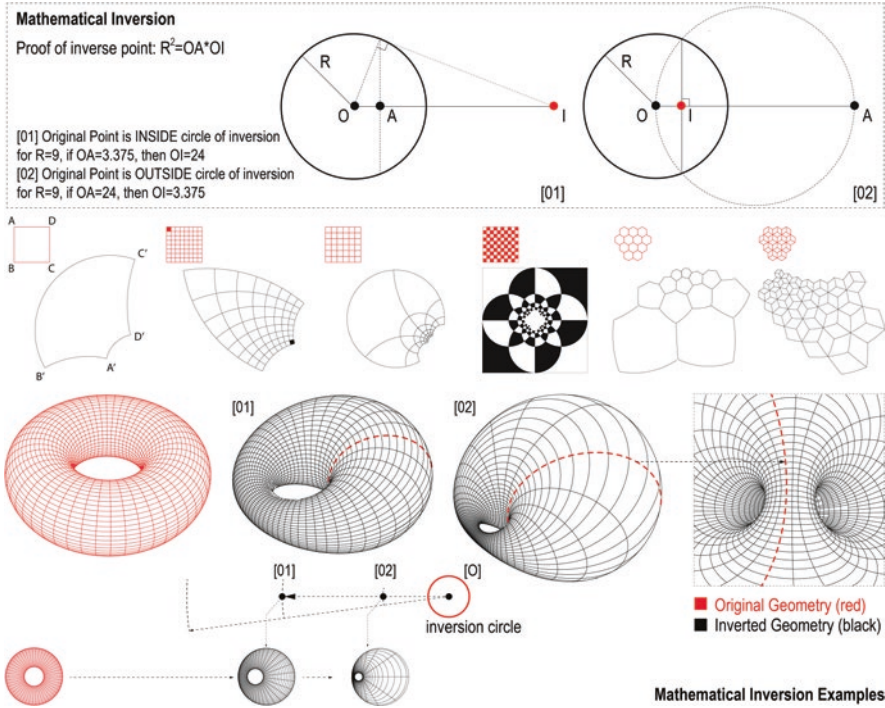
Fig. 9.5 Geometric solution for the inversion formula $R^2 = OA \times OI$. Inversion of orthogonal grids returns curvilinear patterns like the inverted chessboard. For three-dimensional input, a torus is inverted to a *Dupin* cyclide. As the geometry approaches the centre of the inversion (01–02-O), distortion increases, as illustrated by the red dashed line above

Fig. 9.6 Inversion algorithm in parametric modelling software (Grasshopper®). Four stages of deformation are shown for a hyperboloid of revolution
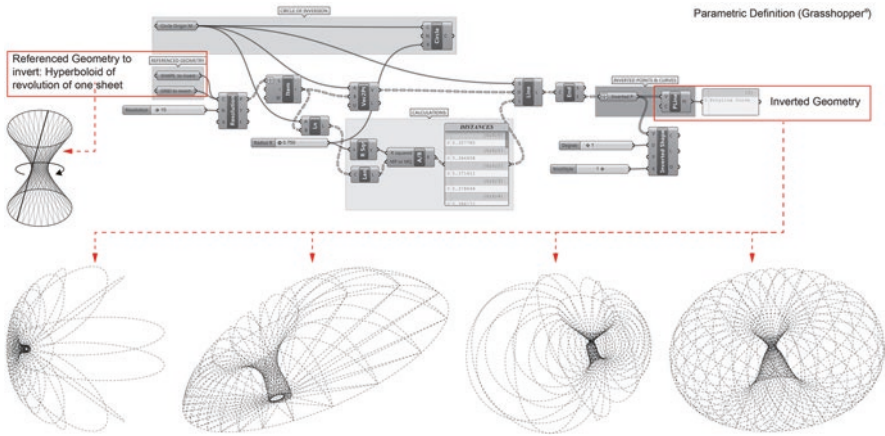
surface topologies, moving the centre of the inversion sphere closer to the hyperboloid of revolution causes greater deformation (and length increase) of the rulings.

A Combined Approach to *Virtual Presence*

We have identified a mathematical logic present in Gaudí's work *vis-à-vis* an equally rigorous analogue numerical methodology by Pickering. Echoes of an underlying codification seem to exist in both; the significance of the *intangible* aspect which drives the final design. In the *Sagrada Familia*, ruled surfaces manifest in the building through their absence, what Mark Burry has called an architecture of *"real absence"* and *"virtual presence"* [2, pp. 128, 136]. To appreciate the built components' complexity, one must imagine the original topologies from which they emerge:

> Gaudí was sculpting geometrically rather than 'physically' as a sculptor would work with hammer and chisel…he was conceiving of the outcome of the geometries' use just as materially as would a sculptor working reductively with stone, but Gaudí was pursuing this outcome by manipulating the geometry of 'what is not there'. [2, p. 145]

In Pickering's work, the translation of certain *regular* topologies into non-Euclidean geometries using *mathematical inversion* is noteworthy, because it switches operations towards the hyperbolic plane. His sculpted volumes warrant similar consideration, asking the observer to decipher complex intersecting topologies by reference to their earlier, straightforward Euclidean counterparts. Pickering often conceals the original surface further, offering instead its *skeleton* in the finished product, which is constructed with the *waffle-grid* method; three-dimensional objects represented as intersected contour planes (Fig. 9.4).

> Pickering doesn't actually represent the equation directly but instead makes a jig on which to hold the answer. It is up to us, as observers, to construct the gossamer mathematical surface ourselves. [8, p. 79]

This notion of ambiguity in visual expression is present in the work of both designers, as one needs to interpret their geometrical intent by tracing back the design transformation steps. If we were to speculate on a possible evolution of Gaudí's methodology by further implementing mathematical rules, it may seem appropriate to integrate additional layers of geometrical complexity like inversion. This can promote even richer results (and perhaps consider other factors from a different point of view, i.e. wall illumination). To this end, we applied the inversion algorithm through a parametric 3D model, generating the inverted option of a window which mimics Gaudí's working protocol of intersecting hyperboloids of revolution. The six original intersected hyperboloids (Fig. 9.3) and their inverted topology are shown in plan in reference to the sphere of inversion (Fig. 9.7).

While the results naturally echo the original surfaces, they are asymmetrically distorted due to the position of the centre of inversion. This asymmetry causes light to behave differently, introducing rich shadows (bottom of Fig. 9.7), which can help highlight more exaggerated deformations. On a more tangible level, the inversion
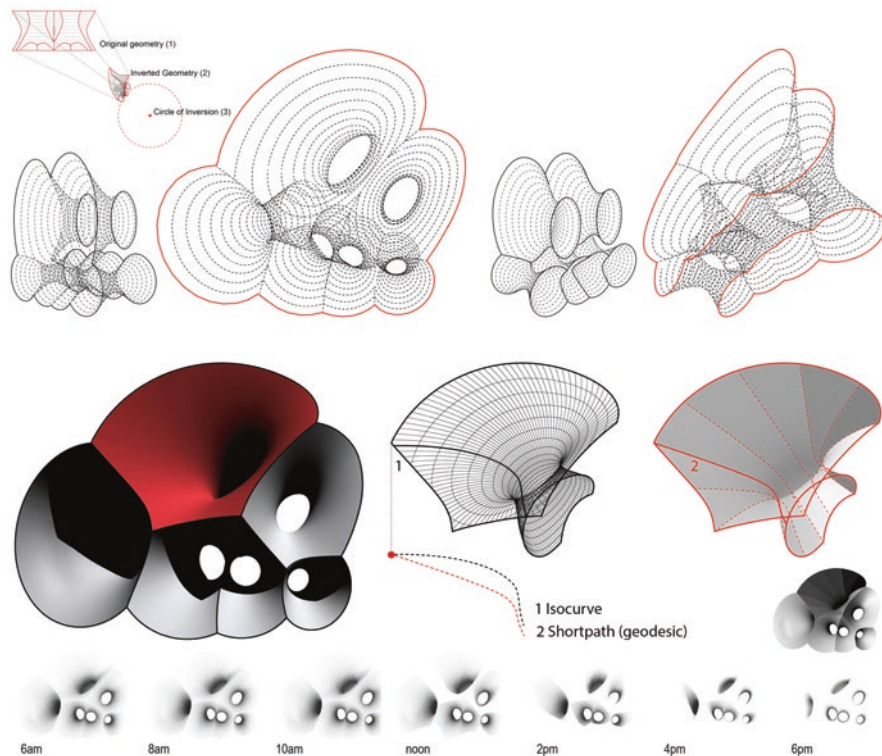
Fig. 9.7 Comparison of original and inverted topologies (front-back, inverted shape outlines are shown in red); conventional isocurve (1) surfaces are re-defined through geodesics (2) to get developable curves for fabrication from straight lengths of material; surface shadows on the inverted window topology are provided at 2-h intervals (6 a.m.–6 p.m.) throughout the day

has changed the properties of the original geometry generators; the rulings are no longer straight lines after the process of inversion. From a formal point of view, this may prove visually attractive as the inverted rulings could develop into an interesting ornamental feature by guiding the carving of the window surfaces similar to the original window ridges in Fig. 9.3. On the other hand, they might present some difficulty in terms of the window fabrication.

Fabrication Strategies: Advantages and Constraints

Even after a century since Gaudí's passing, his design intent for the *Sagrada Familia* proved a challenge to decipher and build, ultimately exploiting parametric modelling, design scripting and robotic fabrication methods for precise stone carving of the complex intersected surfaces. As we have mentioned, the use of a geometrical

language in the *Sagrada Familia* is attributed to a possible intent on the part of Gaudí to help his successors capture his vision for the building and complete the construction. Ruled surfaces were meant to further guide architects and contractors, facilitating the fabrication of vaults and walls [1, p. 106, 9, pp. 149–150]. Producing surfaces which result from combining such intersected geometries with inversive deformation will likely pose an interesting challenge with regard to their constructability. Their lack of developability (in the way of most ruled surfaces) raises questions of feasibility and appropriateness. While the comments of engineer Chris Wise refer to Pickering's work, they may also apply here:

> Pickering's work could certainly be built. As an engineer, I like the rationale of its manufacture (It is a counterpoint to those who doodle away in 3D Studio without a second thought about the practicality of their computerised forms…), but there is a fundamental contradiction in attempting to use his favourite equation for something like 'architecture'. This is because the inversion principle is the equation of a weightless structure. Put it on earth and the pure maths no longer applies… [8, p. 81]

While the fabrication of ruled surfaces is facilitated by the inherent rationalized geometry, relying on straight lines (rulings) to define complex topology, the resulting inverted surfaces discussed herewith are quite complex, and require other methods. Finding a complete strategy for producing templates for stone carving of the inverted surfaces is beyond the scope of this paper, as the inverted vault geometries demonstrate substantial difficulty. My interest is limited to identify possible aspects of interest in various fabrication strategies without going too much in depth.

Differentiating the tectonics of Gaudí's and Pickering's structures should be acknowledged at this point. The *Sagrada Familia* engenders a stereotomic character, using reinforced concrete, stone and brick for walls and vaults, while Pickering's waffle-grids justify another method, likely a metal structural frame. Indicatively, our combined proposal of inverted hyperboloid surfaces may be treated as a skin which lies on a waffle-grid scaffold. In order to obtain a buildable surface that approximates this doubly curved topology, the inverted surfaces would have to become developable. This involved identifying an appropriate discretization strategy. We have briefly discussed two alternative scenarios below.

Fabrication Strategy 1: Unrolling Surfaces to Small Panels Using Dual Graphs (186 Panels)

Obtaining a faithful approximation of the inverted surfaces involves discretizing the surface into a mesh and an additional rationalization process using a parametric plug-in called *Ivy*. *Ivy* uses graph representation of mesh geometry to optimize the subdivision of complex curved surfaces for unrolling (Fig. 9.8), to anticipate architectural fabrication requirements [10, p. 447].
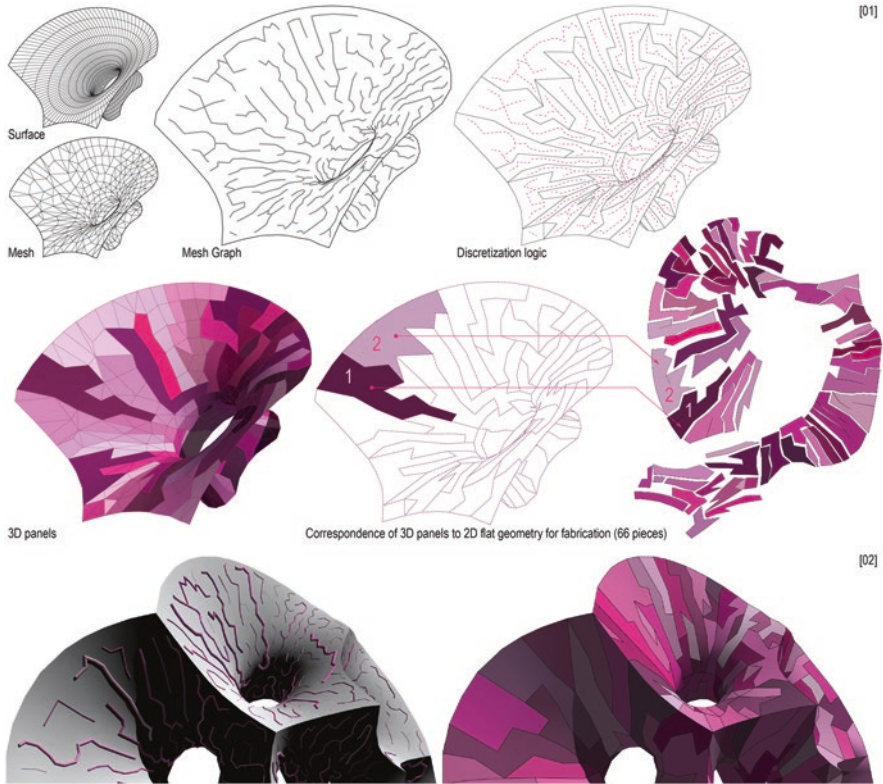
Fig. 9.8 (01) Inverted geometry rationalization for constructability: Surface to Mesh conversion using graph maps to calculate optimum discretization for flattening the pieces in *Ivy* [10] (66 panels); (02) Rendering of 6 panelized, intersected and inverted hyperboloids (compound surface of 186 panels)

The surface is converted into a mesh, whose faces are then reduced to end up with fewer panels. The *Ivy* software produces what is called a *dual graph* in order to establish optimum paths for surface segmentation, thereby converting mesh faces into graph nodes and non-naked edges into graph edges [10, p. 447]. These paths guide the boundaries of each panel; longer paths define larger panels (Fig. 9.8). Following this process, six inverted hyperboloids unfolded into 186 flat panels for fabrication. The three-dimensional surface pieces and the corresponding flat panels are shown in Fig. 9.8. The lower left image shows the final mesh graph; thicker graph nodes denote larger panels. It is important to note that the mesh was reduced significantly (about 25% of its original resolution) prior to the discretization process to decrease the number of panels into a reasonable number. Naturally, a finer mesh resolution will result in a closer approximation of the initial surface but will generate considerably more pieces for fabrication.

Discretization of 6 inverted hyperboloids into smaller panels based using geodesic curves (total 60 panels)   Stitching 10 panels together to form a compound surface
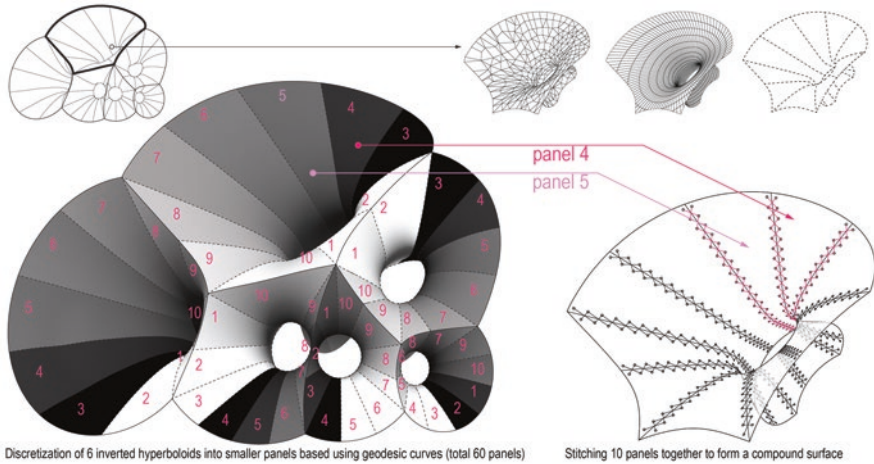
Fig. 9.9 Hyperboloid discretization using geodesic lines (compound surface of 60 panels)

Fabrication Strategy 2: Unrolling Surfaces into Long Panels Defined by Geodesic Lines (60 Panels)

In addition to their inherent mathematical structure, ruled surfaces were preferred by Gaudí because they could use straight lines to produce the formwork for fabrication, for example, in the case of the hyperboloid *Catalan vaults* [9]. Nevertheless, inversion alters the topological nature of the surfaces so that they cannot be defined by straight rulings anymore. To examine the possibility of a simpler fabrication scenario, resulting in a smaller number of panels and higher surface resolution, the inverted surfaces were re-modelled based on geodesic lines between two points, corresponding to divisions on the two naked edges (rings), shown in Fig. 9.9. Each inverted hyperboloid was therefore initially split into 10 surfaces using geodesic[3] lines on connecting division points along the two naked edges of the surface (Fig. 9.7). Then these were unrolled using a variety of methods in 3D software, producing some loss in surface area (usually reduction). It is also possible to apply the first strategy discussed here to subdivide the geodesic-split panels using *Ivy*, but that would result in a larger number of panels. Alternative tessellation methods may include attractors to split surfaces in rectangles based on curvature, but this falls outside the scope of the current paper.

---

[3] A geodesic is the locally shortest path between two points on a surface [11].

Historical Traces of Gaudí's Method to French Baroque Construction

There is a primarily historical significance in resolving developable surfaces for fabrication, which can potentially link contemporary software with traditional craft. Gaudy's ability to conceptualize unprecedented three-dimensional assemblies by intersection echoes construction insights from another period of great virtuosity in stone vault construction, the French Baroque (stereotomy in the sixteenth and seventeenth centuries) and particularly the work of Philibert de L'Orme and his contemporaries, i.e. Abraham Bosse, Amédée-François Frézier [12, pp. 179–180]. Bernard Cache, architect, and pioneer of digital fabrication software in architecture during the 1990s, identified enormous relevance in that period for understanding the current representation of complex topologies and the methods for generating their developed counterparts for construction:

> It is very important to remember that projective geometry has implications much deeper than Brunelleschian representation, and…its fundamental concepts still remain to be integrated within computer-aided design (CAD) systems. As a result, we suggest the next generation of CAD software lies somewhere between 1550 and 1872. [13, p. 103]

Cache's comment alludes to the projective operations necessary to produce construction templates for carving stone to build a particular kind of vault called *Trompe de Montpellier*[4] in sixteenth century's France. De L'Orme and his contemporaries pushed the limits of stereotomy through construction acrobatics which manifest through this doubly curved vault resulting from the intersection of a half-cone and a half-cylinder, the most famous of which was built in the *Château d'Anet* to support the *King's cabinet* (1576). The developed surface requires the use of descriptive geometry to produce a drawing called a *Trait* [12, pp. 179–200]. This analogue process entails a computational logic, as the three-dimensional understanding of the final carved shape of each piece of stone results from projection. By contemporary representation standards, the *Trait* corresponds to the *Unroll Surface* command in Rhino3D software (Fig. 9.10). The beauty of such constructs hinges on removing material from a typical support, by intersecting volumes, to give the projecting vault a "hanging" impression.

A similar process of material removal by intersection enabled Gaudí to create such dramatic sculptural and illumination effects on the walls and ceiling of the *Sagrada Familia*. In Gaudí's case, the act of intersection assumes a generative role, the outcome of which he could nevertheless foresee by means of projective drawing (like the *Trait* in Philibert de L'Orme's time) and physical prototyping. Pickering, on the other hand, had no way of anticipating the intersected geometries from inversion, at least in his early works. Unlike today's script which automatically computes hundreds of three-dimensional coordinates, Pickering had to calculate every point coordinate and interpolate the shapes by hand.

---

[4] The English translation for *trompe* is *squinch*, referring to the pinched geometry of the vault.
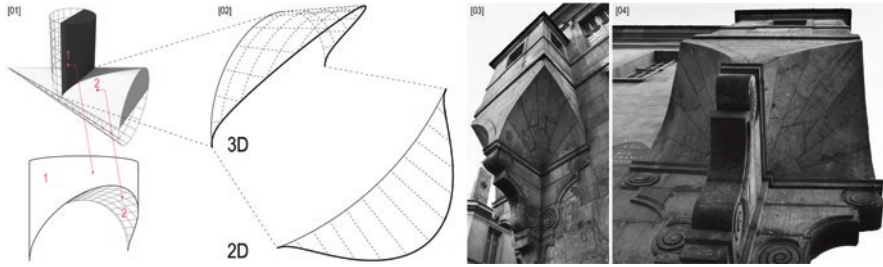
Fig. 9.10 Process of generating a typical trompe by intersecting a cylinder with a cone (01); resulting vault and flat geometry for fabrication (02); A triple *Trompe* vault at *Hôtel de Lamoignon* (previously *Angoulême*), Paris, by J. B. Androuet du Cerceau (1584) (03, 04)

Conclusions

The process we have introduced herewith is able to *augment* Gaudí's work by applying another mathematical layer. Gaudí's and Pickering's methods address, implicitly or otherwise, questions about *efficiency of process, appropriate representation* and *feasibility/commodity* of design outcomes (i.e. potential and prospect for inhabitation).

Pickering's process can be automated via either parametric software or spreadsheets, facilitating the visualization of inverted shapes; this would allow to more quickly intuit the families of possibilities. However, it is difficult to determine a benchmark for combination of parameters, given the possibility to evolve indefinitely in the virtual domain. The particular settings of inversion need to be further calibrated to establish their appropriate application. Which combination of Booleans yields the best outcome? Which inversion circle (or sphere) most successfully deforms an original topology? Mark Burry wonders about the point when one can stop further parametric adjustments and consider the design process as being complete [3]. Because both Gaudí and Pickering were operating with the *intangible* (what is removed), and relied on Boolean combinations, such a calibration may not always be clear. So, to our interest, the process remains inherently cumulative.

It seems that, paradoxically, the constraints of the analogue procedures during the projects' time may have helped their design improve. The physical investigation of both Gaudí and Pickering may also have turned out fruitful because it was liberated from notational conventions; neither produced much in terms of drawings of the *Sagrada Familia* or inversion. In the former case, the complexity of *Sagrada Familia* required a more direct but enabling approach to visualize what was difficult to draw; the prototyping steps undertaken by Gaudí are closer to a pre-Albertian way of working, the kind of *viva voce* tradition used by Brunelleschi for the design progression of the Florence *Duomo*, which—like the *Sagrada Familia*—was built without construction drawings [14, p. 32]. According to Mario Carpo, this direct, hands-on working method circumvents the notational mediator between design intent and its built expression, introduced by Alberti's modern approach to

describing building design. It also confirms Gaudí's insight that some *intangible* aspects of the project could not be adequately imagined by drawing, and could be figured out faster through physical modelling, prior to applying complex descriptive geometry:

> …if you can't draw what you have in mind in order to have others make it for you, you can still try to make it yourself. For example, this is what Antoni Gaudí did, …in the Sagrada Familia, not coincidentally reviving, …some of the technologies and social organization of a late medieval building site. [14, p. 32]

Pickering, similarly, calculated point coordinates and remained on sketching before physically modelling the intersections of his found geometries. We find these working habits noteworthy because they associate older ways of practice with today's complex computational processes.

In considering the utility of Gaudí's and Pickering's work, it is helpful to evaluate their stereotomic character (volume vs surface). Inversive rules open possibilities of spatial inhabitation for Pickering's work, because the topologies possess an interesting quality: due to the inversive deformation, even visually *hard* shapes produce curved topological outcomes which seem more pliable. In reality, however, this is a *hard* process because anything unwanted in the final form cannot be individually edited out—rather the form is seen as a whole—due to the same mathematical rule the whole geometry needs to follow. This of course results from Pickering's choice to construct the scaffold (structure) of the topology and not its surface, as mentioned earlier. In contrast, Gaudí was interested in the surface topology itself, which, together with the mass it envelops, becomes also structural. In both cases, the geometrical intersections (the notches in the *waffle grid* in the former, and the *ridges* ending in *double* or *triple points* in the latter [1]) undertake a structural role for resolving load distribution.

Overall, it has been instructive to see how the work of both designers relies entirely on certain procedures to achieve complexity. As Daniel Giralt-Miracle points out, Gaudí's design was based on *"the use of simple geometry and complex development"* [3, p. 9]; correspondingly, Pickering's inversion formula is fairly simple, yet the design steps progressively afford substantial complexity, illustrating the importance of a process over a product in the act of design. Pickering's choice to execute his investigations physically—much like Gaudí used his own prototypes—lies in a personal, intimate choice, which relates to his ability to appreciate the work through some secondary intangibility. As Chris Wise mentions, Pickering may have treated these three-dimensional topologies as pure scaffolds *"onto which the pure numbers can be projected"* [8, p. 80], ultimately regarding the shapes *"as the memory of his mathematical journey"* [8, p. 80]. His sculptures might preferably remain in the domain of the possible than that of the realized. In a similar fashion, the inverted versions of Gaudí's windows—which are harder to construct than their ruled predecessors—may serve as a thought experiment, an exercise to help us consider the limits of architectural form-finding and its physical manifestation.

Except for Fig. 9.4, all the photos, drawings and diagrams are from the author.

References

1. Burry, M. (2011). Architecture and practical design computation. In A. Menges & S. Ahlquist (Eds.), *Computational design thinking* (pp. 102–119). John Wiley & Sons Ltd.
2. Burry, M. (2011). Scripted productivity: Gaudi's rose windows. In M. Burry (Ed.), *Scripting cultures: Architectural design and programming* (1st ed., pp. 126–151). John Wiley & Sons Ltd.
3. Burry, M., Serrano, J. G., & Grifoll, J. C. (2008). Sagrada Familia s. In *XXI: Gaudi ara-ahora-now*. Ediciones UPC, S.L.
4. Burry, M. (2007). Setting the scene. In M. B. Burry (Ed.), *Gaudí unseen: Completing the Sagrada Familia* (pp. 10–55). Jovis.
5. Mostafavi, M. (2006). So I became anti-nature. In G. Liaropoulos-Legendre (Ed.), *Mathematical form: John Pickering and the architecture of the inversion principle* (p. 7). AA Publications.
6. Hilbert, D., & Cohn-Vossen, S. (1952). The simplest curves and surfaces; differential geometry. In D. Hilbert & S. Cohn-Vossen (Eds.), *Geometry and the imagination* (pp. 10–17, 171-271). Chelsea Publishing Company.
7. Barker, A., & Howison, S. (2015) Models of Geometric Surfaces: Dupin Cyclides. Retrieved from Oxford Mathematical Institute: https://www.maths.ox.ac.uk/about-us/departmental-art/dupin-cyclides
8. Wise, C. (2006). Perfect imperfect. In G. Liaropoulos-Legendre (Ed.), *Mathematical form: John Pickering and the architecture of the inversion principle* (pp. 79–81). AA Publications.
9. Rosell, R. E., & Oller, J. F. (2007). The construction of the project. In M. Burry (Ed.), *Gaudí unseen: Completing the Sagrada Familia* (pp. 141–151). Jovis.
10. Nejur, A., & Steinfeld, K. (2017). Ivy: Progress in developing practical applications for a weighted-mesh representation for use in generative architectural design. Acadia 2017: Disciplines & Disruption [Proceedings of the 37th Annual Conference of the Association for Computer Aided Design in Architecture (pp. 446–455). Cambridge, MA: ACADIA.
11. *Geodesic line*. (2012). Retrieved from encyclopedia of mathematics: https://www.encyclope-diaofmath.org/index.php/Geodesic_line
12. Evans, R. (2000). Chapter 5: Drawn stone. In R. Evans (Ed.), *The projective cast: Architecture and its three geometries* (pp. 179–240). MIT Press.
13. Cache, B. (2004). Towards an associative architecture. In N. Leach, D. Turnbull, & C. Williams (Eds.), *Digital tectonics* (pp. 102–109). John Wiley & Sons Ltd.
14. Carpo, M. (2011). Geometry, algorism and the notational bottleneck. In M. Carpo (Ed.), *The alphabet and the algorithm* (pp. 28–34). MIT Press.

Emmanouil Vermisso   is an Associate Professor of Architecture at Florida Atlantic University and a doctoral candidate at the University of Patras, studying human and computational Creativity. He holds degrees from the University of Westminster and Syracuse University and has practiced in the London firms of Foster+Partners, AHMM and Porphyrios Associates. He is interested in creativity, bottom-up design thinking, analogue computation and architectural organicism. His research includes the use of artificial intelligence in design, analogue form-finding, self-organization, and responsive prototyping, and has been published in the International Journal of Architectural Computing, ACADIA, CAAD Futures, receiving recognition from ACSA, NCARB and AIA.

Chapter 10
An Introduction to Solid Tessellations with Students of Architecture

João Pedro Xavier, José Pedro Sousa, Alexandra Castro, and Vera Viana

Abstract This paper intends to describe an educational experiment accomplished in the *Geometry and Architecture* course of the first year in the Faculty of Architecture of the University of Porto in 2017. In this activity, students were introduced to digital three-dimensional modelling as an additional tool to develop their knowledge of geometry. The subject of solid tessellations was selected as leitmotif because of the structural and architectonic interest and creative potential that the situations in which polyhedra, other than the cuboid, fill space may have for aspiring architects. The time limitations of the academic year impaired the desired breadth for the task, so students had to focus their attention only in six uniform solid tessellations, out of the possible 28. Besides acquiring digital design modelling skills useful for their scholarly and professional practice, this experiment and collaborative assignment allowed students to improve knowledge of polyhedral theory and apply newfound IT skills in architectural design.

Introduction

For several years, the syllabus *Geometry and Architecture* of the first year in the Faculty of Architecture of the University of Porto (FAUP) was entirely concerned with projective geometry and such traditional systems of representation as cartography, topography, orthographic projections, axonometry, and perspective. In FAUP, digital design as a supporting tool for the study of representation and architectural design is usually introduced only in the third year. Recognizing the limitations of this methodological option and, above all, its divergence with contemporary reality and the most updated architectural practices, the professors of the syllabus decided, in 2015, to introduce the computer in the classroom as a tool for students to learn geometry and actively explore digital three-dimensional modelling. Since then, the

J. P. Xavier · J. P. Sousa · A. Castro (✉)
Faculty of Architecture, University of Porto, Porto, Portugal
e-mail: jpx@arq.up.pt; jsousa@arq.up.pt; macastro@arq.up.pt

V. Viana
Faculty of Architecture, CEAU, University of Porto, Porto, Portugal
e-mail: vlopes@arq.up.pt

program of the course has clearly been divided into two parts: the first, corresponding to ca. 2/3 of the total lecturing time, in which traditional representation systems are approached through individual assignments and hand-drawing is taken as privileged learning and investigation tool; in the second, a collaborative assignment is proposed, and the exploration of three-dimensional modelling with computer-aided design (CAD) stimulated.

The investigation of certain concepts in geometry usually takes some time to accomplish within traditional representational systems, while digital modelling allows students to address a broader range of themes and enhance their abilities for spatial visualization, mental rotation, and geometric reasoning, since it provides an accurate representation of geometric objects easily navigable within viewports and representational systems. The geometrical concepts and transformations are then taken as the fundamental concern of their inquiry, rather than the technical procedures of the chosen representational system.

An introduction to digital 3D modelling in the *Geometry and Architecture* syllabus is scheduled for a teamwork activity to be developed in 5–6 weeks so students can explore CAD processes to study and research certain geometric subjects that, from the professors' perspective, may have a sturdy impact on architectural design. Each year, a different topic is proposed so that students may be introduced into themes generally unexplored and whose complexity clearly justifies the use of digital media. So far, the topics for the students' investigations were anamorphosis, in 2015–2016 and 2020–2021, solid tessellations in 2016–2017, surfaces in 2017–2018, and vaults, in 2019–2020.

This paper presents the assignment accomplished by the students on the topic of solid tessellations. A brief insight on the theoretical framework that supported the investigation developed and the goals and methodology proposed for the task will be addressed. In the end, a selection of the students' final works will be presented from a critical standpoint, acknowledging the creative potential of didactic experiments that aim to bridge polyhedral theory and architectural design.

Polyhedra and Solid Tessellations

Polyhedra is a stimulating subject to introduce in any educational context, as Pedersen denotes [1, p. 133] when referring to how students react when instructed to make their models in paper; they usually do not question why they should make them, quite the contrary, they become interested in their characteristics and show a keen interest in modelling other examples. Studying polyhedra may also be a gateway to enhance the students' geometrical knowledge, not only because of the myriad of mathematical contents and branches into which students are introduced [1, p. 135] but also because, by modelling and manipulating geometry in such a tangible form, students seem to recognize geometric concepts and operations more efficiently, becoming capable of developing their geometric reasoning to a different

level.[1] Moreover, studying and virtually modelling different classes of polyhedra within an architecture program help students to widen the repertoire of possibilities to conceive and design space beyond the rigidity of cuboidal forms [2, 3].

To a more in-depth approach of the subject from a theoretical perspective, an expert on polyhedral geometry, who co-authored this study, collaborated with the team of professors to establish a content basis that came to be fundamental for the research done by the students.

The subject was first introduced from a theoretical standpoint,[2] through which students widened their knowledge on polyhedra and were given the chance to manipulate physical models of less common polyhedra and learn how to model some of them virtually. Students then explored geometric transformations and symmetry operations in a digital framework, such as translation, rotation, and reflection, to better understand important notions, such as the duality of polyhedra and the spherical symmetry groups. The words of Coxeter [5, p. 68] were explained to illustrate how, in solid tessellations or honeycombs, polyhedra fit together to fill space just once and every face of each polyhedron belongs to one other polyhedron, as well as the conditions necessary for polyhedra to do so (Fig. 10.1). To better understand these notions, the students modelled the six convex parallelohedra that
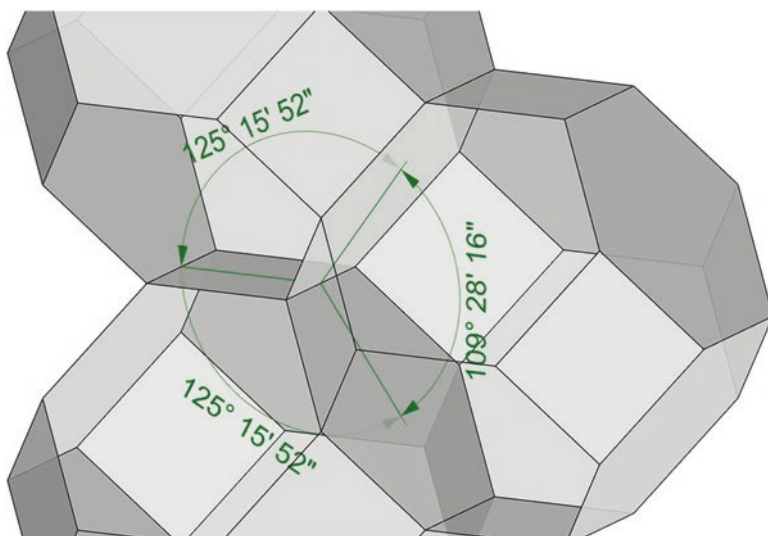
Fig. 10.1 Three truncated octahedra with a common edge fill space because the sum of the dihedral angles around that edge equals 360°

---

[1] The authors recognize that the extent through which the students' geometric reasoning is enhanced within a digitally driven educational approach is yet to be fully understood or certified, but this experiment aims to introduce a modest contribution to the discussion and, at the same time, to stimulate the exploration of polyhedral theory in other higher education settings.

[2] A report on the educational resources explored and the students' opinion on the theoretical segment of the classes accomplished for this didactical experiment has been included in [4].

fill space by translation of their replicas [6], besides other examples of convex and concave polyhedra that infinitely fill space.

In subsequent classes, the notion of uniformity in a tessellation, through which every vertex, equally surrounded, is superimposable under symmetries onto any other, was explained. All 28 convex uniform tessellations [7] were illustrated and some of them virtually modelled by the students. Special attention was given to the 13 honeycombs and their duals, respectively, categorized by Conway, Burgiel, and Goodman-Strauss [8, p. 292–298] as architectonic and catoptric tessellations because of the symmetry properties of their cells.

The Assignment

Out of the 28 convex uniform tessellations, six of the architectonic (Fig. 10.2) were proposed by the team of professors as the leitmotif of the collaborative assignment, not only for the sake of concision and feasibility but also because of their potential interest for architectural design. The idea was for students to overcome the characteristic abstraction of the underlying geometrical structure in each solid tessellation and regard them from an architectural—spatial – standpoint, exploring their intrinsic spatiality. With the intention of adopting computer modelling as a driving force for the students and preparing the presentation of their response to the assignment, Rhinoceros®,[3] one of the most efficient software used in architectural practice and powerful research tool, was selected due to its versatility and easiness to approach geometric modelling.

The time scheduled for the exercise was 6 weeks, and six classes, with an average of 24 students each, organized in groups of 4 or 5 elements, were involved. Each group had to explore one of the six tessellations, with the purpose of creating a spatial structure to be placed at the Garden of Quinta da Póvoa, one of the most interesting exterior spaces in the faculty's campus (Fig. 10.3).

The work was developed following a methodology subdivided into steps: (1) presentation of the theme and theoretical framework; (2) a brief introduction to the software and the commands that would be relevant for the assignment; (3) analysis of the geometric concepts involved based on preliminary modelling experiments; (4) design and development of the project itself; and (5) presentation of the final projects. Each group of students had to manipulate virtual models of the polyhedra involved in their tessellation and find out how those could fill space uniformly. One of the proposals for the task was for students to consider the geometric structure under analysis as a possibility of conceiving a small inhabitable structure but slightly deviating from its rigid configuration. After the theoretical introduction, the work in the CAD environment was developed according to the following phases:

---

[3] *Rhinoceros®* is a 3D computer graphics and computer-aided design application software developed by Robert McNeel & Associates (https://www.rhino3d.com/).
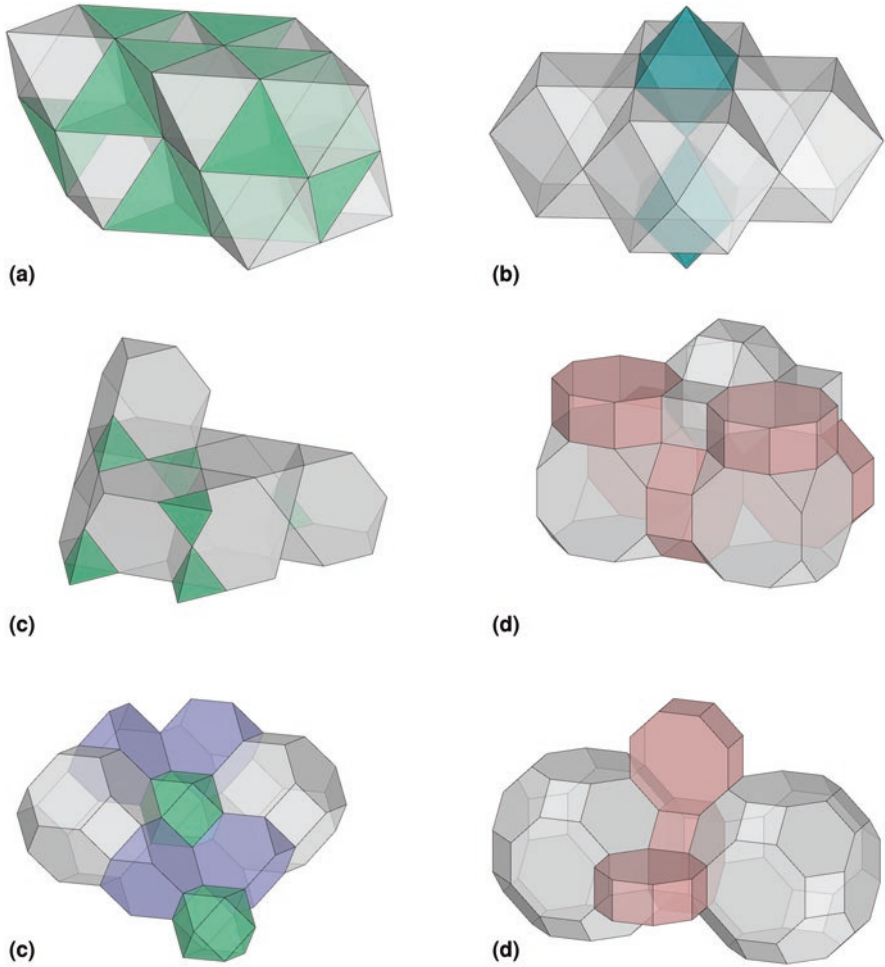
Fig. 10.2 The six architectonic tessellations selected for the teamwork. The designations of polyhedra per vertex according to Wenninger [8]. (**a**) Tetroctahedrille (8 Tetrahedra and 6 Octahedra). (**b**) Cuboctahedrille (2 Octahedra and 4 Cuboctahedra). (**c**) Trunctetrahedrille (2 Tetrahedra and 6 Truncated Tetrahedra). (**d**) 1-RCO-Hedrille (1 Rhombicuboctahedron, 1 Truncated Cube, 1 Cube, and 2 Octagonal Prisms). (**e**) Truncated Tetroctahedrille (1 Cuboctahedron, 2 Truncated Tetrahedra, and 2 Truncated Octahedra). (**f**) b-tCO-Hedrillle (2 Octagonal Prisms and 2 Rhombitruncated Cuboctahedra)

Phase 1: Modelling the Tessellation

The initial approach began with students modelling each polyhedron in the tessellation, after which the possibilities of multiplication through translation and rotations were analyzed, exploring different operations and geometric transformations. This
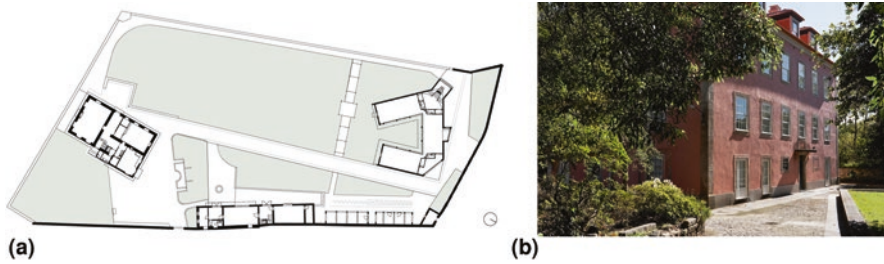
Fig. 10.3 Site Plan of "Casa Cor-de-Rosa, Cavalariças and Pavilhão Carlos Ramos" [10] (left) and Faculty of Architecture – University of Porto, Casa Cor-de-Rosa/Álvaro Siza [11] (right)

allowed students to get to know in further detail the tessellation assigned to them and begin to recognize its intrinsic spatial characteristics.

Phase 2: Incorporating the Polyhedral Composition within the garden's Context

Students chose a specific area of the garden and began thinking about adapting the structure to the location by refining its overall scale, dimension, and orientation. In this stage, architectonic topics, such as the configuration of the structure, its spatial features, and how it would physically interact with the site itself, began to be considered.

Phase 3: Definition of the Structure's Materiality

While combining polyhedra to achieve the desired shape, students were proposed to include a cutting plane, meant as a disruptive yet creative element in the overall structure. The plane would trim the form either at its base, to facilitate its integration in the garden's ground or elsewhere. Once the spatial structure was outlined, students had to conceive its materialization, attending to the following requirements: (1) having structural bars in every edge of each polyhedron while some of its faces are left open; (2) enclosing the space within some cells in the structure with the faces as panels.

Phase 4: Presentation of the Project

In the last phase of their project, the students presented a poster based on a template provided for the assignment, where they inserted: CAD-produced images aimed to display; the architectonic tessellation assigned for the group; the geometric composition conceived in a wireframe and surface appearance; and the overall result shown from complementary points of view. The poster had to include a conceptual hand-sketch, a plan and an elevation, and a photomontage of the inhabitable structure inserted in the garden's context. In addition to the poster, students produced a small video showing the architectonic composition both from the outside and the inside or, alternatively, a cardboard model.

A Selection of the Projects Developed by the Students

The results were diverse, given that, for this assignment, the six classes involved conceived a total of 33 geometric structures from six different uniform tessellations. The variety in the solutions found by the students for the inhabitable structures and the interest they have shown throughout the whole project were a clear testimony of the creative potential that polyhedra and solid tessellations meant for the aspiring undergraduate architects involved. We will analyze in more detail three of their works[4] conceived from the same tessellation, the cuboctahedrille (Fig. 10.2b). This tessellation turned out to be the one that led to the more interesting results, and the reasons for this might be the fact that only two different polyhedra were involved or its clear connection to the tetraoctahedral spaceframe and the face-centered cubic lattice. Nonetheless, each group conducted their studies independently and conceived very different results, both in the spatial concept and the architectonic image of the geometric structure devised.

Project a: Stopping Point

In this project (Fig. 10.4), the group conceived a small pavilion, very compact in its overall form. Placed under a big tree, the pavilion is strongly marked by its closed panels and the entrances opposed to each other. One interesting detail of the project is the configuration of the cells sectioned by the cutting plane proposed in the assignment. Segmenting the overall form was a decisive step in the design process that generated an interesting irregularity for the structure, which included three small openings on the upper part of the volume so that natural light might penetrate its interior.

---

[4] Other examples of the students' work besides Projects A, B and C, are shown in [9].
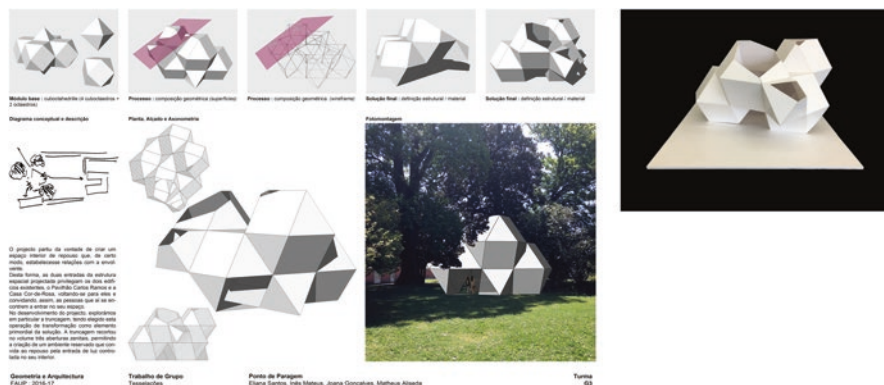
Fig. 10.4 Project A: "Stopping point" by Eliana Santos, Inês Mateus, Joana Gonçalves and Matheus Aliseda, 2016/2017 (Presentation poster and cardboard model)
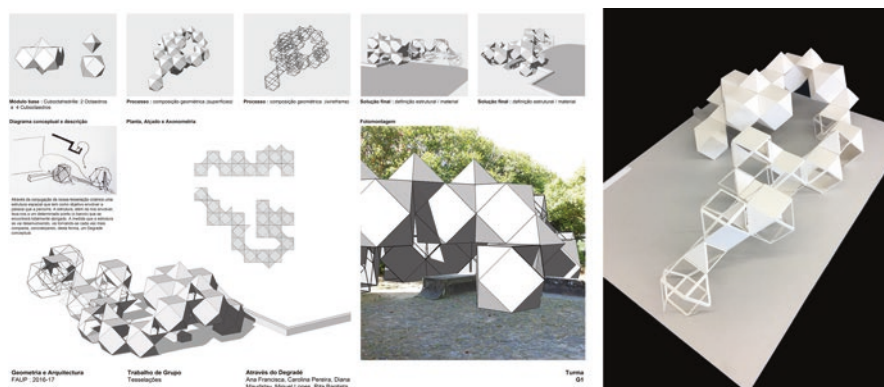
Fig. 10.5 Project B: "Through the gradient" by Ana Francisca, Carolina Pereira, Diana Maudslay, Miguel Lopes and Rita Baptista, 2016/2017 (Presentation poster and cardboard model)

Project B: Through the Gradient

In this project (Fig. 10.5), the students decided to expand the composition and place it along an existing path close to a sitting area of the garden so that people would walk along and throughout the architectonic structure before reaching the meeting point enclosed by a granite bench. A distinctive aspect of the proposal is the composition configuration that departed from an idea of gradation. As the poster illustrates, the inhabitable structure starts with a single *open* polyhedral cell to which more and more elements were added, and the base module multiplied until the structure finishes in the preexistent sitting area. Much the same way, the initial cells do not include panels to be read as open and progressively developed into closed cells. This detail ensures transparency as an important structure element and enhances the honeycomb's legibility.

Project C: (In)Tangible

In this example (Fig. 10.6), the students developed a spatial concept very different from the last two. Envisaging the structure as a kind of tent-like shape, they placed the faceted volume in an open area of the garden, along a connecting path, that visually links a small door existing on the facade of the Pavilion designed by the architect Álvaro Siza Vieira and an old gazebo from which one can look out over the river and the sea.

Conclusions

From the results here presented, we may conclude that the impact of this didactic experiment was extremely positive on many levels. First, because of the students' engagement with the challenge itself and the easiness and spontaneity with which they manipulated the geometric structures in search of an architectural shape. Secondly, for the important contribution of the digital tools to support the investigation and how they provided students the control of such complex forms. In the context of the *Geometry and Architecture* course, this possibility posed a stimulating challenge since it allowed to open the syllabus to different topics which are less commonly explored yet very pertinent in the context of contemporary architectural
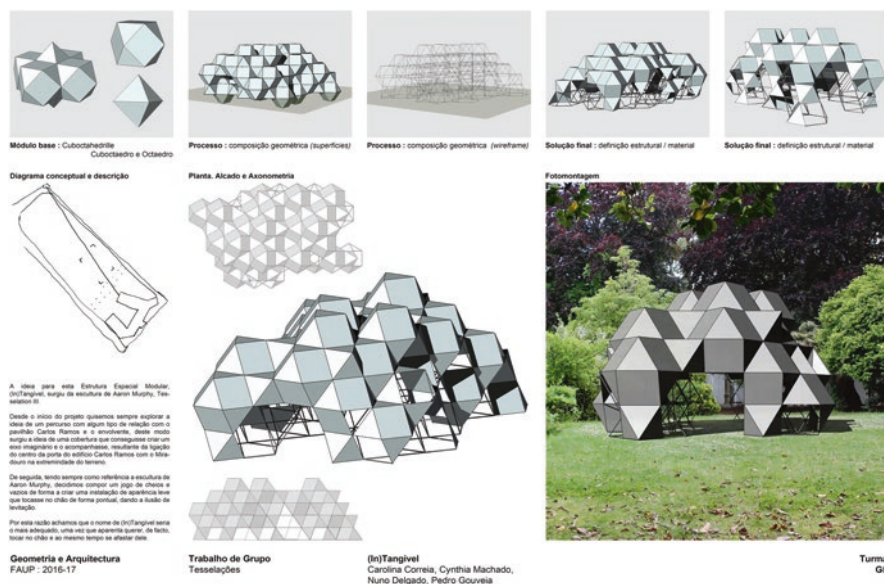
Fig. 10.6 Project C: "(In)Tangible" by Carolina Correia, Cynthia Machado, Nuno Delgado and Pedro Gouveia, 2016/2017 (Presentation poster)

practice. Thirdly, for the contribution of a brief introduction to polyhedral theory to the development of the spatial intelligence of the students' and their overall knowledge on geometry.

In this regard, we must highlight how studying and modelling polyhedra in higher education are an interesting subject through which geometry and architecture may be creatively explored, not only for the tangibility of the operations involved but also for the numerous mathematical concepts and transformations that the students are able to interact and better understand. For higher education courses in which modelling, materializing and structuring space is a topmost concern, such as Architecture, research on polyhedra is certainly a valuable subject matter, especially if students are given the possibility to explore 3Dmodelling software to improve their knowledge of geometry.

References

1. Pedersen, J. (1988). Why study polyhedra? In M. Senechal & G. M. Fleck (Eds.), *Shaping space: A polyhedral approach* (pp. 133–147). Birkhäuser.
2. Gabriel, J. (1997). *Beyond the cube: The architecture of space frames and polyhedra*. J. Wiley.
3. Burry, J., & Burry, M. (2012). *The new mathematics of architecture*. Thames e Hudson.
4. Viana, V (2020). *Aplicações didácticas sobre poliedros para o ensino da geometria / Didactic Applications on Polyhedra for the teaching of Geometry* (http://hdl.handle.net/10348/10337) [Tese de Doutoramento, Universidade de Trás-os-Montes e Alto Douro]. Repositório Científico da UTAD. 243–251.
5. Coxeter, H. S. M. (1973). *Regular Polytopes*. Dover Publications.
6. Grünbaum, B., & Shephard, G. C. (1980). Tilings with congruent tiles. *Bulletin of the American Mathematical Society, 3*(3), 951–974. https://doi.org/10.1090/s0273-0979-1980-14827-2
7. Grünbaum, B. (1994). Uniform tilings of 3-space. *Geombinatorics, 4*, 49–56.
8. Conway, J. H., Burgiel, H., & Goodman-Strauss, C. (2008). *The symmetries of things*. A.K. Peters.
9. Viana, V. (2018). Architectonic tessellations as constructive modules. In K. Williams & M. Bevilacqua (Eds.), *Nexus 2018 architecture and mathematics conference book* (pp. 325–328). Kim Williams Books.
10. Site Plan of "Casa Cor-de-Rosa, Cavalariças and Pavilhão Carlos Ramos" – FAUP © CEFA.
11. Faculty of Architecture – University of Porto, Casa Cor-de-Rosa/Álvaro Siza © Luis Ferreira Alves/FAUP.

João Pedro Xavier is an Architect and Full Professor at the Faculty of Architecture, University of Porto, where he received his degree in 1985 and his Ph.D. in Architecture in 2005.

He worked in Álvaro Siza's office from 1986 to 1999. At the same time, he established his own practice as an architect.

Xavier is a member the research teams *Architecture: Theory, Project, History* and *Digital Fabrication Laboratory*. The relationship between architecture and mathematics, especially perspective, is his main research interest.

He is correspondent editor of the *Nexus Network Journal*, and Council member of the *European Association for Architectural Education*.

José Pedro Sousa is an Assistant Professor at the Faculty of Architecture of the University of Porto (FAUP) teaching courses on geometry, computational design, and fabrication. At FAUP, he founded and coordinates the Digital Fabrication Laboratory (DFL), which is a research group dedi-

cated to investigating the impact of digital technologies in architectural thinking, design, and construction. He is currently a member of the High-Level Roundtable of the New European Bauhaus movement.

Alexandra Castro is an Invited Assistant at the Faculty of Architecture at the University of Porto (FAUP), where she teaches Geometry. She is currently developing her PhD research, focused on the relationship between geometry and contemporary architecture from the perspective of the impact that digital tools have on design practice, with the work of Herzog & de Meuron as central case-study. In 2013, she joined the CEAU-FAUP as a researcher, where she investigates geometry, digital modelling, and architectural representation. In 2010, she founded with Nicola Natali, the architectural office Castro Natali, based in Porto.

Vera Viana is a Researcher in the Faculty of Architecture, University of Porto, and Director of the Portuguese Geometry and D.rawing Teachers' Association.

With research interests on polyhedral geometry, the history of polyhedra, the relationships between architecture and mathematics and the transformative potential of digital culture in mathematics education, Viana authored a Ph.D. thesis, papers, lectures, workshops, and a website on these subjects.

Viana organizes the *Geometrias* conferences and contributes to other conferences as scientific reviewer and sessions moderator. Co-Chair of the *IS4SI2021 Summit* and the *Symmetry Art and Science: 12th SIS-Symmetry Congress*. Editorial Board member of the *Nexus Network Journal*.